

# Computation of whispering gallery modes for spherical symmetric, heterogeneous Helmholtz problems with piecewise smooth refractive index

Bouchra Bensiali\*

Stefan Sauter†

February 19, 2026

## Abstract

In this paper, we develop a numerical method for the computation of (quasi-)resonances in spherical symmetric, heterogeneous Helmholtz problems with piecewise smooth refractive index. Our focus lies in resonances very close to the real axis, which characterize the so-called whispering gallery modes. Our method involves a modal equation incorporating fundamental solutions to decoupled problems, extending the known modal equation to the case of piecewise smooth coefficients. We first establish the well-posedness of the fundamental system, then we formulate the problem of resonances as a nonlinear eigenvalue problem, whose determinant will be the modal equation in the piecewise smooth case. In combination with the numerical approximation of the fundamental solutions using a spectral method, we propose a Newton method to solve the nonlinear modal equation with a proper scaling. We prove the local convergence of the algorithm in the piecewise constant case by showing the simplicity of the roots. We confirm our approach through a series of numerical experiments in the piecewise constant as well as in the variable case.

**Keywords:** *Helmholtz problem, WGM, resonances, nonlinear eigenvalue problem, fundamental system, spectral method, Newton method, special functions.*

**MSC:** *65H17, 65N80, 35J05, 33C10, 34B30.*

## 1 Introduction

Whispering gallery modes (WGM) are one type of interference phenomena of waves characterized by their localization along the jump interface of the wave speed. These modes occur in general at high frequencies and are associated with complex scattering resonances very close to the real axis. These waves have many applications such as in whispering gallery modes resonators in optics (with important applications in medicine) where the goal is to confine light waves in a local region of an ambient medium [29, 10]. The determination of geometric and material configurations for such interference phenomena is an important task in order to improve the performance of the system. The study of whispering gallery modes thus requires the study of high-frequency scattering problems, that are usually modelled by the Helmholtz equation. In this paper, we propose a numerical method to detect the critical states associated with scattering resonances for heterogeneous Helmholtz problems with piecewise smooth refractive index. The developed software allows for an efficient computation of many (quasi-)resonances for spherical symmetric problems with varying coefficients.

Different numerical methods have been suggested in the literature for computing resonances in Helmholtz problems. Some of them rely on the perfectly matched layer technique [39, 32], while others are based on a Dirichlet-to-Neumann map [8, 7]. Further approaches are boundary integral methods [54, 49, 26] and Hardy space methods [28, 40]. All these methods have in common that the problem for resonances is formulated as a non-selfadjoint or nonlinear eigenvalue problem.

After discretization, the nonlinear eigenvalue problem can be reduced to the general form: given an holomorphic matrix function  $T: \Omega \rightarrow \mathbb{C}^{n \times n}$  on an open set  $\Omega \subset \mathbb{C}$ , find  $(u, k) \in \mathbb{C}^n \times \Omega$  with  $u \neq 0$  such that

$$T(k)u = 0. \tag{1}$$

This type of nonlinear matrix eigenvalue problems can be solved for instance using a Newton method [33] or a contour integration based method [9, 12, 54], among other methods. While Newton's method consists in solving a nonlinear equation (for instance  $\det(T(k)) = 0$ ), the contour integral method consists in finding all eigenvalues and eigenvectors inside a given contour in the complex plane by reducing the original nonlinear eigenvalue problem to a linear eigenvalue problem that has identical eigenvalues in the domain. It is well known that Newton-type methods are sensitive to the initial starting point and can thus miss some eigenvalues, moreover, different formulations of Newton-type methods may exhibit non-robust convergence behavior [30]. On the other hand, the contour integration method is free from fixed point iterations required in Newton's method; however, it relies on a considerable number of control parameters: the choice of the contour itself (the

\* (bouchra.bensiali@centrale-casablanca.ma), École Centrale Casablanca, Ville Verte, 27182 Bouskoura, Morocco

† (stas@math.uzh.ch), Institut für Mathematik, Universität Zürich, Winterthurerstr 190, CH-8057 Zürich, Switzerland

radius and midpoint if the contour is a circle), quadrature points for the approximation of the contour integral and thresholds for the singular value decomposition filtering. A comparison between the two methods thus requires an extensive analysis of numerical experiments to assess the robustness, accuracy and speed of convergence of each one of them; see the review papers of Voß [57], and Güttel and Tisseur [24], which contain a presentation of various Newton-type methods and contour integration methods for certain types of nonlinear eigenvalue problems.

In the physical community, whispering gallery modes are also studied numerically, e.g., for the applications mentioned earlier. Numerical codes are used for this purpose, based on Finite Difference Time Domain [25] or Finite Elements [17]. Another widely used physical approach is based on the coupled mode theory (CMT) [27, 20], but this method is limited to specific geometries and refractive indices where the modes can be explicitly computed. For complex systems or those with significant variations in material properties, alternative modeling approaches may be necessary to capture the full dynamics. For the computation of resonances associated with whispering gallery modes, it is also common in the physical literature to truncate the domain with non transparent boundary conditions [48]. Other recent works provide asymptotic expansion of WGM resonances at high polar frequency for cavities with radially varying optical index [10].

Next, we will sketch our new approach for spherical symmetric, heterogeneous Helmholtz problems with piecewise smooth refractive index. As the starting point we write the Helmholtz equation in spherical coordinates so that the equation for the radially dependent part becomes a Bessel-type ordinary differential equation with a transmission condition at the interface point. The solution is a linear combination of two linear independent solutions (fundamental system) in each of the two sub-intervals and the linearity of the problem allows us to express explicitly two of the four coefficients in their linear combinations by the boundary conditions. The remaining two coefficients are determined by the transmission conditions and are the solution of a  $2 \times 2$  system whose entries depend on the fundamental system and on the wavenumber. Since also the fundamental system depends on the wavenumber, the problem is highly non-linear. For varying refractive index the fundamental system as well as its dependence on the wavenumber is not known explicitly. To determine the resonances, i.e., the wavenumbers such that the determinant of the  $2 \times 2$  system is zero we propose a Newton method which takes into account the fact that, for changing wavenumber in the Newton iteration, also the corresponding fundamental systems have to be updated (numerically) along their derivatives with respect to the wavenumber. The resulting algorithm allows us to compute the WGM for varying refractive index to high accuracy for a large range of modes.

The paper is organized as follows. After presenting the problem setting, the formulation of the problem of resonances as a nonlinear eigenvalue problem is presented and analyzed using a system of fundamental solutions in Section 2. In Section 3, the Newton method is presented and the local convergence result under suitable assumptions. We investigate in Section 4 the simplicity of the roots, and in Section 5 the impact of scaling on the Newton algorithm. Finally, we present our final approach in Section 6 through targeted numerical experiments, before concluding remarks. By concentrating on Newton’s approach, this work provides a focused analysis that can serve as a basis for more extensive methodological benchmarks in future research.

## 2 Problem formulation

### 2.1 Polar coordinates and fundamental systems

We consider the following heterogeneous Helmholtz problem in a spherical symmetric setting in dimension  $d = 2$ :

$$\begin{cases} -\Delta u - (kn)^2 u = 0 & \text{in } \Omega := B_1^2 := \{x \in \mathbb{R}^2, |x| < 1\}, \\ \frac{\partial u}{\partial \nu} - T_{k\hat{n}(1)} u = g & \text{on } \gamma_1 := \partial\Omega, \end{cases} \quad (2)$$

where  $k \in \mathbb{C}^*$  (set of nonzero complex numbers) denotes the wavenumber, and  $n^2$  the refractive index. In the following we restrict to piecewise Lipschitz continuous coefficient  $n$  and formulate these equations as a transmission problem. We will need the sets  $\mathbb{C}_{\geq 0}^* := \{\zeta \in \mathbb{C}^* \mid \text{Im } \zeta \geq 0\}$  and  $\mathbb{C}_{< 0} := \{\zeta \in \mathbb{C}^* \mid \text{Im } \zeta < 0\}$ . Here  $\partial/\partial\nu$  is the (outward) normal derivative at  $\partial\Omega$ . Since we are interested in spherical symmetric problems we assume that the refractive index only varies in radial direction:  $n(x) = \hat{n}(|x|)$  for some univariate function  $\hat{n} \in L^\infty(\tau)$ ,  $\tau := ]0, 1[$ , which is piecewise smooth and positive. More precisely, we assume that there exists a *jump point*  $\xi \in ]0, 1[$  which divides  $\tau$  into the subintervals  $\tau_1 := ]0, \xi[$ ,  $\tau_2 := ]\xi, 1[$  and the domain into  $\Omega_j := \{x \in \mathbb{R}^2 \mid |x| \in \tau_j\}$ ,  $j \in \{1, 2\}$ . The interface is denoted by  $\gamma_\xi := \overline{\Omega_1} \cap \Omega_2$ . The exterior complement of  $\Omega$  is  $\Omega^+ := \mathbb{R}^2 \setminus \overline{\Omega}$ . We assume that there are positive constants  $n_{\min}$ ,  $n_{\max}$  such that the restrictions of  $\hat{n}$  to the subintervals  $\tau_1$ ,  $\tau_2$  satisfy

$$\begin{aligned} \hat{n}_j &:= \hat{n}|_{\tau_j} \in C^\infty(\tau_j) \\ 0 < n_{\min} &:= \inf_{r \in ]0, 1[} \hat{n}(r) \leq \sup_{r \in ]0, 1[} \hat{n}(r) =: n_{\max} < \infty. \end{aligned}$$

Finally we set  $n_j(x) := \hat{n}_j(|x|)$ . To express functions in polar coordinates  $x = r \begin{pmatrix} \cos \theta \\ \sin \theta \end{pmatrix}$  with  $r := |x|$  and  $\theta \in [-\pi, \pi[$  we use the “hat notation”:  $\hat{u}(r, \theta) := u \left( r \begin{pmatrix} \cos \theta \\ \sin \theta \end{pmatrix} \right)$ . If  $\hat{u}$  is independent of  $\theta$  we write short  $\hat{u}(r)$  for  $\hat{u}(r, \theta)$ . We consider

Dirichlet-to-Neumann boundary conditions, which are equivalent to an outgoing radiation condition (for  $g = 0$ ). We employ the definition of the Dirichlet-to-Neumann operator  $T_\kappa$  on the sphere  $\gamma_1$  by a series expansion. For  $\varphi \in H^{1/2}(\gamma_1)$  with Fourier expansion

$$\varphi(x, y) = \sum_{m \in \mathbb{Z}} \varphi_m e^{im\theta} \quad \text{for } (x, y) = (\cos \theta, \sin \theta) \in \gamma_1$$

the operator  $T_\kappa$  is given by

$$(T_\kappa \varphi)(x, y) = \sum_{m \in \mathbb{Z}} \kappa \frac{H'_m(\kappa)}{H_m(\kappa)} \varphi_m e^{im\theta}, \quad (3)$$

where  $H_m(r) := H_m^{(1)}(r)$  is the Hankel function of first kind and order  $m$  [41]. From [58, §15.7] it follows that the total number of zeros of  $H_m$  does not exceed  $m+1$  and all of them are located in  $\mathbb{C}_{<0}$ . In this way,  $\mathcal{Z} := \{z \in \mathbb{C} \mid \exists m \in \mathbb{Z} \ H_m(z) = 0\} \subset \mathbb{C}_{<0}$  is countable and we assume that  $k\hat{n}(1) \notin \mathcal{Z}$  in (2). It is shown, e.g., in [22] that the series in (3) defines a continuous mapping from  $H^{1/2}(\gamma_1) \rightarrow H^{-1/2}(\gamma_1)$  for all  $\kappa \in \mathbb{C}_{\geq 0}^*$ .

We consider the nonlinear PDE eigenvalue problem associated with (2)

$$\begin{cases} \text{Find } (k, u) \in \mathbb{C}^* \times (H^1(\Omega) \setminus \{0\}) \text{ such that} \\ -\Delta u = (kn)^2 u & \text{in } \Omega_1 \cup \Omega_2, \\ [u]_{\gamma_\varepsilon} = [\nabla u \cdot \nu]_{\gamma_\varepsilon} = 0, & \text{interface condition,} \\ \frac{\partial u}{\partial \nu} = T_{k\hat{n}(1)} u & \text{on } \gamma_1. \end{cases} \quad (4)$$

**Proposition 1.** *All solutions (resonances) of problem (4) satisfy  $k \in \mathbb{C}_{<0}$ .*

*Proof.* Assume by contradiction that there exists a non-trivial solution  $(k, u) \in \mathbb{C}_{\geq 0}^* \times H^1(\Omega) \setminus \{0\}$ . Then, the weak form of (4) reads

$$a(u, v) := (\nabla u, \nabla v)_{L^2(\Omega)} + k^2 (n^2 u, v)_{L^2(\Omega)} - (T_{k\hat{n}(1)} u, v)_{L^2(\partial\Omega)} = 0 \quad \forall v \in H^1(\Omega).$$

We choose  $v = \mu u$  with  $\mu = -ik/|k|$  and obtain for the real part

$$\begin{aligned} \operatorname{Re} a(u, \mu u) &= \frac{\operatorname{Im} k}{|k|} \left( \|\nabla u\|_{L^2(\Omega)}^2 + |k|^2 \|nu\|_{L^2(\Omega)}^2 \right) \\ &\quad - \operatorname{Re} \left( \bar{\mu} (T_{k\hat{n}(1)} u, u)_{L^2(\partial\Omega)} \right) = 0 \quad \forall u \in H^1(\Omega). \end{aligned}$$

Since  $\operatorname{Im} k \geq 0$  we get

$$0 = \operatorname{Re} a(u, \mu u) \geq -\operatorname{Re} \left( \bar{\mu} (T_{k\hat{n}(1)} u, u)_{L^2(\partial\Omega)} \right).$$

From [37, (3.4b,c)] and [22] we conclude that

$$-\operatorname{Re} \left( \bar{\mu} (T_{k\hat{n}(1)} u, u)_{L^2(\partial\Omega)} \right) \geq C (\operatorname{Im} k) \|u\|_{L^2(\partial\Omega)}^2 \quad \forall u \in H^{1/2}(\partial\Omega) \quad (5)$$

so that  $u|_{\partial\Omega} = 0$ . The homogeneous DtN boundary conditions on  $\partial\Omega$  in (4) then imply  $\partial u / \partial \nu = 0$  on  $\partial\Omega$ . For  $\operatorname{Im} k = 0$  we apply the unique continuation principle for piecewise Lipschitz continuous refractive index (see [31], [2] and, e.g., [21, Thm. 2.4]) and obtain  $u = 0$  which is a contradiction. For  $\operatorname{Im} k > 0$  we use (5) and conclude directly from

$$0 = \operatorname{Re} a(u, \mu u) \geq \frac{\operatorname{Im} k}{|k|} \left( \|\nabla u\|_{L^2(\Omega)}^2 + |k|^2 \|nu\|_{L^2(\Omega)}^2 \right)$$

that  $u = 0$  which again is a contradiction. □

Using polar coordinates, the solution and the boundary data can be expanded as a Fourier series via the ansatz

$$\begin{cases} u(x, y) = \hat{u}(r, \theta) = \sum_{m \in \mathbb{Z}} \hat{u}_m(r) e^{im\theta} \\ g(x, y) = \hat{g}(\theta) = \sum_{m \in \mathbb{Z}} \hat{g}_m e^{im\theta} \end{cases} \quad (6a)$$

which leads to a system of ODEs for the Fourier coefficients

$$\hat{u}_{j,m} := \hat{u}_m|_{\tau_j} \quad j \in \{1, 2\}. \quad (6b)$$

Let the differential operator  $L_{j,k}^m$  be given by

$$L_{j,k}^m v := -\frac{1}{r} (rv'(r))' + \left( \frac{m^2}{r^2} - (k\hat{n}_j(r))^2 \right) v(r) \quad \text{in } \tau_j$$

and the boundary operators by

$$B_{1,k}^m(0)v := \begin{cases} v(0) & \text{for odd } m, \\ v'(0) & \text{for even } m, \end{cases} \quad \text{and} \quad B_{2,k}^m(1)v := v'(1) - k\hat{n}_2(1) \frac{H'_m(k\hat{n}_2(1))}{H_m(k\hat{n}_2(1))} v(1),$$

where we again assume that  $k\hat{n}_2(1)$  does not belong to the set of zeros  $\mathcal{Z}$  (see [52] for the distinction between odd and even  $m$  for the boundary condition at 0). In this paper we investigate resonances which are caused by the jump of the refractive coefficient across the interface at  $\xi$ . Then, we consider the problem

$$\begin{cases} L_{j,k}^m \hat{u}_{j,m} = 0 & \text{in } \tau_j, \\ [\hat{u}_m]_\xi = [\hat{u}'_m]_\xi = 0 & \text{transmission condition,} \\ B_{2,k}^m(1)\hat{u}_{2,m} = \hat{g}_m & \text{DtN boundary conditions at 1,} \\ B_{1,k}^m(0)\hat{u}_{1,m} = 0 & \text{boundary condition at 0.} \end{cases} \quad (7)$$

*Remark 1.* The restriction to two-dimensional domains is only made to simplify the exposition. For general dimension, spherical coordinates can be used to transform (2) to a Bessel-type ordinary differential equation in analogy to (7), see, e.g., [52, §2.2].

In the next step we derive equations for a fundamental system of  $L_{j,k}^m$ . We define the functions  $f_{j,\ell,k}^m$ ,  $(j, \ell) \in \{(1, 1), (2, 1), (2, 2)\}$  as the solutions of

$$\begin{cases} L_{1,k}^m f_{1,1,k}^m = 0 & \text{in } \tau_1 \\ B_{1,k}^m(0) f_{1,1,k}^m = 0 \\ \left( f_{1,1,k}^m \right)'(\xi) - \beta_{1,k}^m(\xi) f_{1,1,k}^m(\xi) = h_{1,1,k}^m \neq 0 \end{cases} \quad (8)$$

$$\begin{cases} L_{2,k}^m f_{2,1,k}^m = 0 \\ - \left( f_{2,1,k}^m \right)'(\xi) - \beta_{2,k}^m(\xi) f_{2,1,k}^m(\xi) = 0 \\ \left( f_{2,1,k}^m \right)'(1) - \beta_{2,k}^m(1) f_{2,1,k}^m(1) = h_{2,1,k}^m \neq 0 \end{cases} \quad \text{in } \tau_2 \quad (9) \quad \begin{cases} L_{2,k}^m f_{2,2,k}^m = 0 \\ - \left( f_{2,2,k}^m \right)'(\xi) - \beta_{2,k}^m(\xi) f_{2,2,k}^m(\xi) = h_{2,2,k}^m \neq 0 \\ \left( f_{2,2,k}^m \right)'(1) - \beta_{2,k}^m(1) f_{2,2,k}^m(1) = 0 \end{cases} \quad \text{in } \tau_2 \quad (10)$$

for multipliers  $\beta_{j,k}^m(\xi) \in \mathbb{C}$  which are fixed later. They should be chosen such that a) problems (8)-(10) are well-posed and b) the dependence on the parameter  $k$  is smooth either on the whole  $\mathbb{C}^*$ , or on the half plane  $\mathbb{C}_{\geq 0}^*$ , or, more relevant in view of Proposition 1, on the half plane  $\mathbb{C}_{< 0}$ .

Let

$$\mathcal{J} := \{(1, \xi), (2, \xi), (2, 1)\}$$

and introduce for  $(j, x_0) \in \mathcal{J}$ , the operators

$$\mathfrak{R}_{j,k}(x_0)(\hat{u}_j) = \sum_{m \in \mathbb{Z}} \beta_{j,k}^m(x_0) \hat{u}_{j,m}(x_0) e^{im\theta}. \quad (11)$$

The coefficients  $h_{j,\ell,k}^m$  induce anti-linear forms via

$$\mathfrak{F}_{j,\ell,k}(v) := \begin{cases} \int_{\gamma_\xi} \mathfrak{h}_{1,1,k} \bar{v} & \text{for problem (8), i.e., } (j, \ell) = (1, 1) \\ \int_{\gamma_1} \mathfrak{h}_{2,1,k} \bar{v} & \text{for problem (9), i.e., } (j, \ell) = (2, 1) \\ \int_{\gamma_\xi} \mathfrak{h}_{2,2,k} \bar{v} & \text{for problem (10), i.e., } (j, \ell) = (2, 2) \end{cases} \quad \text{for } \mathfrak{h}_{j,\ell,k} := \sum_{m \in \mathbb{Z}} h_{j,\ell,k}^m e^{im\theta}. \quad (12)$$

**Assumption 2.** The coefficients  $\beta_{j,k}^m(\xi)$ ,  $\beta_{2,k}^m(1)$  are such that the resulting operators  $\mathfrak{R}_{j,k}(x_0) : H^{1/2}(\gamma_{x_0}) \rightarrow H^{-1/2}(\gamma_{x_0})$  in (11) are bounded linear operators.

The coefficients  $h_{j,\ell,k}^m$  are such that the resulting anti-linear forms  $\mathfrak{F}_{j,\ell,k} : H^{1/2}(\gamma_{x_0}) \rightarrow \mathbb{C}$  in (12) are bounded.

**Example 3.**

- The choice  $\beta_{j,k}^m(x_0) = ik\hat{n}_j(x_0)$  for all  $m \in \mathbb{Z}$  corresponds to Robin boundary conditions  $\mathfrak{R}_{j,k}(x_0)u = ik\hat{n}_j(x_0)u|_{\gamma_{x_0}}$  and
- the choice  $\beta_{j,k}^m(x_0) = -ik\hat{n}_j(x_0)$  to its flipped version  $\mathfrak{R}_{j,k}(x_0)u = -ik\hat{n}_j(x_0)u|_{\gamma_{x_0}}$ .
- The choice  $\beta_{2,k}^m(1) = k\hat{n}(1) \frac{(H_m^{(1)})'(k\hat{n}(1))}{H_m^{(1)}(k\hat{n}(1))}$  corresponds to the DtN operator:  $\mathfrak{R}_{2,k}(1)u = T_{k\hat{n}(1)}(u|_{\gamma_1})$ .

## 2.2 Well-posedness of ODEs for the fundamental system

Next, we will investigate the well-posedness of the problems (8)-(10). The idea is to switch back from the ODE in polar coordinates to an elliptic PDE on  $\Omega_j$ . We define the sesquilinear form  $a_j : H^1(\Omega_j) \times H^1(\Omega_j) \rightarrow \mathbb{C}$  by

$$a_j(u, v) := (\nabla u, \nabla v)_{\Omega_j} - k^2 (n^2 u, v)_{\Omega_j} - (\mathfrak{R}_{j,k}(\xi) u, v)_{\gamma_\xi} - \begin{cases} 0 & \text{for } j = 1, \\ (\mathfrak{R}_{j,k}(1) u, v)_{\gamma_1} & \text{for } j = 2, \end{cases}$$

where  $(\cdot, \cdot)_{\Omega_j}$  and  $(\cdot, \cdot)_{\gamma_x}$  denote the  $L^2(\Omega_j)$  and  $L^2(\gamma_x)$  scalar products. The problems (8)-(10) are then equivalent to

$$\begin{aligned} \text{find } f_{1,1,k} &\in H^1(\Omega_1) \text{ s. t. } a_1(f_{1,1,k}, v) = \mathfrak{F}_{1,1,k}(v) \quad \forall v \in H^1(\Omega_1), \\ \text{find } f_{2,1,k} &\in H^1(\Omega_2) \text{ s. t. } a_2(f_{2,1,k}, v) = \mathfrak{F}_{2,1,k}(v) \quad \forall v \in H^1(\Omega_2), \\ \text{find } f_{2,2,k} &\in H^1(\Omega_2) \text{ s. t. } a_2(f_{2,2,k}, v) = \mathfrak{F}_{2,2,k}(v) \quad \forall v \in H^1(\Omega_2). \end{aligned}$$

By choosing  $v = \mu u$  for  $\mu := -i k / |k|$  as a test function and considering the real part we obtain for  $j \in \{1, 2\}$ :

$$0 = \operatorname{Re} a_j(u, \mu u) = \frac{\operatorname{Im} k}{|k|} \left( \|\nabla u\|_{\Omega_j}^2 + |k|^2 \|n u\|_{\Omega_j}^2 \right) - \sum_{x:(j,x) \in \mathcal{J}} \operatorname{Re} \left( \bar{\mu} (\mathfrak{R}_{j,k}(x) u, u)_{\gamma_x} \right). \quad (13)$$

Note that

$$-\operatorname{Re} \left( \bar{\mu} (\mathfrak{R}_{j,k}(x) u, u)_{\gamma_x} \right) = \frac{\operatorname{Re} k \operatorname{Im} (\mathfrak{R}_{j,k}(x) u, u)_{\gamma_x} - \operatorname{Im} k \operatorname{Re} (\mathfrak{R}_{j,k}(x) u, u)_{\gamma_x}}{|k|}$$

for  $(j, x) \in \mathcal{J}$ .

**Lemma 4.** *Let Assumption 2 be satisfied.*

1. Assume that there exists a non-negative function  $\mu_{\mathbb{R}} : \mathbb{C}_{\geq 0}^* \rightarrow \mathbb{R}_{\geq 0}$  with  $\mu_{\mathbb{R}} : \mathbb{C}_{> 0} \rightarrow \mathbb{R}_{> 0}$  such that for all  $(j, x) \in \mathcal{J}$ ,  $k \in \mathbb{C}_{\geq 0}^*$ , and  $u \in H^{1/2}(\gamma_x) \setminus \{0\}$ :

$$-\operatorname{Re} (\mathfrak{R}_{j,k}(x) u, u)_{\gamma_x} \geq \mu_{\mathbb{R}}(k) \|u\|_{\gamma_x}^2, \quad \text{for } \operatorname{Im} k > 0, \quad (14)$$

$$(\operatorname{sign} \operatorname{Re} k) \operatorname{Im} (\mathfrak{R}_{j,k}(x) u, u)_{\gamma_x} > 0 \quad \text{for } \operatorname{Re} k \neq 0.$$

Then, problems (8)-(10) are well-posed for any  $k \in \mathbb{C}_{\geq 0}^*$ .

2. Assume that there exists a non-negative function  $\mu_{\mathbb{R}} : \mathbb{C}_{\leq 0}^* \rightarrow \mathbb{R}_{\geq 0}$  with  $\mu_{\mathbb{R}} : \mathbb{C}_{< 0} \rightarrow \mathbb{R}_{> 0}$  such that for all  $(j, x) \in \mathcal{J}$ ,  $k \in \mathbb{C}_{< 0}$  and  $u \in H^{1/2}(\gamma_x) \setminus \{0\}$

$$-\operatorname{Re} (\mathfrak{R}_{j,k}(x) u, u)_{\gamma_x} \geq \mu_{\mathbb{R}}(k) \|u\|_{\gamma_x}^2 \quad \text{for } \operatorname{Im} k < 0, \quad (15)$$

$$-(\operatorname{sign} \operatorname{Re} k) \operatorname{Im} (\mathfrak{R}_{j,k}(x) u, u)_{\gamma_x} > 0 \quad \text{for } \operatorname{Re} k \neq 0.$$

Then, problems (8)-(10) are well-posed for any  $k \in \mathbb{C}_{< 0}$ .

*Proof.* It follows, e.g., as in [18, Prop. 2.5] that the sesquilinear form  $a_j(\cdot, \cdot)$  is continuous in  $H^1(\Omega_j)$  and satisfies a Gårding inequality. The anti-linear forms  $\mathfrak{F}_{j,\ell,k}$  are continuous so that well-posedness can be concluded from Fredholm's alternative via uniqueness, i.e., from the implication

$$(a_j(u, v) = 0 \quad \forall v \in H^1(\Omega_j)) \implies (u = 0). \quad (16)$$

We start with some consideration of the boundary terms in  $a_j(\cdot, \cdot)$ .

**First case:** Let  $k \in \mathbb{C}_{\geq 0}^*$  and the corresponding conditions in the lemma be satisfied.

Then, for  $(j, x) \in \mathcal{J}$  it holds

$$-\operatorname{Re} \left( \bar{\mu} (\mathfrak{R}_{j,k}(x) u, u)_{\gamma_x} \right) \geq \frac{\operatorname{Re} k}{|k|} \operatorname{Im} (\mathfrak{R}_{j,k}(x) u, u)_{\gamma_x} + \mu_{\mathbb{R}}(k) \frac{\operatorname{Im} k}{|k|} \|u\|_{\gamma_x}^2,$$

where we recall  $\bar{\mu} = i \bar{k} / |k|$ . It follows from (14) that both summands are non-negative and we split the analysis into two cases:

1.  $\operatorname{Im} k > 0$ . Then

$$-\operatorname{Re} \left( \bar{\mu} (\mathfrak{R}_{j,k}(x) u, u)_{\gamma_x} \right) \geq \left( \mu_{\mathbb{R}}(k) \frac{\operatorname{Im} k}{|k|} \right) \|u\|_{\gamma_x}^2. \quad (17)$$

Since  $\operatorname{Im} k > 0$  we have  $\mu_{\mathbb{R}}(k) > 0$  so that the prefactor  $\left( \mu_{\mathbb{R}}(k) \frac{\operatorname{Im} k}{|k|} \right)$  in the right-hand side of (17) is positive.

2.  $\text{Im } k = 0$ . Since  $k \neq 0$ , we have  $\text{Re } k \neq 0$  and

$$-\text{Re} \left( \bar{\mu} (\mathfrak{R}_{j,k}(x) u, u)_{\gamma_x} \right) \geq \frac{|\text{Re } k|}{|k|} (\text{sign } \text{Re } k) \text{Im} (\mathfrak{R}_{j,k}(x) u, u)_{\gamma_x} > 0$$

for all  $H^{1/2}(\gamma_x) \setminus \{0\}$ . Hence, in both cases the implication

$$\left( \text{Re} \left( \bar{\mu} (\mathfrak{R}_{j,k}(x) u, u)_{\gamma_x} \right) = 0 \right) \implies \left( u|_{\gamma_x} = 0 \right) \quad (18)$$

follows.

**Second case:** Let  $k \in \mathbb{C}_{<0}$  and the corresponding conditions in the Lemma be satisfied.

In a similar way we obtain for  $k \in \mathbb{C}_{<0}$  the estimate

$$\begin{aligned} -\text{Re} \left( \bar{\mu} (\mathfrak{R}_{j,k}(x) u, u)_{\gamma_x} \right) &\leq \frac{\text{Re } k}{|k|} \text{Im} (\mathfrak{R}_{j,k}(x) u, u)_{\gamma_x} + \mu_{\text{R}}(k) \frac{\text{Im } k}{|k|} \|u\|_{\gamma_x}^2 \\ &\leq \left( \mu_{\text{R}}(k) \frac{\text{Im } k}{|k|} \right) \|u\|_{\gamma_x}^2. \end{aligned}$$

This time, the pre-factor  $\left( \mu_{\text{R}}(k) \frac{\text{Im } k}{|k|} \right)$  is negative yielding also in this case the implication

$$\left( \text{Re} \left( \bar{\mu} (\mathfrak{R}_{j,k}(x) u, u)_{\gamma_x} \right) = 0 \right) \implies \left( u|_{\gamma_x} = 0 \right). \quad (19)$$

We insert this into the left-hand side in (16) and use (13) to get

$$\begin{aligned} 0 = |\text{Re } a_j(u, \mu u)| &\geq \frac{|\text{Im } k|}{|k|} \left( \|\nabla u\|_{\Omega_j}^2 + |k|^2 \|nu\|_{\Omega_j}^2 \right) + \sum_{x:(j,x) \in \mathcal{J}} \left| \text{Re} \left( \bar{\mu} (\mathfrak{R}_{j,k}(x) u, u)_{\gamma_x} \right) \right| \\ &\geq \sum_{x:(j,x) \in \mathcal{J}} \left| \text{Re} \left( \bar{\mu} (\mathfrak{R}_{j,k}(x) u, u)_{\gamma_x} \right) \right|. \end{aligned}$$

Conditions (18) and (19) imply  $u|_{\partial\Omega_j} = 0$ . The (homogeneous) boundary conditions  $\partial u / \partial \nu - \mathfrak{R}_{j,k}(\xi)(u) = 0$  at  $\gamma_\xi$  for the strong formulation of the left-hand side in (16) yield  $\partial u / \partial \nu|_{\gamma_\xi} = 0$ . This, in combination with the unique continuation principle (see [2]) leads to  $u = 0$ .  $\square$

### Example 5.

- If  $\text{Im } k \geq 0$ , the boundary conditions  $\mathfrak{R}_{j,k}(x) u = i k \hat{n}_j(x) u$  satisfy (14) with  $\mu_{\text{R}} = |\text{Im } k| \hat{n}_j(x)$  and  $(\text{sign } \text{Re } k) \text{Im} (\mathfrak{R}_{j,k}(x) u, u)_{\gamma_x} = |\text{Re } k| \hat{n}_j(x) \|u\|_{\gamma_x}^2$  so that all conditions in (14) are satisfied.
- If  $\text{Im } k < 0$ , the boundary conditions  $\mathfrak{R}_{j,k}(x) u = -i k \hat{n}_j(x) u$  satisfy (15) with  $\mu_{\text{R}} = |\text{Im } k| \hat{n}_j(x)$  and  $-(\text{sign } \text{Re } k) \text{Im} (\mathfrak{R}_{j,k}(x) u, u)_{\gamma_x} = |\text{Re } k| \hat{n}_j(x) \|u\|_{\gamma_x}^2$ .
- If  $k \in \mathbb{C}_{\geq 0}^*$ , the boundary condition  $\mathfrak{R}_{2,k}(1) u = T_{k\hat{n}(1)} u$  satisfy (14) with  $\mu_{\text{R}}(k) = c > 0$  independent of  $k$ . This is proved in [22].

The choices of boundary conditions as in Examples 3.b and 5.b imply that the corresponding equations (8)-(10) have unique solutions  $f_{1,1,k}^m, f_{2,1,k}^m, f_{2,2,k}^m$  for  $k \in \mathbb{C}_{<0}$ . According to Proposition 1 all possible resonances of problem (4) belong to  $\mathbb{C}_{<0}$  and this choice of boundary conditions is justified. Any solution  $u$  in (4) with Fourier coefficients  $\hat{u}_{j,m}$  as in (6) then can be written in the form

$$\begin{aligned} \hat{u}_{1,m} &= A_{1,1}^m f_{1,1,k}^m \\ \hat{u}_{2,m} &= A_{2,1}^m f_{2,1,k}^m + A_{2,2}^m f_{2,2,k}^m \end{aligned} \quad (20)$$

and the conditions for the coefficients  $A_{1,1}^m, A_{2,1}^m, A_{2,2}^m$  are such that  $\hat{u}_{j,m}$  satisfy the two transmission conditions as well as the DtN boundary condition at  $\gamma_1$ :

$$\begin{bmatrix} f_{1,1,k}^m(\xi) & -f_{2,1,k}^m(\xi) & -f_{2,2,k}^m(\xi) \\ \left( f_{1,1,k}^m \right)'(\xi) & -\left( f_{2,1,k}^m \right)'(\xi) & -\left( f_{2,2,k}^m \right)'(\xi) \\ 0 & \left( f_{2,1,k}^m \right)'(1) - \beta_{2,k}^m(1) f_{2,1,k}^m(1) & \left( f_{2,2,k}^m \right)'(1) - \beta_{2,k}^m(1) f_{2,2,k}^m(1) \end{bmatrix} \begin{pmatrix} A_{1,1}^m \\ A_{2,1}^m \\ A_{2,2}^m \end{pmatrix} = 0 \quad (21)$$

with the Fourier multiplier corresponding to DtN boundary conditions

$$\beta_{2,k}^m(1) = k\hat{n}(1) \frac{\left(H_m^{(1)}\right)'(k\hat{n}(1))}{H_m^{(1)}(k\hat{n}(1))}. \quad (22)$$

We denote the  $3 \times 3$  matrix in (21) by  $T_+^m(k)$  and problem (4) is equivalent to find resonances  $k \in \mathbb{C}_{<0}$  such that  $\det T_+^m(k) = 0$ . In the following we will simplify the problem by imposing the following assumption, to ensure that the resonances of the non-linear eigenvalue problem (4) are not simultaneously critical frequencies for the auxiliary problems in (23).

**Assumption 6.** *Let  $(k, u) \in \mathbb{C}_{<0} \times H_0^1(\Omega) \setminus \{0\}$  be a resonance of problem (4) and  $m \in \mathbb{Z}$ . Then, there exists a complex neighborhood  $\omega_k \subset \mathbb{C}_{<0}$  of  $k$  such that the problems*

$$\left\{ \begin{array}{l} L_{1,k}^m f_{1,1,k}^m = 0 \quad \text{in } \tau_1 \\ B_{1,k}^m(0) f_{1,1,k}^m = 0 \\ \left(f_{1,1,k}^m\right)'(\xi) - ik\hat{n}_1(\xi) f_{1,1,k}^m(\xi) = h_{1,1,k}^m \neq 0 \end{array} \right\}, \quad \left\{ \begin{array}{l} L_{2,k}^m f_{2,2,k}^m = 0 \quad \text{in } \tau_2 \\ -\left(f_{2,2,k}^m\right)'(\xi) - ik\hat{n}_2(\xi) f_{2,2,k}^m(\xi) = h_{2,2,k}^m \neq 0, \\ \left(f_{2,2,k}^m\right)'(1) - \beta_{2,k}^m(1) f_{2,2,k}^m(1) = 0 \end{array} \right\} \quad (23)$$

for  $\beta_{2,k}^m(1)$  as in (22) have unique solutions.

This allows to reduce the non-linear eigenvalue problem (21) by using the ansatz

$$\hat{u}_{j,m} = A_j^m f_{j,j,k}^m \quad \forall j \in \{1, 2\}$$

and obtaining from the jump relations the condition

$$T^m(k)A = \begin{bmatrix} f_{1,1,k}^m(\xi) & -f_{2,2,k}^m(\xi) \\ \left(f_{1,1,k}^m\right)'(\xi) & -\left(f_{2,2,k}^m\right)'(\xi) \end{bmatrix} \begin{pmatrix} A_1^m \\ A_2^m \end{pmatrix} = 0, \quad (24)$$

thus the link to an algebraic nonlinear eigenvalue problem (S-Appendix B<sup>1</sup>). Going back to the system of ODEs (7), this is equivalent to finding  $k$  such that there exists a nontrivial solution  $\hat{u}_m$  of (7) for  $\hat{g}_m = 0$ , which is a nonlinear eigenvalue problem since the DtN boundary conditions depend in a nonlinear way on  $k$ . In turn, this is equivalent to finding scattering resonances  $k$  such that there exists a nontrivial solution  $u$  of (2) with  $g = 0$ ; [8]. In the spherical symmetric setting, we thus have reduced the nonlinear PDE eigenvalue problem (4) to an algebraic nonlinear eigenvalue problem (24).

Thus the condition for critical complex  $k$  (for which the equation (7) is not well-posed) is given by

$$\det(k) := \det(T(k)) = -[f_{1,1,k}(\xi) f_{2,2,k}'(\xi) - f_{1,1,k}'(\xi) f_{2,2,k}(\xi)] = 0, \quad (25)$$

where we skipped the superscript  $m$ .

### 2.3 Quasi-resonances

We will also be interested in quasi-resonances  $\underline{k} = \text{Re}(k) \neq 0$  where  $k$  is a resonance of problem (4). Since  $\underline{k}$  is real, problem (2) is well posed. Using similar reasoning as in the proof of Lemma 4 (see Examples 3.a- 5.a and Examples 3.c-5.c), we can show that the problems

$$\left\{ \begin{array}{l} L_{1,\underline{k}}^m f_{1,1,\underline{k}}^m = 0 \\ B_{1,\underline{k}}^m(0) f_{1,1,\underline{k}}^m = 0 \\ \left(f_{1,1,\underline{k}}^m\right)'(\xi) - i\underline{k}\hat{n}_1(\xi) f_{1,1,\underline{k}}^m(\xi) = h_{1,1,\underline{k}}^m \neq 0 \end{array} \right. \quad \text{in } \tau_1 \quad (26)$$

$$\left\{ \begin{array}{l} L_{2,\underline{k}}^m f_{2,1,\underline{k}}^m = 0 \\ -\left(f_{2,1,\underline{k}}^m\right)'(\xi) - i\underline{k}\hat{n}_2(\xi) f_{2,1,\underline{k}}^m(\xi) = 0 \\ \left(f_{2,1,\underline{k}}^m\right)'(1) - \beta_{2,\underline{k}}^m(1) f_{2,1,\underline{k}}^m(1) = \hat{g}_m \end{array} \right. \quad \text{in } \tau_2 \quad (27)$$

$$\left\{ \begin{array}{l} L_{2,\underline{k}}^m f_{2,2,\underline{k}}^m = 0 \\ -\left(f_{2,2,\underline{k}}^m\right)'(\xi) - i\underline{k}\hat{n}_2(\xi) f_{2,2,\underline{k}}^m(\xi) = h_{2,2,\underline{k}}^m \neq 0 \\ \left(f_{2,2,\underline{k}}^m\right)'(1) - \beta_{2,\underline{k}}^m(1) f_{2,2,\underline{k}}^m(1) = 0 \end{array} \right. \quad \text{in } \tau_2 \quad (28)$$

are well-posed for  $\beta_{2,\underline{k}}^m(1)$  as in (22).

<sup>1</sup>See Supplementary Material.

We thus can express the solution of (7) for a quasi-resonance  $\underline{k}$  in terms of local homogeneous solutions via the ansatz

$$\hat{u}_{1,m} = A_{1,1}^m f_{1,1,\underline{k}}^m \quad \text{and} \quad \hat{u}_{2,m} = f_{2,1,\underline{k}}^m + A_{2,2}^m f_{2,2,\underline{k}}^m, \quad (29)$$

and the transmission conditions lead to a linear system for the coefficients:

$$\begin{pmatrix} f_{1,1,\underline{k}}^m(\xi) & -f_{2,2,\underline{k}}^m(\xi) \\ (f_{1,1,\underline{k}}^m)'(\xi) & -(f_{2,2,\underline{k}}^m)'(\xi) \end{pmatrix} \begin{pmatrix} A_{1,1}^m \\ A_{2,2}^m \end{pmatrix} = \begin{pmatrix} f_{2,1,\underline{k}}^m(\xi) \\ (f_{2,1,\underline{k}}^m)'(\xi) \end{pmatrix}. \quad (30)$$

In this way, the function (29) with  $A_{1,1}^m$  and  $A_{2,2}^m$  chosen as in (30) solves the boundary value problem (7) for  $k \leftarrow \underline{k}$ .

For a resonance  $k$  very close to the real axis (i.e. with small imaginary part), we expect the matrix of the system (30) to be close to being singular and we refer to this case as a quasi-mode (see Section 6.5).

### 3 A Newton method for determining critical $k$ 's

For a compact formulation, we suppress the superscript  $m$  in the operators  $L_{j,k}^m$ , the functions  $f_{j,\ell,k}^m$ , and the data  $\beta_{2,k}^m(1)$  and  $h_{j,\ell,k}^m$ . We want to determine the zeros of  $\det(k)$  (25) in  $\mathbb{C}^*$  knowing only approximations of  $f_{1,1,k}$  and  $f_{2,2,k}$  given by an ODE solver (see Section 6.1 for details on the ODE solver). For this purpose, we formulate a Newton method. Since Newton's method requires the derivative of  $\det(k)$  with respect to  $k$ , we have to evaluate  $\partial_k f_{1,1,k}(\xi)$  and  $\partial_k f_{2,2,k}(\xi)$  along  $\partial_k f_{1,1,k}'(\xi)$  and  $\partial_k f_{2,2,k}'(\xi)$ . In order to avoid finite-difference approximation, we are going to establish the equations satisfied by  $\partial_k f_{1,1,k}$  and  $\partial_k f_{2,2,k}$  (see Proposition 7). Also, the choice of boundary conditions at  $r = \xi$  on  $f_{1,1,k}$  (8) and  $f_{2,2,k}$  (10) allows us to write

$$\begin{cases} f_{1,1,k}'(\xi) = ikn_1(\xi)f_{1,1,k}(\xi) + h_{1,1,k} \\ f_{2,2,k}'(\xi) = -ikn_2(\xi)f_{2,2,k}(\xi) - h_{2,2,k} \end{cases} \quad (31)$$

without additional approximation. For the sake of simplicity, and where there is no ambiguity, we will use the notations  $n_1$  and  $n_2$  instead of  $\hat{n}_1$  and  $\hat{n}_2$ .

The expressions of the determinant and its derivative are then given by

$$\begin{aligned} \det(k) &= -[f_{1,1,k}(\xi)(-ikn_2(\xi)f_{2,2,k}(\xi) - h_{2,2,k}) - (ikn_1(\xi)f_{1,1,k}(\xi) + h_{1,1,k})f_{2,2,k}(\xi)] \\ &= ik(n_2(\xi) + n_1(\xi))f_{1,1,k}(\xi)f_{2,2,k}(\xi) + h_{2,2,k}f_{1,1,k}(\xi) + h_{1,1,k}f_{2,2,k}(\xi) \end{aligned} \quad (32)$$

and

$$\begin{aligned} \partial_k \det(k) &= i(n_2(\xi) + n_1(\xi))(f_{1,1,k}(\xi)f_{2,2,k}(\xi) + k\partial_k f_{1,1,k}(\xi)f_{2,2,k}(\xi) + kf_{1,1,k}(\xi)\partial_k f_{2,2,k}(\xi)) \\ &\quad + h_{2,2,k}\partial_k f_{1,1,k}(\xi) + \partial_k h_{2,2,k}f_{1,1,k}(\xi) + h_{1,1,k}\partial_k f_{2,2,k}(\xi) + \partial_k h_{1,1,k}f_{2,2,k}(\xi). \end{aligned} \quad (33)$$

**Proposition 7.** *Let  $(\tilde{k}, \tilde{u}) \in \mathbb{C}_{<0} \times H^1(\Omega) \setminus \{0\}$  be a resonance pair of (4) and Assumption 6 be satisfied for some  $\omega_{\tilde{k}} \subset \mathbb{C}_{<0}$ . The equations satisfied by  $\partial_k f_{1,1,k}$  and  $\partial_k f_{2,2,k}$  are the following:*

$$\begin{cases} L_{1,k}(\partial_k f_{1,1,k}) = 2kn_1^2 f_{1,1,k} & \text{in } \tau_1 \\ B_{1,k}(0)(\partial_k f_{1,1,k}) = 0 & \text{Dirichlet or Neumann boundary conditions} \\ (\partial_k f_{1,1,k})'(\xi) - ikn_1(\xi)\partial_k f_{1,1,k}(\xi) = \partial_k h_{1,1,k} + in_1(\xi)f_{1,1,k}(\xi) & \text{Robin boundary conditions} \end{cases} \quad (34)$$

$$\begin{cases} L_{2,k}(\partial_k f_{2,2,k}) = 2kn_2^2 f_{2,2,k} & \text{in } \tau_2 \\ -(\partial_k f_{2,2,k})'(\xi) - ikn_2(\xi)\partial_k f_{2,2,k}(\xi) = \partial_k h_{2,2,k} + in_2(\xi)f_{2,2,k}(\xi) & \text{Robin boundary conditions} \\ (\partial_k f_{2,2,k})'(1) - \beta_{2,k}(1)\partial_k f_{2,2,k}(1) = (\partial_k \beta_{2,k}(1))f_{2,2,k}(1) & \text{DtN boundary conditions} \end{cases} \quad (35)$$

where  $\beta_{2,k}(1) = kn_2(1) \frac{H_m'(kn_2(1))}{H_m(kn_2(1))}$ .

These equations are well-posed in  $V = H^1(\tau_1)$  (even  $m$ ) or  $V = \{v \in H^1(\tau_1), v(0) = 0\}$  (odd  $m$ ), and  $H^1(\tau_2)$  respectively, for all  $k \in \omega_{\tilde{k}}$ .

*Proof.* These results can be established by switching back from spherical to Cartesian coordinates, and passing to the limit  $\varepsilon \rightarrow 0$  ( $\varepsilon \in \mathbb{C}^*$ ) in the equation satisfied by  $\frac{\tilde{f}_{k+\varepsilon} - \tilde{f}_k}{\varepsilon}$ , where for instance  $\tilde{f}_k(x) = f_{1,1,k}(r)e^{im\theta}$ , see [11, §3].  $\square$

### 3.1 Newton's algorithm

We use Newton's method for complex differentiable functions:

---

#### Algorithm 1 Newton's algorithm

---

Newton( $k_0, \varepsilon, l_{\max}$ )

**for**  $l = 0 \dots$  until stopping criterion is reached **do**

- Start with  $k = k_l$ ;
- Solve two two-point BVPs (23) exactly or numerically for  $k = k_l$ : result: approximations  $f_{1,1,k}$  and  $f_{2,2,k}$  to (23);
- Compute the derivatives with respect to  $k$ ,  $\partial_k f_{1,1,k}$  and  $\partial_k f_{2,2,k}$ , as the solutions of two two-point BVPs (34)-(35);
- Compute  $\det(k_l)$  by using (32) and  $\partial_k \det(k_l)$  by (33);
- Compute

$$k_{l+1} = k_l - \frac{\det(k_l)}{\partial_k \det(k_l)}; \quad (36)$$

- $l \leftarrow l + 1$ ;

The stopping criterion is given by  $\frac{|\det(k_l)|}{\|T(k_l)\|_F} \leq \varepsilon$  or when a maximal number of iterations  $l_{\max}$  is reached.

**end for**

---

We use a stopping criterion based on the relative residual  $\frac{|\det(k_l)|}{\|T(k_l)\|_F}$ , where  $\|\cdot\|_F$  is the Frobenius norm, as in [24].

*Remark 2.* We used the direct computation of the determinant since  $T$  is a  $2 \times 2$  matrix, but for larger matrices (as in the case of multiple jump points), it would be more pertinent to use the following formula, holding for  $k$  such that  $\det(k) \neq 0$ ,

$$\partial_k \det(k) = \det(k) \operatorname{trace}(T^{-1}(k) \partial_k T(k)), \quad (37)$$

leading to the *Newton-trace* iteration (see [24, Eq. (4.2)–(4.3)])

$$k_{l+1} = k_l - \frac{1}{\operatorname{trace}(T^{-1}(k_l) \partial_k T(k_l))}. \quad (38)$$

### 3.2 Starting values

Since we are interested in whispering gallery modes (WGM) which are associated with complex scattering resonances very close to the real axis, we will consider these different choices for the starting values of  $k$  in the Newton method:

- Trust region strategies [57, 61]:
  - Start from the real axis
  - Start from asymptotic expansions: in [10, 39], asymptotic expansion of WGM resonances when  $m \rightarrow \infty$  for cavities with radially varying optical index are proposed in some configurations. Even if our problem may differ from the one of [10], their asymptotics could represent a good first guess of the critical states in our case. For instance, considering the leading term in the asymptotics (S-Appendix C), a possible starting point is

$$k = \frac{m}{\xi n_0} \quad \text{where} \quad n_0 = \lim_{r \nearrow \xi} n(r). \quad (39)$$

- Homotopy methods [16]:
  - If Newton's method does not converge for a given refractive index and a given starting value  $k_0$ , it could be useful to first solve the problem for a piecewise constant refractive index case or an intermediate case close to  $n$  for which the algorithm converges, and then take the resulting  $k$  as a starting value for the initial problem.

### 3.3 Local convergence

We state here an important result of this paper, which deals with the local convergence of the suggested complex Newton method in Section 3.1, under suitable conditions. We assume here that  $\det(k)$  (32) and  $\partial_k \det(k)$  (33) are evaluated using the exact fundamental system for some  $k$ .

**Theorem 8.** *Let  $n: (0,1) \rightarrow \mathbb{R}_+^*$  be piecewise smooth (on  $(0,\xi)$  and  $(\xi,1)$ ) and bounded from above and below by positive numbers. Let  $k_\infty \in \mathbb{C}_{<0}$  be a resonance of (4) and Assumption 6 be satisfied for some  $\omega_{k_\infty} \subset \mathbb{C}_{<0}$ . Then  $\det: \omega_{k_\infty} \rightarrow \mathbb{C}$*

is analytic. If  $k_\infty \neq 0$  is a simple root of  $\det$  then there exists  $\delta > 0$  such that for any starting point  $k_0 \in B(k_\infty, \delta)$ , the sequence

$$k_{l+1} = k_l - \frac{\det(k_l)}{\partial_k \det(k_l)}$$

converges to  $k_\infty$  and the convergence is quadratic.

*Proof. Step 1:* Analyticity of  $\det$

Under the assumptions on  $n$ , we know from Assumption 6 that the solutions  $f_{1,1,k}$  and  $f_{2,2,k}$  exist and are unique in  $H^1(0, \xi)$  and  $H^1(\xi, 1)$  respectively for all  $k \in \omega_{k_\infty}$ . Thus  $\det$  in (32) is well defined as a function from  $\omega_{k_\infty}$  to  $\mathbb{C}$ .

We also established in Proposition 7 that  $\partial_k f_{1,1,k}$  and  $\partial_k f_{2,2,k}$  exist and are unique in  $H^1(0, \xi)$  and  $H^1(\xi, 1)$  respectively for all  $k \in \omega_{k_\infty}$ . Thus  $\det$  is complex-differentiable, and hence analytic in  $\omega_{k_\infty}$ .

**Step 2:** Convergence of the complex Newton method

Since  $\det$  is analytic, the local quadratic convergence of the complex Newton method to a simple root starting sufficiently close to the root follows classically [47, 3, 60].  $\square$

## 4 Simplicity of the roots

In order to apply Theorem 8 providing the local convergence of the Newton algorithm, it remains to show that the roots of  $\det$  (32) are simple.

### 4.1 Piecewise constant case

In the piecewise constant case, we have explicit expressions of  $f_{1,1,k}$  and  $f_{2,2,k}$  in terms of Bessel and Hankel functions, leading to an explicit expression of the determinant (25):

$$\det(k)/k = -[J_m(kn_1\xi)n_2H'_m(kn_2\xi) - n_1J'_m(kn_1\xi)H_m(kn_2\xi)] = D(k), \quad (40)$$

which is exactly Eq.(1.6) in [10] with  $n_2 = 1$ ,  $n_1 = n_0$  and  $\xi = R$  (see also [39, 38]). By forming  $K = kn_2\xi$  and  $N = \frac{n_1}{n_2}$  in (40),

$$D(k) = Nn_2J'_m(NK)H_m(K) - n_2J_m(NK)H'_m(K) = n_2\tilde{D}_N(K), \quad (41)$$

where

$$\tilde{D}_N(K) = NJ'_m(NK)H_m(K) - J_m(NK)H'_m(K). \quad (42)$$

Thus if  $n_1$  and  $n_2$  are given such that  $N > 1$  then we can recover the zeros  $k_0$  of  $D$  for a given  $\xi$  from the zeros  $K_0$  of  $\tilde{D}_N$  using  $k_0 = \frac{K_0}{n_2\xi}$ . Thus we are interested in the zeros of the following function of  $z$  (by replacing  $N \leftarrow n$  and  $K \leftarrow z$  in (42)):

$$D(z) = nJ'_m(nz)H_m(z) - J_m(nz)H'_m(z) \quad (43)$$

whose derivative with respect to  $z$  is given by

$$D'(z) = n^2J''_m(nz)H_m(z) - J_m(nz)H''_m(z). \quad (44)$$

**Theorem 9.** *Let  $D$  be as in (43) and  $n > 1$ . For  $m \geq 0$ , all roots of  $D$  except, possibly,  $z = 0$  are simple.*

*Proof.* We start by simplifying the expression of the derivative  $D'$  (44) to remove the second derivatives. We know that  $J_m$  and  $H_m$ , for  $m \in \mathbb{R}$ , are solutions of the Bessel differential equation

$$z^2y''(z) + zy'(z) + (z^2 - m^2)y(z) = 0, \quad (45)$$

i.e., for  $z \neq 0$ ,

$$y''(z) = -\frac{y'(z)}{z} - \left(1 - \frac{m^2}{z^2}\right)y(z). \quad (46)$$

Thus

$$\begin{aligned} D'(z) &= n^2 \left[ -\frac{J'_m(nz)}{nz} - \left(1 - \frac{m^2}{(nz)^2}\right)J_m(nz) \right] H_m(z) - J_m(nz) \left[ -\frac{H'_m(z)}{z} - \left(1 - \frac{m^2}{z^2}\right)H_m(z) \right] \\ &= -n \frac{J'_m(nz)}{z} H_m(z) - \left(n^2 - \frac{m^2}{z^2}\right) J_m(nz) H_m(z) + J_m(nz) \frac{H'_m(z)}{z} + \left(1 - \frac{m^2}{z^2}\right) J_m(nz) H_m(z) \\ &= -\frac{1}{z} \left[ nJ'_m(nz)H_m(z) - J_m(nz)H'_m(z) \right] - (n^2 - 1)J_m(nz)H_m(z) \\ &= -\frac{D(z)}{z} - (n^2 - 1)J_m(nz)H_m(z). \end{aligned} \quad (47)$$

If  $z_0 \neq 0$  is a zero of  $D(z)$  with multiplicity  $\geq 2$ , then we have  $D(z_0) = D'(z_0) = 0$ . Since  $n > 1$  and  $z_0 \neq 0$ , it follows from the differential equation (47) that  $z_0$  is also a zero of  $J_m(nz)H_m(z)$ . Since, for  $m \geq -1$ , the Bessel function  $J_m(z)$  has only real zeros [1][58, §15.25], and  $D(z) \neq 0$  for all  $z \in \mathbb{R} \setminus \{0\}$  (recall that resonances  $z \neq 0$  must satisfy  $\Im(z) < 0$ ), we obtain that  $z_0$  is a zero of  $H_m(z)$ . Using  $D(z_0) = H_m(z_0) = 0$  in (43), we get also  $H'_m(z_0) = 0$  (since  $J_m(nz_0) \neq 0$  for the same reasons stated earlier). Thus  $z_0$  is a multiple zero of  $H_m$ . But all zeros of  $H_m$ , except  $z = 0$ , are simple [58, §15.21] [55]. This is a contradiction.  $\square$

## 4.2 Piecewise smooth case

We prove here the geometric simplicity of eigenvalues (see definition in [57] and S-Appendix B) that is necessary for the roots to be simple. The study of the algebraic simplicity of eigenvalues (which is equivalent to the simplicity of the roots) is reported in [11, §5.1.2].

**Proposition 10.** *Let  $\lambda \in \mathbb{C}^*$  be an eigenvalue of the nonlinear eigenvalue problem (24) (under Assumption 6). Then  $\lambda$  is geometrically simple.*

*Proof.* Let  $\begin{pmatrix} x_1 \\ x_2 \end{pmatrix} \in \mathbb{C}^2 \setminus \{0\}$  be an eigenvector corresponding to the eigenvalue  $\lambda$ , i.e.,

$$f'_{1,1,\lambda}(\xi)f_{2,2,\lambda}(\xi) - f_{1,1,\lambda}(\xi)f'_{2,2,\lambda}(\xi) = 0 \quad (48)$$

and

$$\begin{cases} f_{1,1,\lambda}(\xi)x_1 - f_{2,2,\lambda}(\xi)x_2 = 0 \\ f'_{1,1,\lambda}(\xi)x_1 - f'_{2,2,\lambda}(\xi)x_2 = 0. \end{cases} \quad (49)$$

From  $f'_{1,1,\lambda}(\xi) - i\lambda n_1(\xi)f_{1,1,\lambda}(\xi) = h_{1,1,\lambda} \neq 0$  (8) (resp.  $-f'_{2,2,\lambda}(\xi) - i\lambda n_2(\xi)f_{2,2,\lambda}(\xi) = h_{2,2,\lambda} \neq 0$  (10)), we get that  $f_{1,1,\lambda}(\xi)$  and  $f'_{1,1,\lambda}(\xi)$  cannot vanish simultaneously (resp.  $f_{2,2,\lambda}(\xi)$  and  $f'_{2,2,\lambda}(\xi)$  cannot vanish simultaneously). Moreover, from (48),  $f_{1,1,\lambda}(\xi) = 0$  if and only if  $f_{2,2,\lambda}(\xi) = 0$  (resp.  $f'_{1,1,\lambda}(\xi) = 0$  if and only if  $f'_{2,2,\lambda}(\xi) = 0$ ). By using this in (49) we conclude that, there exists a nonzero complex constant  $C_\lambda \in \left\{ \frac{f_{2,2,\lambda}(\xi)}{f_{1,1,\lambda}(\xi)}, \frac{f'_{2,2,\lambda}(\xi)}{f'_{1,1,\lambda}(\xi)} \right\}$  such that

$$x_1 = C_\lambda x_2, \quad (50)$$

and any eigenvector corresponding to the same eigenvalue  $\lambda$  can be written  $x_2 \begin{pmatrix} C_\lambda \\ 1 \end{pmatrix}$  hence  $\dim(\ker(T(\lambda))) = 1$ , i.e., the eigenvalue  $\lambda$  is geometrically simple.  $\square$

*Remark 3.* One could also adapt the proof of the simplicity of eigenvalues for Sturm-Liouville problems [14, Thm. 11.2.3] [50, Thm. 2.4] to our case, and show the simplicity of eigenvalues for the ODE (7) with  $\hat{g}_m = 0$  and then deduce the geometric simplicity of the eigenvalues for the corresponding nonlinear eigenvalue problem.

## 5 A proper conditioning

The functions  $f_{1,1,k}$  and  $f_{2,2,k}$  in (23) depend on the choice of  $h_{1,1,k}$ ,  $h_{2,2,k}$  and have impact to the performance of the Newton method. Our concrete choice of these control parameters is motivated by the following consideration for piecewise constant refractive index. In this case, the unique solutions  $f_{1,1,k}$  and  $f_{2,2,k}$  of (23) (under Assumption 6) are given by  $r \mapsto J_m(kn_1 r)$  and  $r \mapsto H_m(kn_2 r)$  respectively, for a specific choice of  $h_{1,1,k}$  and  $h_{2,2,k}$  namely

$$\begin{cases} h_{1,1,k} = kn_1(\xi)J'_m(k\xi n_1(\xi)) - ikn_1(\xi)J_m(k\xi n_1(\xi)) = kn_1(\xi)[J'_m(k\xi n_1(\xi)) - iJ_m(k\xi n_1(\xi))] =: \frac{1}{c_{1,k}} \\ h_{2,2,k} = -kn_2(\xi)H'_m(k\xi n_2(\xi)) - ikn_2(\xi)H_m(k\xi n_2(\xi)) = -kn_2(\xi)[H'_m(k\xi n_2(\xi)) + iH_m(k\xi n_2(\xi))] =: \frac{1}{c_{2,k}}. \end{cases} \quad (51)$$

**Lemma 11.** *For all  $k \in \mathbb{C}_{>0}^*$  and all  $\xi \in ]0, 1[$ ,  $J'_m(k\xi n_1(\xi)) - iJ_m(k\xi n_1(\xi)) \neq 0$  and  $H'_m(k\xi n_2(\xi)) + iH_m(k\xi n_2(\xi)) \neq 0$ .*

*Proof.* Let  $k \in \mathbb{C}_{>0}^*$ . Following Lemma 4 (Examples 3.a-5.a), the function  $r \mapsto J_m(kn_1(\xi)r)$  is the unique solution of the differential equation

$$\begin{cases} -y''(r) - \frac{1}{r}y'(r) + \left(\frac{m^2}{r^2} - k^2 n_1^2(\xi)\right)y(r) = 0 & \text{in } (0, \xi) \\ y'(\xi) - ikn_1(\xi)y(\xi) = kn_1(\xi)J'_m(k\xi n_1(\xi)) - ikn_1(\xi)J_m(k\xi n_1(\xi)) & \text{Robin boundary conditions} \\ y(0) = 0 & \text{for odd } m \\ y'(0) = 0 & \text{for even } m. \end{cases} \quad (52)$$

If there exists  $k \in \mathbb{C}_{\geq 0}^*$  such that  $J'_m(k\xi n_1(\xi)) - iJ_m(k\xi n_1(\xi)) = 0$  then the solution  $r \mapsto J_m(kn_1(\xi)r)$  is identically zero. This is a contradiction.<sup>2</sup> For the result concerning  $H_m$ , we use a similar reasoning considering the unique solution of the differential equation

$$\begin{cases} -y''(r) - \frac{1}{r}y'(r) + \left(\frac{m^2}{r^2} - k^2n_2^2(\xi)\right)y(r) = 0 & \text{in } (\xi, 1) \\ -y'(\xi) - ikn_2(\xi)y(\xi) = -kn_2(\xi)H'_m(k\xi n_2(\xi)) - ikn_2(\xi)H_m(k\xi n_2(\xi)) & \text{Robin boundary conditions} \\ y'(1) - kn_2(\xi)\frac{H'_m(kn_2(\xi))}{H_m(kn_2(\xi))}y(1) = 0 & \text{DtN boundary conditions} \end{cases} \quad (53)$$

since  $H_m(kn_2(\xi)) \neq 0$  for  $k \in \mathbb{C}_{\geq 0}^*$  (for integer orders  $m$ , the zeros of the Hankel function of the first kind always have negative imaginary parts [1]).  $\square$

**Lemma 12.** *Let Assumption 6 be satisfied in the piecewise constant case, for a resonance  $(\tilde{k}, \tilde{u}) \in \mathbb{C}_{<0} \times H^1(\Omega) \setminus \{0\}$  of problem 4 and neighborhood  $\omega_{\tilde{k}}$  as in Assumption 6. Then, for any  $k \in \omega_{\tilde{k}}$ ,  $J'_m(k\xi n_1(\xi)) - iJ_m(k\xi n_1(\xi)) \neq 0$  and  $H'_m(k\xi n_2(\xi)) + iH_m(k\xi n_2(\xi)) \neq 0$ .*

*Proof.* Under Assumption 6, problems (23) are well posed for all  $k \in \omega_{\tilde{k}}$ . Using the same reasoning as in the proof of Lemma 11, it follows that for any  $k \in \omega_{\tilde{k}}$ ,  $J'_m(k\xi n_1(\xi)) - iJ_m(k\xi n_1(\xi)) \neq 0$  and  $H'_m(k\xi n_2(\xi)) + iH_m(k\xi n_2(\xi)) \neq 0$ , since the contrary leads to a contradiction.  $\square$

*Remark 4.* It follows that, in the piecewise constant case, the resonances of the auxiliary problems in (23) are respectively the zeros of  $\frac{1}{c_{1,k}}$  and the zeros of  $\frac{1}{c_{2,k}}$  (51).

For the simplest choice  $h_{1,1,k} = h_{2,2,k} = 1$ , it holds

$$\begin{cases} f_{1,1,k}(r) = c_{1,k}J_m(kn_1r) \\ f_{2,2,k}(r) = c_{2,k}H_m(kn_2r), \end{cases} \quad (54)$$

when the fundamental system (23) is well posed, and the Newton algorithm on this choice (leading to “det<sub>2</sub>”) could have a different behavior than the one (“det<sub>1</sub>”) in (40) as, even if

$$\det_2(k) = c_{1,k}c_{2,k}\det_1(k) = \alpha(k)\det_1(k) \quad (55)$$

for some function  $\alpha$  satisfying  $\alpha(k) \neq 0$  for all  $k \in \omega_{\tilde{k}}$  (Lemma 12)<sup>3</sup>, one has

$$\frac{\partial_k \det_2(k)}{\det_2(k)} = \frac{\partial_k c_{1,k}}{c_{1,k}} + \frac{\partial_k c_{2,k}}{c_{2,k}} + \frac{\partial_k \det_1(k)}{\det_1(k)} \neq \frac{\partial_k \det_1(k)}{\det_1(k)}, \quad (56)$$

so that different choices of  $h_{1,1,k}$  and  $h_{2,2,k}$  lead to different scalings of the fundamental solutions and hence to different scalings of the determinant, which in turn may affect the Newton algorithm.

Indeed, in our experiments, the use of det<sub>2</sub> may cause some roundoff problems as the ratio  $\frac{\partial_k \det_2(k)}{\det_2(k)}$  may be close to zero in contrast to  $\frac{\partial_k \det_1(k)}{\det_1(k)}$ , see Figure 14.

Another observation regarding the use of the Newton method with det<sub>2</sub> starting from the real axis is that, often, the first iterate has in our experiments a positive imaginary part which is not optimal knowing that the roots satisfy  $\Im(k) < 0$ . This is related to the sign of  $\Im\left(\frac{\det(k_0)}{\partial_k \det(k_0)}\right)$ : if it is positive then the first iterate has a negative imaginary part, otherwise it has a positive imaginary part. We plot this quantity  $\Im\left(\frac{\det(k_0)}{\partial_k \det(k_0)}\right)$  for  $k_0 \in \mathbb{R}_{>0}$  in Figure 2 for different choices of determinants: det<sub>1</sub> or det<sub>2</sub>, we also considered det<sub>scal</sub> corresponding to the scaling

$$\det_{\text{scal}}(k) = k^2 \det_2(k) \quad (57)$$

in order to investigate whether a simpler scaling than multiplying det<sub>2</sub> by  $\frac{1}{c_{1,k}c_{2,k}}$  would be suitable in practice.

As shown in Figure 2, the considered quantity is always positive for det<sub>1</sub> in contrast to det<sub>2</sub> which has an oscillatory behavior. It appears that the simpler scaling by  $k^2$  does not resolve the problem of negative imaginary parts on the real axis, and it seems that a scaling that is oscillatory with  $k$  is advantageous. For certain values of  $k_0$ , however, the quantity  $\frac{\det_2(k_0)}{\partial_k \det_2(k_0)}$  may be positive, and the Newton algorithm should work better for these initial starting points (tests performed for  $k_0 = 17$  or  $k_0 = 22$  for  $\xi = 0.5$ ,  $n_1 = 1.5$ ,  $n_2 = 1$  and  $m = 10$ ). For example, Figure S-2 and Table S-21 in S-Appendix A show the Newton iterations in the complex plane for two choices of the initial guess on the real axis, where one can observe either a convergence or a gross divergence using det<sub>2</sub>.

<sup>2</sup>Note that this reasoning (and adapted one to  $\mathbb{C}_{<0}$ ) also allows us to obtain another proof of the simplicity of the zeros of  $J_m$  that was used in the proof of Theorem 9.

<sup>3</sup>Note that the relation (55) holds when both det<sub>1</sub> and det<sub>2</sub> are defined, i.e. in the piecewise constant case for  $k \in \mathbb{C}_{\geq 0}^* \cup (\mathbb{C}_{<0} \setminus Z)$  where  $Z$  is the set of the zeros of  $\frac{1}{c_{1,k}}$  or  $\frac{1}{c_{2,k}}$  (Remark 4).

<sup>4</sup>The comparison should be considered only for  $k$  outside the set  $Z$  since the plotted det<sub>1</sub> is the exact one (40), while the constructed det<sub>1</sub> obtained solving  $f_{1,1,k}$  and  $f_{2,2,k}$  with  $h_{1,1,k} = \frac{1}{c_{1,k}}$  and  $h_{2,2,k} = \frac{1}{c_{2,k}}$  is also undefined for  $k \in Z$ .

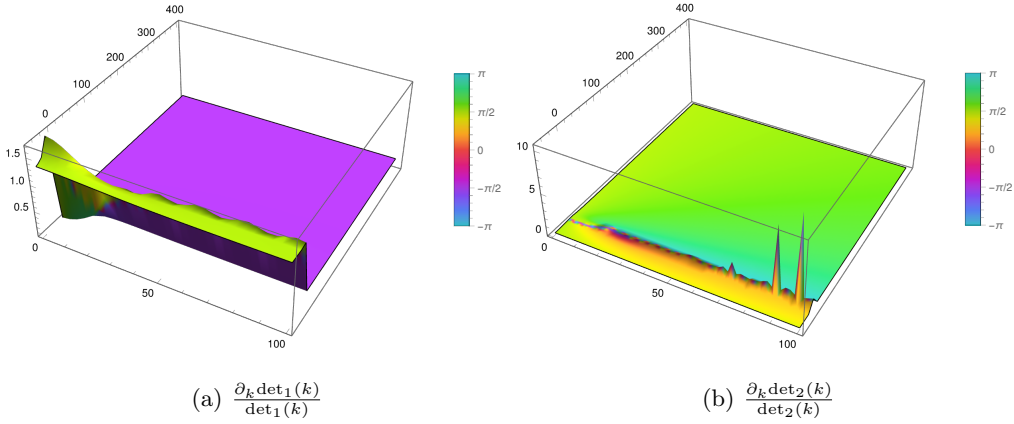


Figure 1: Comparison between  $\frac{\partial_k \det_2(k)}{\det_2(k)}$  and  $\frac{\partial_k \det_1(k)}{\det_1(k)}$  for  $\xi = 0.5$ ,  $n_1 = 1.5$ ,  $n_2 = 1$  and  $m = 10$ . Here  $k$  is varying over the complex rectangle with vertices  $-50i$  and  $100 + 400i$ .

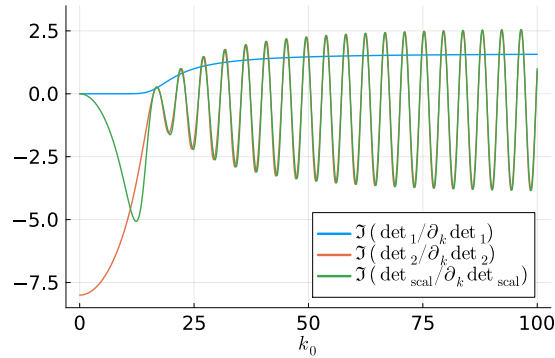


Figure 2: Plot of  $\Im\left(\frac{\det(k_0)}{\partial_k \det(k_0)}\right)$  on the real axis for  $\xi = 0.5$ ,  $n_1 = 1.5$ ,  $n_2 = 1$  and  $m = 10$ .

An important observation affecting the Newton method using the different scalings can be found in the plots (see Fig. 3) of  $\text{sign}\left(\Im\left(\frac{\partial_k \det(k)}{\det(k)}\right)\right)$  related to the phase of  $\frac{\partial_k \det(k)}{\det(k)}$  in the complex plane, extending the plot made on the real axis (Figure 2): one significant advantage of  $\det_1$  over the other scalings is that it could be observed in Figure 3d that the considered quantity is always negative for  $\Im(k) \geq 0$ , meaning that if a given iterate  $k_l$  in the Newton algorithm is such that  $\Im(k_l) \geq 0$ , then the next applications of the Newton algorithm will have a tendency to send it back to the region  $\Im(k) < 0$  where we are looking for zeros. The other scalings  $\det_2$  (Figure 3e) and  $\det_{\text{scal}}$  (Figure 3f) lack this property, which could explain why for some starting points on the real axis, the next iterates could have their imaginary part that keeps increasing in the region  $\Im(k) > 0$  (case of  $\det_2$  where a big region inside  $\Im(k) > 0$  has a wrong sign), or may have an oscillatory behavior in some sub-region  $0 < \Im(k) < \alpha$  where the plotted sign is not constant (case of both  $\det_2$  and  $\det_{\text{scal}}$ ).

Given that we intend to propose a Newton technique that starts on the real axis, we recommend to start the algorithm with a first iteration in the fourth quadrant, so that  $\Im(k_1) < 0$ . The insights gained from the piecewise constant case will be useful to ensure that the problem is scaled properly also in the variable case, where we recommend, by analogy, the use of the scaling (51) for the aforementioned benefits. For this purpose, we will need an additional assumption in the variable case:

**Assumption 13.** Let  $(\tilde{k}, \tilde{u}) \in \mathbb{C}_{<0} \times H_0^1(\Omega) \setminus \{0\}$  be a resonance of problem (4) and  $m \in \mathbb{Z}$ . Then, there exists a complex neighborhood  $\omega_{\tilde{k}} \subset \mathbb{C}_{<0}$  of  $\tilde{k}$  such that  $\frac{1}{c_{1,k}} \neq 0$  and  $\frac{1}{c_{2,k}} \neq 0$  for all  $k \in \omega_{\tilde{k}}$ .

In this way, it is assumed that the resonances of the non-linear eigenvalue problem (4) are not simultaneously zeros of  $\frac{1}{c_{1,k}}$  or  $\frac{1}{c_{2,k}}$ .<sup>5</sup>

<sup>5</sup>Note that these zeros coincide with the critical frequencies for the auxiliary problems in (23) in the piecewise constant case (Remark 4), thus the additional Assumption 13 is already included in Assumption 6 in this case, but these assumptions are in general different in the variable case.

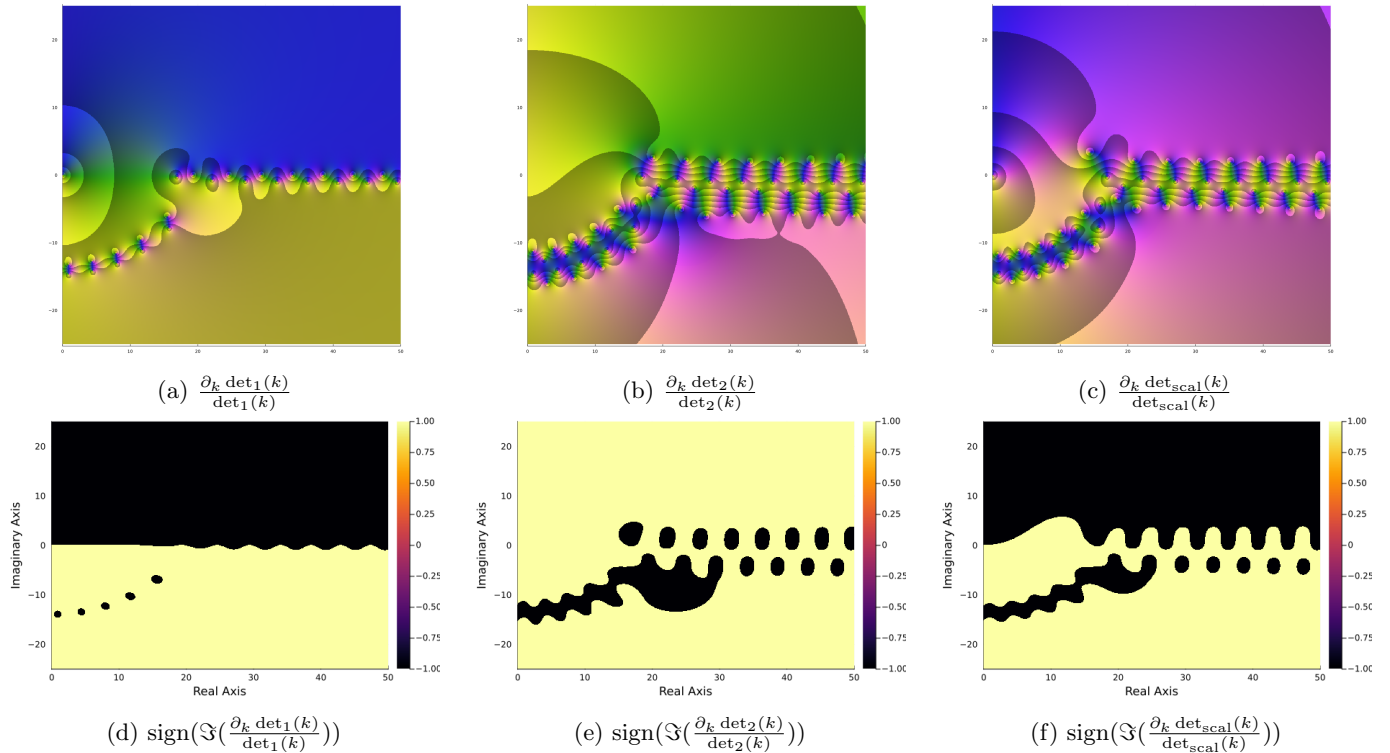


Figure 3: Complex plots of different scalings of  $\frac{\partial_k \det(k)}{\det(k)}$  for  $\xi = 0.5$ ,  $n_1 = 1.5$ ,  $n_2 = 1$  and  $m = 10$ .

## 6 Numerical experiments

### 6.1 BVP solver

In the variable case, the Newton method requires to solve the boundary value problems numerically for  $f_{1,1,k}$ ,  $f_{2,2,k}$ ,  $\partial_k f_{1,1,k}$  and  $\partial_k f_{2,2,k}$  to evaluate the determinant and its derivative. Hence, there is a need for reliable BVP solver of these two-point boundary value problems.

Since the problems posed in  $(0, \xi)$  and  $(\xi, 1)$  are Bessel-type equations, their numerical approximation can be challenging given the singularities in the equation and the oscillatory behavior of the solution. To circumvent these problems, we use spectral methods in order to achieve high accuracy approximation. This is based on the asymptotic expansion of the solution on a given basis and we adopt the `ApproxFun` package in Julia language [44, 46, 56, 45]. This appears to be more efficient and reliable for our application than using `NDSolve` of MATHEMATICA<sup>®</sup> and it is more suitable for numerical computations.

### 6.2 Newton method for variable refractive index

Based on the previous sections, we present here the full Newton algorithm to find (quasi-)resonances in the variable case. We specify in particular the choice of boundary conditions (BC), following §5, and starting values, following §3.2. The Newton algorithm we suggest is the following<sup>6</sup>

<sup>6</sup>A sample Julia code for this algorithm is available at <https://github.com/HankelGretel/WGM>.

---

**Algorithm 2** Newton’s algorithm for variable refractive index
 

---

 Newton\_var( $\xi, n_1(r)$  on  $(0, \xi), n_2(r)$  on  $(\xi, 1), m \in \mathbb{N}, \varepsilon, l_{\max}$ )

- Take the starting value:  $k_0 = \frac{m}{\xi n_1(\xi)}$ ;

**for**  $l = 0 \dots$  until stopping criterion is reached **do**

- Start with  $k = k_l$ ;
- Solve two two-point BVPs numerically for  $k = k_l$ : result: approximations  $f_{1,1,k}$  and  $f_{2,2,k}$  to (23) with the BC

$$\begin{cases} h_{1,1,k} := kn_1(\xi)(J'_m(k\xi n_1(\xi)) - iJ_m(k\xi n_1(\xi))) & \text{(assumed to be } \neq 0) \\ h_{2,2,k} := -kn_2(\xi)(H'_m(k\xi n_2(\xi)) + iH_m(k\xi n_2(\xi))) & \text{(assumed to be } \neq 0); \end{cases} \quad (58)$$

- Compute numerically the derivatives with respect to  $k$ ,  $\partial_k f_{1,1,k}$  and  $\partial_k f_{2,2,k}$ , as the solution of two two-point BVPs (34), (35);
- Compute  $\det(k_l)$  by using (32) and  $\partial_k \det(k_l)$  by (33);
- Compute

$$k_{l+1} = k_l - \frac{\det(k_l)}{\partial_k \det(k_l)}; \quad (59)$$

- $l \leftarrow l + 1$ ;

 The stopping criterion is given by  $\frac{\det(k_l)}{\|T(k_l)\|_F} \leq \varepsilon$  or when a maximal number of iterations  $l_{\max}$  is reached.

**end for**


---

### 6.3 Numerical setups

We fix without loss of generality  $\xi = 0.5$  and consider the following numerical setups, including piecewise constant cases, and non-constant cases for  $n_1$  of affine or parabolic types. We also consider a special variable  $n_1$  with explicit solution ( $n_1(r) = \sqrt{2 - r^2}$ ), corresponding to the Luneburg lens [13, 34, 35, 36] (see S-Appendix D). Finally, we consider a more general case, where  $n_1$  and  $n_2$  are both variable, making it outside of the scope of the theorems of [10] regarding the asymptotics for resonances. The different setups are summarized in Table 1 and the considered cases for variable  $n_1$  are illustrated in Figure 4.

$n_1(r)$	<b>1.5</b>	<b>5</b>	$2 - r$	$1.5 + r$	$1 + r$	$3(1 - r)$	$-2.8r + 2.5$	$1.5 + 6r(\xi - r)$	$1.5 - 6r(\xi - r)$	$3 - r(r + 1)$	$\sqrt{2 - r^2}$			
$n_2(r)$	<b>1</b>		1					1			<b>1</b>	$r + 0.5$	$1 + (r - 0.5)^3$	
Thm.	1.A		1.A		1.B		1.C		1.B		1.A		1.A	NA
Table	S-5	S-6	S-7	S-8	S-9	S-10	S-11 S-12 S-13	S-14		S-15 S-16	S-17	S-18	S-19	S-20

Table 1: Summary of the setups considered in the numerical experiments.

The results of the Newton algorithm are reported in the indicated Tables of the Supplementary Material. We also report on the tables the value  $k_{\text{asympt}}$  corresponding to the first terms of the asymptotics of  $k_0(m)$  up to  $O(m^{-1})$  for Thm. 1.A and Thm. 1.C, and up to  $O(m^{-\frac{1}{2}})$  for Thm. 1.B (S-Appendix C).

Our algorithm is first validated in cases where fundamental solutions are known explicitly (cases in bold in Table 1) by comparing the results obtained using the Newton method with **ApproxFun** and using the exact expression of the determinant in Tables S-1, S-2, S-3 and S-4. The results are very close (difference of order  $10^{-11} - 10^{-15}$ ), which validates our methodology and implementation.

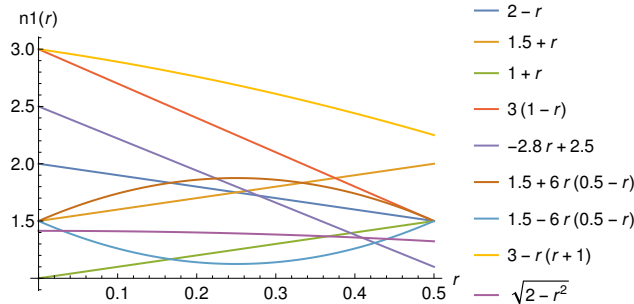


Figure 4: Different test cases in the non-constant case.

## 6.4 Interpretation of results

Based on the numerical experiments, the following observations can be made regarding the convergence of the Newton method presented in Section 6.2.

### Piecewise constant case:

- The Newton method converges for  $n_1 = 1.5$  and  $n_2 = 1$  (Table S-5), for all the considered  $m \leq 60$  in a number of iterations  $l \leq 10$ .
- In high-contrast media, e.g.  $n_1 = 5$  and  $n_2 = 1$  (Table S-6), the Newton method also converges for all the considered  $m \leq 60$  in a number of iterations  $l \leq 11$ . The use of the stopping criterion based on the relative residual  $\frac{\det(k)}{\|T(k)\|_F}$  is crucial in this context, as the computed determinant can be very large yet negligible compared to the magnitude of  $T$ . This allows us to remove the sensitivity of the Newton algorithm with respect to the jump in the refractive index  $n^2$  at the interface (low/high-contrast media).
- The obtained  $k$  is close to the corresponding theoretical asymptotic  $k_{\text{asympt}}$ , with a difference of order  $10^{-2}$  (low-contrast media) and  $10^{-4}$  (high-contrast media) for high values of  $m \geq 28$ .

### Variable case:

- The Newton method converges in all the considered cases using the same formula for the initial guess ( $\frac{m}{\xi n_1(\xi)}$ ), in a number of iterations  $l \leq 19$ .
- The Newton method also converges in the case with the highest contrast in the refractive index at the interface (see Figure 4 and corresponding Table S-17), when using the aforementioned stopping criterion, whereas it may fail (maximal number of iterations can be reached) if one uses the simplest stopping criterion  $|\det k| \leq \varepsilon$ , for the same reasons as in the piecewise constant case. We note that the imaginary part of the resonance in these cases approaches 0 (values of order  $10^{-12} - 10^{-17}$  for high values of  $m$ ).
- The considered example satisfying Thm. 1.C converges starting from  $k_0 = \frac{m}{\xi n_1(\xi)}$  (Table S-11) which is different from the leading term in the asymptotics in this case (which is  $\frac{m}{\xi_0 n_1(\xi_0)}$  with  $\xi_0 = \frac{25}{56} \approx 0.44$ , see S-Appendix C). A comparison with the results obtained starting from  $k_{\text{asympt}}$  (Table S-13) gives comparable results for large  $m$  that are also close to  $k_{\text{asympt}}$ . However, starting from the leading term  $\frac{m}{\xi_0 n_1(\xi_0)}$  (Table S-12) gives different results for the resonances, that are quite far from  $k_{\text{asympt}}$ . This shows a high sensitivity of the algorithm to the initial guess, especially in this case. In the other cases (Thm. 1.A or Thm. 1.B), the obtained resonances are close to  $k_{\text{asympt}}$  when starting from the leading term of the asymptotics ( $k_0 = \frac{m}{\xi n_1(\xi)}$  for these theorems), with a difference of orders ranging from  $10^{-1}$  to  $10^{-3}$  for high values of  $m$ , except in one case (Tables S-15 and S-16). This difference of behavior for Thm. 1.C may be linked to the fact that quasi-resonances are not of whispering gallery type in this case: the quasi-modes are strictly localized inside the cavity (around  $r = \xi_0 < \xi$ ) [10]. Nevertheless, this is a good point for our algorithm 2 where we specified the same initial guess independently of the verified theorem. This is particularly interesting when none of the theorems is valid (see next point).
- In the case of variable  $n_1$  and  $n_2$ , theoretical asymptotic expansions are not available. In the considered cases (Tables S-19 and S-20), taking  $n_2$  such that  $n_2(\xi) = 1$  and  $n_2'(\xi) = n_2''(\xi) = 0$  (Table S-20) gives results that are asymptotically close to the case  $n_2 = 1$  (Table S-18), while a different variable  $n_2$  satisfying only  $n_2(\xi) = 1$  (Table S-19) yields different results.

## 6.5 Quasi-resonance solutions and exact modes

After computing a resonance  $k^*$ , we can solve (30) for the quasi-resonance  $k = \underline{k} = \Re(k^*)$  and plot the solution  $\hat{u}_m(r)$  (29) and  $\Re[\hat{u}_m(r)e^{im\theta}]$  in Figure 6. We observe that they concentrate around the interface  $r = \xi$  as  $m$  gets large ( $\Im(k^*)$  gets closer to 0). In Figure 5, we represented the norm  $\|(T^m(k))^{-1}\|_2$  with respect to  $k$  for the different values of  $m$  considered: we observe spikes in this norm when  $k$  is a quasi-resonance, since the matrix is close to being singular in this case ( $\det(T^m(\underline{k})) \approx \det(T^m(k^*)) = 0$ ).

We also plot the exact modes for a given resonance  $k^*$ : they are given, up to a complex multiplicative constant by,

$$u(r) = \begin{cases} \frac{f_{1,1,k^*}(r)}{f_{1,1,k^*}(\xi)} & r \in (0, \xi) \\ \frac{f_{2,2,k^*}(r)}{f_{2,2,k^*}(\xi)} & r \in (\xi, 1) \end{cases} \quad \text{or} \quad u(r) = \begin{cases} \frac{f_{1,1,k^*}(r)}{f'_{1,1,k^*}(\xi)} & r \in (0, \xi) \\ \frac{f_{2,2,k^*}(r)}{f'_{2,2,k^*}(\xi)} & r \in (\xi, 1), \end{cases} \quad (60)$$

see Proposition 10. The exact modes are shown in Figure 7 for the Luneburg case (see Table S-18), exhibiting the same localization behavior at the interface for large  $m$  as the “quasi-modes” in Figure 6.

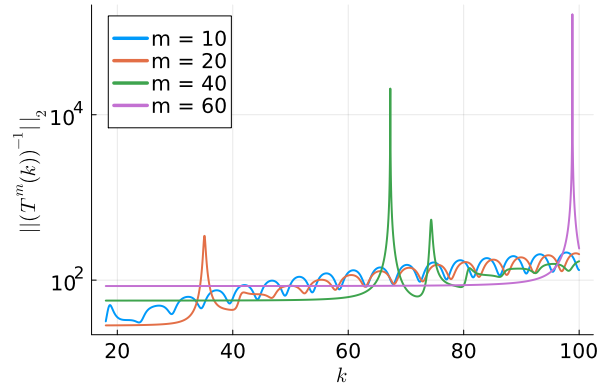
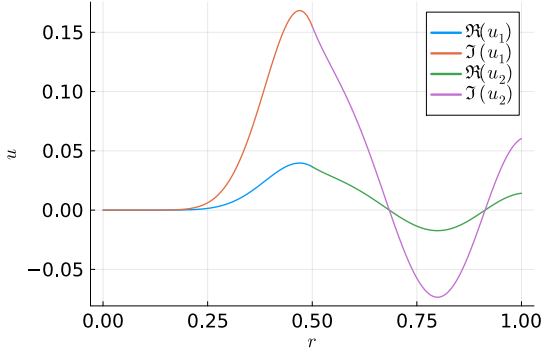


Figure 5: Plot of  $\|(T^m(k))^{-1}\|_2$  with respect to  $k$  for different values of  $m$ , in the Luneburg case  $n_1(r) = \sqrt{2 - r^2}$ ,  $n_2(r) = 1$  and  $\xi = 0.5$ . Here  $h_{1,1,k} = h_{2,2,k} = 1$ .

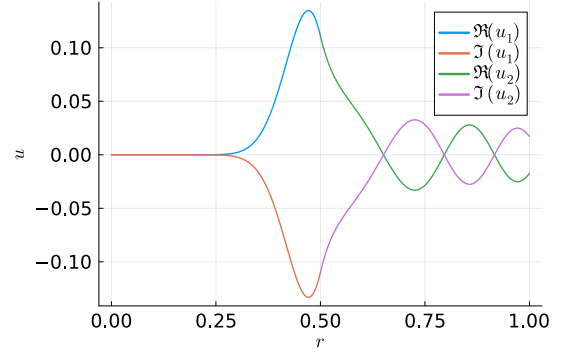
## 7 Conclusion and outlook

In this paper, we have considered the problem of computing quasi-resonances in spherical symmetric heterogeneous Helmholtz problems with piecewise smooth refractive index. We have developed a general approach based on the splitting of the problem into decoupled problems on each domain and one problem at the interface (skeleton). In the spherical symmetric setting, we have reduced the problem to one-dimensional Sturm-Liouville problems. Using fundamental solutions, the problem of resonances is expressed as a nonlinear eigenvalue problem  $T(k)x = 0$  involving the values of the fundamental solutions and their derivatives at the interface. We then developed a numerical approach using Newton's method to solve the nonlinear equation  $\det(T(k)) = 0$  where the fundamental solutions and their derivatives are approximated numerically at each iteration. In the piecewise constant case, we prove the simplicity of the roots, providing a local quadratic convergence of the algorithm. In the variable case, we have specified the initial guess based on known asymptotic expansions, and suggested a proper scaling for the fundamental system in analogy with the piecewise constant case. Various numerical experiments, investigating the convergence and comparing the results to explicit solutions or asymptotic expansions, validate the results and our methodology. Perspectives include comparing the Newton method with other approaches developed for nonlinear eigenvalue problems, such as the contour integral method [12, 9] or rational approximation [15, 51, 23], and investigating the extension of this method to more general settings following for instance [5, 6, 4]. It would also be interesting to consider a piecewise smooth refractive index with  $p$  jump points as in [52], for its potential relevance in physical applications (layered or stratified media) [13, 36].

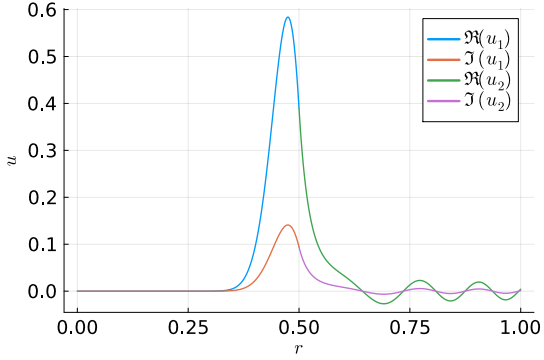
**Acknowledgements.** Part of the research was carried out while the first author was visiting the Institut für Mathematik at the University of Zürich as part of the CIMPA-ICTP Fellowship 2024 “Research in Pairs”. The first author thanks CIMPA and ICTP for the grant and the Institut für Mathematik for the hospitality. We thank Monique Dauge, Andrea Moiola and Zoïs Moitier for helpful discussions on WGM at the WAVES 2024 conference, and for pointing out the simplicity of eigenvalues for Sturm-Liouville problems.



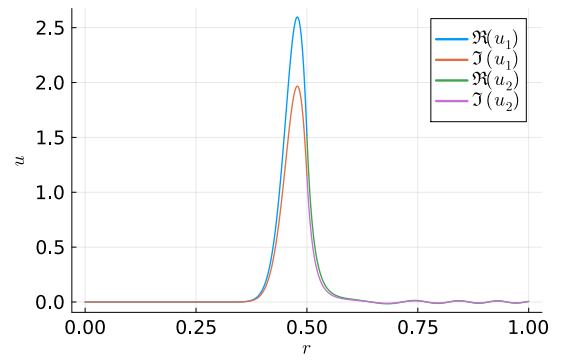
(a)  $m = 10, k = 18.588963438926466$



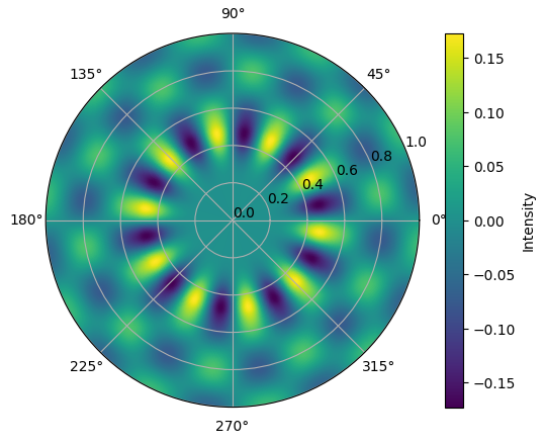
(b)  $m = 20, k = 35.09408648067281$



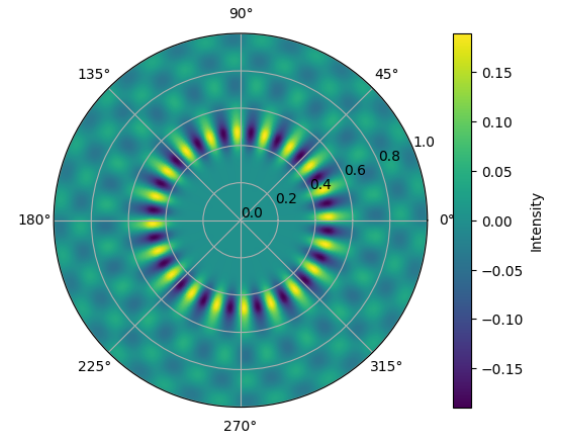
(c)  $m = 40, k = 67.28740148972052$



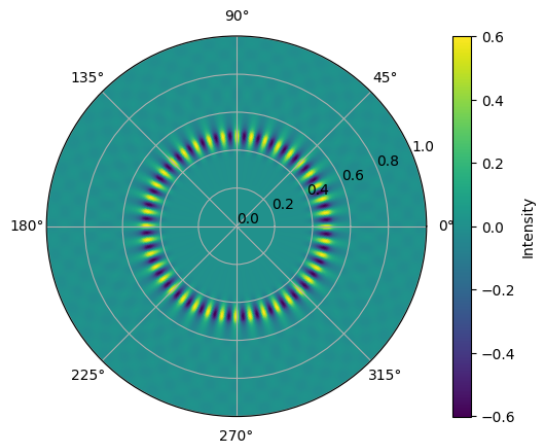
(d)  $m = 60, k = 98.82822050605951$



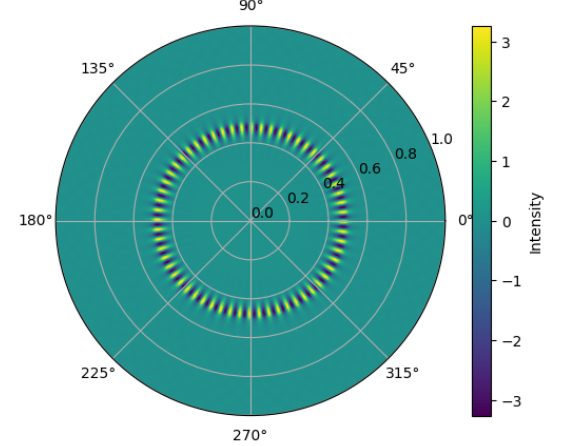
(e) Case (a)



(f) Case (b)

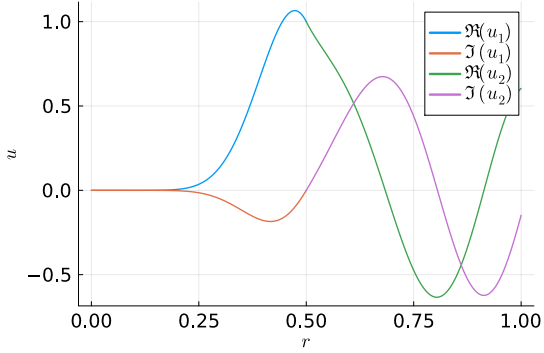


(g) Case (c)

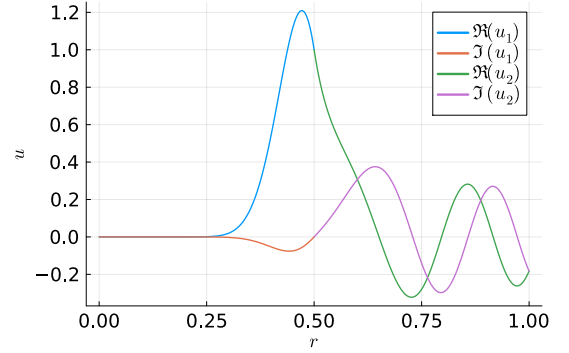


(h) case (d)

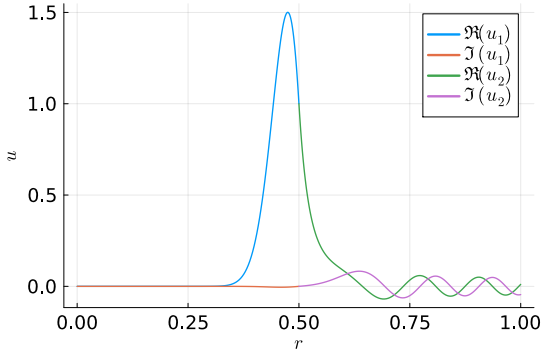
Figure 6: (a)-(d): Plots of  $\Re(\hat{u}_m(r))$  and  $\Im(\hat{u}_m(r))$ ; (e)-(h): Polar plots of  $\Re[\hat{u}_m(r)e^{im\theta}]$ , for  $\hat{u}_m(r)$  solution of (7) in the Luneburg case  $n_1(r) = \sqrt{2-r^2}$ ,  $n_2(r) = 1$  and  $\xi = 0.5$ , where  $k$  is a quasi-resonance (close to a resonance), see Table S-18. Here  $\hat{g}_m = 1$ .



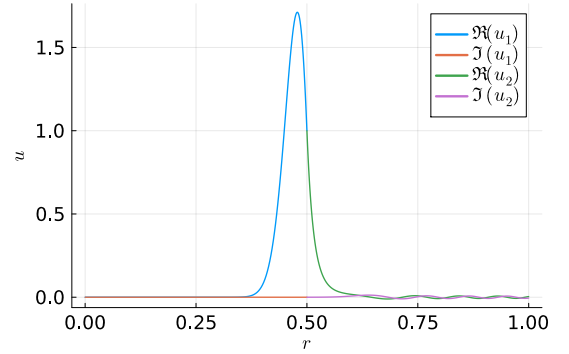
(a)  $m = 10$ ,  $k = 18.588963438926466 - 0.6154425735324377 i$



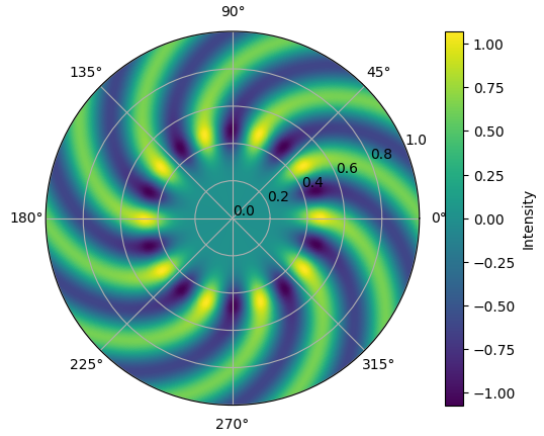
(b)  $m = 20$ ,  $k = 35.09408648067281 - 0.19327141118804717 i$



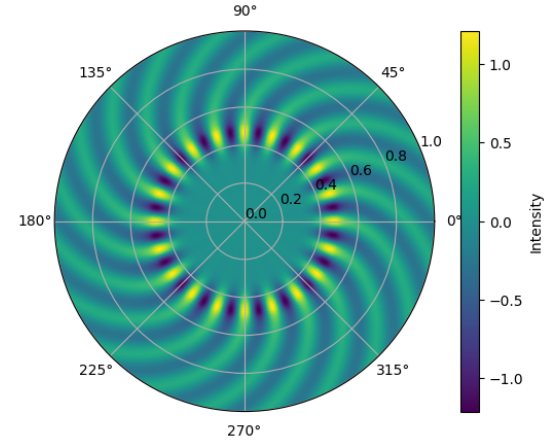
(c)  $m = 40$ ,  $k = 67.28740148972052 - 0.008096455718707863 i$



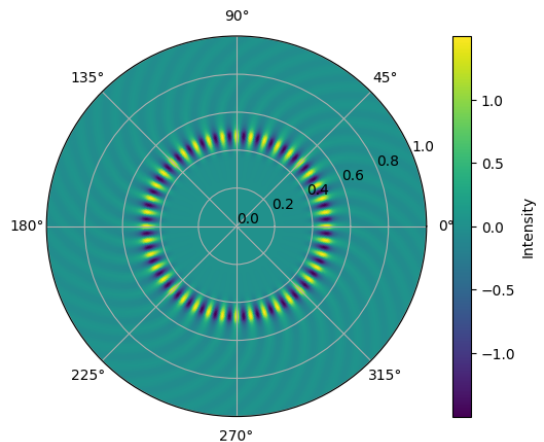
(d)  $m = 60$ ,  $k = 98.82822050605951 - 0.0001666858070041872 i$



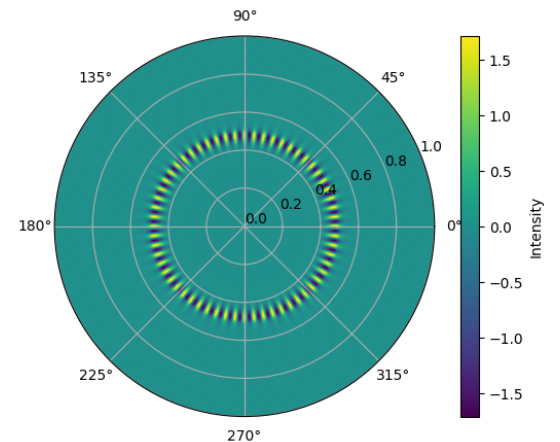
(e) Case (a)



(f) Case (b)



(g) Case (c)



(h) Case (d)

Figure 7: (a)-(d): Plots of  $\Re(\hat{u}_m(r))$  and  $\Im(\hat{u}_m(r))$ ; (e)-(h): Polar plots of  $\Re[\hat{u}_m(r)e^{im\theta}]$ , for the exact mode  $\hat{u}_m(r)$  (60) solution of (7) for  $\hat{g}_m = 0$ , where  $k$  is a resonance, in the Luneburg case  $n_1(r) = \sqrt{2 - r^2}$ ,  $n_2(r) = 1$  and  $\xi = 0.5$ , see Table S-18.

## References

- [1] M. Abramowitz and I. A. Stegun. *Handbook of mathematical functions with formulas, graphs, and mathematical tables*, volume 55. US Government printing office, 1968.
- [2] G. Alessandrini. Strong unique continuation for general elliptic equations in 2D. *J. Math. Anal. Appl.*, 386(2):669–676, 2012.
- [3] D. S. Alexander, F. Iavernaro, A. Rosa, et al. *Early days in complex dynamics: a history of complex dynamics in one variable during 1906-1942*. American Mathematical Society Providence, RI, USA, 2012.
- [4] C. Alves, A. Karageorghis, V. Leitão, and S. Valtchev. *Advances in Trefftz methods and their applications*. Springer, 2020.
- [5] C. J. Alves and P. R. Antunes. Numerical determination of the resonance frequencies and eigenmodes using the MFS. In *Computational Methods*, pages 1385–1389. Springer, 2006.
- [6] C. J. Alves and P. R. Antunes. Wave scattering problems in exterior domains with the method of fundamental solutions. *Numerische Mathematik*, 156(2):375–394, 2024.
- [7] J. C. Araujo-Cabarcas and C. Engström. On spurious solutions in finite element approximations of resonances in open systems. *Computers & Mathematics with Applications*, 74(10):2385–2402, 2017.
- [8] J. C. Araujo-Cabarcas, C. Engström, and E. Jarlebring. Efficient resonance computations for Helmholtz problems based on a Dirichlet-to-Neumann map. *Journal of Computational and Applied Mathematics*, 330:177–192, 2018.
- [9] J. Asakura, T. Sakurai, H. Tadano, T. Ikegami, and K. Kimura. A numerical method for nonlinear eigenvalue problems using contour integrals. *JSIAM Letters*, 1:52–55, 2009.
- [10] S. Balac, M. Dauge, and Z. Moitier. Asymptotics for 2D whispering gallery modes in optical micro-disks with radially varying index. *IMA Journal of Applied Mathematics*, 86(6):1212–1265, 2021.
- [11] B. Bensiali and S. A. Sauter. Computation of whispering gallery modes for spherical symmetric heterogeneous Helmholtz problems with piecewise smooth refractive index (extended version). Technical Report arXiv 2503.15765, 2025.
- [12] W.-J. Beyn. An integral method for solving nonlinear eigenvalue problems. *Linear Algebra and its Applications*, 436(10):3839–3863, 2012.
- [13] A. V. Boriskin and A. I. Nosich. Whispering-gallery and Luneburg-lens effects in a beam-fed circularly layered dielectric cylinder. *IEEE transactions on antennas and propagation*, 50(9):1245–1249, 2002.
- [14] W. E. Boyce and R. C. DiPrima. *Elementary differential equations*, volume 6. Wiley New York, 2012.
- [15] O. P. Bruno, M. A. Santana, and L. N. Trefethen. Evaluation of resonances via AAA rational approximation of randomly scalarized boundary integral resolvents. *arXiv preprint arXiv:2405.19582*, 2024.
- [16] E. Daya and M. Potier-Ferry. A numerical method for nonlinear eigenvalue problems application to vibrations of viscoelastic structures. *Computers & Structures*, 79(5):533–541, 2001.
- [17] S. Degtyarev, V. Podlipnov, P. Verma, and S. Khonina. 3d simulation of silicon micro-ring resonator with comsol. In *International Conference on Micro-and Nano-Electronics 2016*, volume 10224, pages 398–402. SPIE, 2016.
- [18] W. Dörfler and S. A. Sauter. A posteriori error estimation for highly indefinite Helmholtz problems. *Comput. Methods Appl. Math.*, 13(3):333–347, 2013.
- [19] B. R. Fabijonas, D. W. Lozier, and F. W. Olver. Computation of complex Airy functions and their zeros using asymptotics and the differential equation. *ACM Transactions on Mathematical Software (TOMS)*, 30(4):471–490, 2004.
- [20] E. F. Franchimon, K. R. Hiremath, R. Stoffer, and M. Hammer. Interaction of whispering gallery modes in integrated optical microring or microdisk circuits: hybrid coupled mode theory model. *JOSA B*, 30(4):1048–1057, 2013.
- [21] I. G. Graham and S. A. Sauter. Stability and finite element error analysis for the Helmholtz equation with variable coefficients. *Math. Comp.*, 89(321):105–138, 2020.
- [22] B. Gräßle and S. A. Sauter. Dirichlet-to-Neumann operator for the Helmholtz problem with general wavenumbers on the  $n$ -sphere. Technical Report arXiv:2503.18837, 2025.

- [23] S. Güttel, D. Kressner, and B. Vandereycken. Randomized sketching of nonlinear eigenvalue problems. *SIAM Journal on Scientific Computing*, 46(5):A3022–A3043, 2024.
- [24] S. Güttel and F. Tisseur. The nonlinear eigenvalue problem. *Acta Numerica*, 26:1–94, 2017.
- [25] S. Hagness, D. Rafizadeh, S. Ho, and A. Taflove. FDTD microcavity simulations: design and experimental realization of waveguide-coupled single-mode ring and whispering-gallery-mode disk resonators. *Journal of lightwave technology*, 15(11):2154–2165, 1997.
- [26] P. Heider. Computation of scattering resonances for dielectric resonators. *Computers & Mathematics with Applications*, 60(6):1620–1632, 2010.
- [27] K. Hiremath, R. Stoffer, and M. Hammer. Modeling of circular integrated optical microresonators by 2-d frequency domain coupled mode theory. *Optics communications*, 257(2):277–297, 2006.
- [28] T. Hohage and L. Nannen. Hardy space infinite elements for scattering and resonance problems. *SIAM Journal on Numerical Analysis*, 47(2):972–996, 2009.
- [29] V. S. Ilchenko and A. B. Matsko. Optical resonators with whispering-gallery modes-part II: applications. *IEEE Journal of selected topics in quantum electronics*, 12(1):15–32, 2006.
- [30] E. Jarlebring. Convergence factors of Newton methods for nonlinear eigenvalue problems. *Linear algebra and its applications*, 436(10):3943–3953, 2012.
- [31] D. Jerison and C. E. Kenig. Unique continuation and absence of positive eigenvalues for Schrödinger operators. *Ann. of Math. (2)*, 121(3):463–494, 1985.
- [32] S. Kim and J. Pasciak. The computation of resonances in open systems using a perfectly matched layer. *Mathematics of Computation*, 78(267):1375–1398, 2009.
- [33] D. Kressner. A block Newton method for nonlinear eigenvalue problems. *Numerische Mathematik*, 114:355–372, 2009.
- [34] J. A. Lock. Scattering of an electromagnetic plane wave by a Luneburg lens. I. Ray theory. *JOSA A*, 25(12):2971–2979, 2008.
- [35] J. A. Lock. Scattering of an electromagnetic plane wave by a Luneburg lens. II. Wave theory. *JOSA A*, 25(12):2980–2990, 2008.
- [36] J. A. Lock. Scattering of an electromagnetic plane wave by a Luneburg lens. III. Finely stratified sphere model. *JOSA A*, 25(12):2991–3000, 2008.
- [37] J. M. Melenk and S. A. Sauter. Convergence Analysis for Finite Element Discretizations of the Helmholtz equation with Dirichlet-to-Neumann boundary condition. *Math. Comp*, 79:1871–1914, 2010.
- [38] A. Moiola and E. A. Spence. Acoustic transmission problems: wavenumber-explicit bounds and resonance-free regions. *Mathematical Models and Methods in Applied Sciences*, 29(02):317–354, 2019.
- [39] Z. Moitier. *Étude mathématique et numérique des résonances dans une micro-cavité optique*. PhD thesis, Rennes 1, 2019.
- [40] L. Nannen, T. Hohage, A. Schädle, and J. Schöberl. Exact sequences of high order Hardy space infinite elements for exterior Maxwell problems. *SIAM Journal on Scientific Computing*, 35(2):A1024–A1048, 2013.
- [41] J.-C. Nédélec. *Acoustic and electromagnetic equations: integral representations for harmonic problems*, volume 144. Springer, 2001.
- [42] A. Neumaier. Residual inverse iteration for the nonlinear eigenvalue problem. *SIAM Journal on Numerical Analysis*, 22(5):914–923, 1985.
- [43] F. Olver, A. O. Daalhuis, D. Lozier, B. Schneider, R. Boisvert, C. Clark, B. Miller, B. Saunders, H. Cohl, and M. McClain. *NIST Digital Library of Mathematical Functions*. Release 2016. <http://dlmf.nist.gov/>.
- [44] S. Olver, G. Goretkin, R. M. Slevinsky, A. Townsend, and other contributors. ApproxFun.jl. <https://github.com/JuliaApproximation/ApproxFun.jl>, 2013–2015.
- [45] S. Olver and A. Townsend. A fast and well-conditioned spectral method. *SIAM Review*, 55(3):462–489, 2013.

- [46] S. Olver and A. Townsend. A practical framework for infinite-dimensional linear algebra. In *Proceedings of the 1st Workshop for High Performance Technical Computing in Dynamic Languages – HPTCDL ‘14*. IEEE, 2014.
- [47] A. M. Ostrowski. *Solution of equations in Euclidean and Banach spaces*. Academic Press, New York, 1973.
- [48] M. Oxborrow. Traceable 2-d finite-element simulation of the whispering-gallery modes of axisymmetric electromagnetic resonators. *IEEE Transactions on Microwave Theory and Techniques*, 55(6):1209–1218, 2007.
- [49] O. Poisson. Étude numérique des pôles de résonance associés à la diffraction d’ondes acoustiques et élastiques par un obstacle en dimension 2. *ESAIM: Mathematical Modelling and Numerical Analysis*, 29(7):819–855, 1995.
- [50] J. D. Pryce. *Numerical solution of Sturm-Liouville problems*. Oxford University Press, 1993.
- [51] M. A. Santana, L. N. Trefethen, and O. P. Bruno. Computation of Cavity Resonances via AAA Rational Approximation of Randomly Scalarized Boundary Integral Resolvents. In *Book of Abstracts, The 16th International Conference on Mathematical and Numerical Aspects of Wave Propagation (WAVES 2024)*. Edmond, 2024.
- [52] S. Sauter and C. Torres. The heterogeneous Helmholtz problem with spherical symmetry: Green’s operator and stability estimates. *Asymptotic Analysis*, 125(3-4):289–325, 2021.
- [53] K. Schreiber. *Nonlinear eigenvalue problems: Newton-type methods and nonlinear Rayleigh functionals*. PhD thesis, TU Berlin, Germany, 2008.
- [54] O. Steinbach and G. Unger. Combined boundary integral equations for acoustic scattering-resonance problems. *Mathematical Methods in the Applied Sciences*, 40(5):1516–1530, 2017.
- [55] C. Sturm. *Mémoire sur les équations différentielles linéaires du second ordre*. Springer, 2009.
- [56] A. Townsend and S. Olver. The automatic solution of partial differential equations using a global spectral method. *Journal of Computational Physics*, 299:106–123, 2015.
- [57] H. Voss. Nonlinear eigenvalue problems. *Handbook of Linear Algebra*, 164, 2013.
- [58] G. N. Watson. *A Treatise on the Theory of Bessel Functions*. Cambridge University Press, 1966.
- [59] E. T. Whittaker and G. N. Watson. *A course of modern analysis: an introduction to the general theory of infinite processes and of analytic functions; with an account of the principal transcendental functions*. University press, 1920.
- [60] J. H. Wilkinson. *The algebraic eigenvalue problem*. Oxford University Press, Inc., 1988.
- [61] C. Yang, J. C. Meza, and L.-W. Wang. A trust region direct constrained minimization algorithm for the Kohn–Sham equation. *SIAM Journal on Scientific Computing*, 29(5):1854–1875, 2007.

# Supplementary Material: Computation of whispering gallery modes for spherical symmetric, heterogeneous Helmholtz problems with piecewise smooth refractive index

Bouchra Bensiali and Stefan Sauter

## Note

This document provides the detailed results of the numerical experiments performed using Algorithm 2 (Newton’s algorithm for variable refractive index). We also include some appendices providing supporting information. We recall that  $k_0$  is the initial guess and  $k_{\text{asymppt}}$  corresponds to the first terms of the asymptotics of  $\underline{k}_0(m)$  up to  $O(m^{-1})$  for Thm. 1.A and Thm. 1.C, and up to  $O(m^{-\frac{1}{2}})$  for Thm. 1.B (see S-Appendix C).

## Contents

<b>S1 Piecewise constant case validation</b>	<b>S-2</b>
<b>S2 Variable case validation: A special variable case with explicit solution (Luneburg lens)</b>	<b>S-5</b>
<b>S3 Piecewise constant cases</b>	<b>S-7</b>
S3.1 Low-contrast media . . . . .	S-7
S3.2 High-contrast media . . . . .	S-8
<b>S4 Variable cases</b>	<b>S-9</b>
S4.1 $n_1$ variable and $n_2 = 1$ . . . . .	S-9
S4.2 $n_1$ and $n_2$ variable . . . . .	S-21
<b>S-Appendix A Additional figures</b>	<b>S-23</b>
<b>S-Appendix B Basic properties of nonlinear eigenvalue problems [57]</b>	<b>S-24</b>
<b>S-Appendix C Asymptotic expansions of quasi-resonances in dimension 2 [10]</b>	<b>S-24</b>
<b>S-Appendix D Special variable <math>n</math> with explicit solution (Luneburg lens)</b>	<b>S-25</b>

# S1 Piecewise constant case validation

$k_0$	$l$	$k$	$ D(k) $	$ \partial_k D(k) $	Difference in $k$
1	10	16.92320186058385 - 0.23954559046213897im	8.43e-11	1.19e-01	2.86e-14
	10	16.923201860583823 - 0.23954559046216217im	8.43e-11	1.19e-01	
2	9	16.923201860607477 - 0.239545590346429im	7.06e-11	1.19e-01	1.16e-13
	9	16.923201860607584 - 0.23954559034648804im	7.06e-11	1.19e-01	
3	8	16.923201958814623 - 0.23954567846387156im	1.58e-08	1.19e-01	2.73e-13
	8	16.92320195881486 - 0.2395456784639192im	1.58e-08	1.19e-01	
4	8	16.923201860703298 - 0.2395455900407501im	3.34e-11	1.19e-01	1.26e-13
	8	16.923201860703177 - 0.23954559004071005im	3.34e-11	1.19e-01	
5	7	16.92320302561573 - 0.23954583736498444im	1.42e-07	1.19e-01	6.36e-15
	7	16.923203025615667 - 0.2395458373649745im	1.42e-07	1.19e-01	
6	7	16.923201876723557 - 0.2395456186602138im	3.93e-09	1.19e-01	1.83e-13
	7	16.923201876723734 - 0.23954561866023547im	3.93e-09	1.19e-01	
7	7	16.9232018606048 - 0.23954559035873113im	7.21e-11	1.19e-01	2.07e-14
	7	16.923201860604816 - 0.23954559035875164im	7.21e-11	1.19e-01	
8	6	16.92320662364213 - 0.23954499539025922im	5.73e-07	1.19e-01	1.10e-13
	6	16.923206623642024 - 0.23954499539021604im	5.73e-07	1.19e-01	
9	6	16.923202147984654 - 0.2395457528343357im	3.94e-08	1.19e-01	4.70e-15
	6	16.923202147984608 - 0.2395457528343282im	3.94e-08	1.19e-01	
10	6	16.923201864447833 - 0.2395456022787395im	1.55e-09	1.19e-01	1.79e-13
	6	16.92320186444801 - 0.2395456022787569im	1.55e-09	1.19e-01	
11	6	16.923201860726405 - 0.2395455899902375im	2.69e-11	1.19e-01	1.54e-13
	6	16.923201860726255 - 0.23954558999018935im	2.69e-11	1.19e-01	
12	5	16.92320391421663 - 0.2395457509419893im	2.46e-07	1.19e-01	4.91e-14
	5	16.923203914216863 - 0.23954575094203084im	2.46e-07	1.19e-01	
13	5	16.92320189408275 - 0.23954563529149417im	6.72e-09	1.19e-01	2.25e-14
	5	16.923201894082876 - 0.2395456352915151im	6.72e-09	1.19e-01	
14	5	16.92320186069578 - 0.2395455900546274im	3.52e-11	1.19e-01	3.42e-14
	5	16.92320186069587 - 0.2395455900546616im	3.52e-11	1.19e-01	
15	4	16.92320227549268 - 0.2395457990936466im	5.54e-08	1.19e-01	2.29e-15
	4	16.923202275492653 - 0.23954579909366866im	5.54e-08	1.19e-01	
16	4	16.923201860781877 - 0.2395455898294696im	1.07e-11	1.19e-01	4.43e-14
	4	16.92320186078177 - 0.2395455898294269im	1.06e-11	1.19e-01	
17	3	16.923201862834166 - 0.23954559087875893im	2.67e-10	1.19e-01	1.16e-14
	3	16.923201862834055 - 0.23954559087876123im	2.67e-10	1.19e-01	
18	4	16.923200862599433 - 0.2395464356945639im	1.56e-07	1.19e-01	1.20e-14
	4	16.923200862599412 - 0.23954643569455172im	1.56e-07	1.19e-01	
19	1000	-16.717608272660037+ 0.7591717411433029im	1.24e-01	1.30e-01	1.07e-13
	1000	-16.717608272660062 + 0.7591717411434057im	1.24e-01	1.30e-01	
20	6	22.119804063752024 - 0.7063456283412871im	3.82e-09	6.03e-02	6.21e-15
	6	22.119804063752017 - 0.7063456283412931im	3.82e-09	6.03e-02	

Table S-1: Comparison between the Newton method using ApproxFun (down) in the piecewise constant case and the Newton method using the exact expression (40) of  $D(k)$  (up) for  $\xi = 0.5$ ,  $m = 10$ ,  $n_1 = 1.5$  and  $n_2 = 1$ . We took here  $\varepsilon = 1e-6$  and  $l_{\max} = 1000$ .

$k_0$	$l$	$k$	$ D(k) $	$ \partial_k D(k) $	Difference in $k$
21	4	22.119804057435196 - 0.7063456946543558im	3.00e-10	6.03e-02	1.26e-14
	4	22.1198040574352 - 0.706345694654344im	3.00e-10	6.03e-02	
22	3	22.11980251129046 - 0.7063450854527952im	1.00e-07	6.03e-02	7.10e-15
	3	22.119802511290455 - 0.7063450854527893im	1.00e-07	6.03e-02	
23	4	22.119804096508354 - 0.706345754755474im	4.35e-09	6.03e-02	5.12e-15
	4	22.119804096508357 - 0.7063457547554691im	4.35e-09	6.03e-02	
24	5	16.92320279370931 - 0.23954483086628545im	1.44e-07	1.19e-01	1.80e-13
	5	16.923202793709482 - 0.2395448308663334im	1.44e-07	1.19e-01	
25	5	31.730346846554976 - 0.9553141417588785im	7.90e-08	4.30e-02	2.70e-15
	5	31.730346846554987 - 0.9553141417588782im	7.90e-08	4.30e-02	
26	4	27.04249139796374 - 0.8848480038591856im	3.98e-07	4.93e-02	1.71e-14
	4	27.042491397963737 - 0.8848480038592026im	3.98e-07	4.93e-02	
27	4	27.042488355965958 - 0.8848405153357658im	1.31e-10	4.93e-02	1.26e-14
	4	27.04248835596597 - 0.8848405153357701im	1.31e-10	4.93e-02	
28	5	27.042488356712457 - 0.8848405174101011im	3.00e-11	4.93e-02	1.83e-14
	5	27.042488356712454 - 0.8848405174101192im	3.00e-11	4.93e-02	
29	7	16.92320259545549 - 0.23954508315910544im	1.06e-07	1.19e-01	1.96e-14
	7	16.923202595455503 - 0.23954508315912526im	1.06e-07	1.19e-01	
30	7	36.2794673729414 - 0.9907691069700367im	3.96e-10	3.83e-02	2.52e-14
	7	36.279467372941376 - 0.9907691069700371im	3.96e-10	3.83e-02	
31	4	31.73034262206993 - 0.9553087127872721im	2.33e-07	4.30e-02	2.08e-14
	4	31.73034262206995 - 0.9553087127872671im	2.33e-07	4.30e-02	
32	4	31.730344889489842 - 0.9553135682753766im	9.74e-09	4.30e-02	7.80e-15
	4	31.730344889489842 - 0.9553135682753844im	9.74e-09	4.30e-02	
33	6	31.73034327288489 - 0.9553121097293579im	1.00e-07	4.30e-02	2.11e-14
	6	31.73034327288491 - 0.9553121097293374im	1.00e-07	4.30e-02	
34	6	92.23783269919007 - 1.06289908087784im	4.07e-11	1.60e-02	1.13e-14
	6	92.23783269919007 - 1.0628990808778287im	4.07e-11	1.60e-02	
35	6	36.27946761966935 - 0.9907688668035165im	1.36e-08	3.83e-02	6.90e-15
	6	36.27946761966934 - 0.9907688668035097im	1.36e-08	3.83e-02	
36	4	36.27946660785861 - 0.9907693889504177im	3.09e-08	3.83e-02	7.10e-15
	4	36.27946660785862 - 0.9907693889504107im	3.09e-08	3.83e-02	
37	5	36.279467367290934 - 0.9907691165798495im	9.81e-11	3.83e-02	2.86e-14
	5	36.279467367290906 - 0.9907691165798471im	9.81e-11	3.83e-02	
38	5	31.730342433122015 - 0.9553140640209747im	1.18e-07	4.30e-02	5.70e-15
	5	31.73034243312201 - 0.9553140640209804im	1.18e-07	4.30e-02	
39	5	45.14774543822885 - 1.0249856558400918im	1.86e-10	3.16e-02	4.96e-14
	5	45.147745438228895 - 1.0249856558400874im	1.86e-10	3.16e-02	
40	5	40.74237122193321 - 1.0115554177751054im	1.58e-10	3.46e-02	2.50e-14
	5	40.74237122193319 - 1.0115554177751027im	1.58e-10	3.46e-02	

Table S-2: (Cont'd) Comparison between the Newton method using ApproxFun (down) in the piecewise constant case and the Newton method using the exact expression (40) of  $D(k)$  (up) for  $\xi = 0.5$ ,  $m = 10$ ,  $n_1 = 1.5$  and  $n_2 = 1$ . We took here  $\varepsilon = 1e-6$  and  $l_{\max} = 1000$ .

*Remark 5.* For the validation (§S1-S2), the Newton algorithm was applied on  $D(k) = \frac{\det(k)}{k}$  and stopping criterion  $|D(k)| \leq \varepsilon$ .

*Remark 6.* Investigating the iterations for the case where  $k_0 = 19$ , one finds that the process terminates by oscillating between two values  $-16.71760827266006 + 0.7591717411434071i$  and  $-17.13411129251172 - 0.09502475320676629i$ . It is worth noting that, if one works with  $\det$  instead of  $D$ , this case converges.

*Remark 7.* For information, the behavior of  $\frac{\partial_k D(k)}{D(k)}$  is shown in Figure S-1 to be compared with Figure 3.

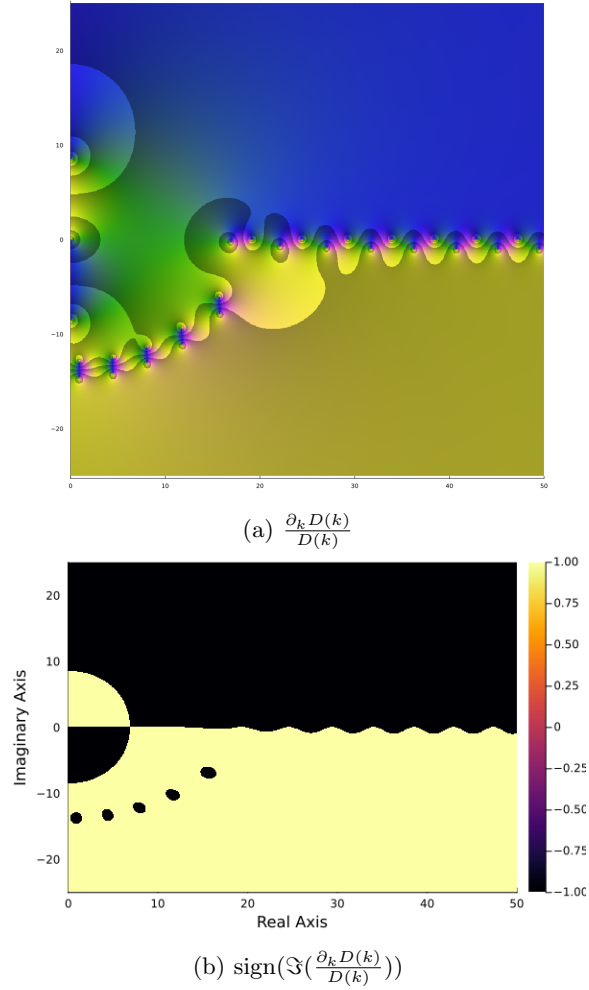


Figure S-1: Complex plots of  $\frac{\partial_k D(k)}{D(k)}$  where  $D(k) = \frac{\det_1(k)}{k}$  (40) for  $\xi = 0.5$ ,  $n_1 = 1.5$ ,  $n_2 = 1$  and  $m = 10$ .

## S2 Variable case validation: A special variable case with explicit solution (Luneburg lens)

$k_0$	$l$	$k$	$ D(k) $	$ \partial_k D(k) $	Difference in $k$
1	9	18.58896340188007 - 0.6154425719496848im	2.74e-09	6.84e-02	1.75e-14
	9	18.588963401880036 - 0.615442571949669im	2.74e-09	6.84e-02	
2	8	18.58896340488882 - 0.6154425690916594im	2.51e-09	6.84e-02	3.46e-15
	8	18.588963404888805 - 0.6154425690916552im	2.51e-09	6.84e-02	
3	7	18.58896695779626 - 0.6154417792268551im	2.47e-07	6.84e-02	1.14e-14
	7	18.588966957796284 - 0.6154417792268659im	2.47e-07	6.84e-02	
4	7	18.58896341614563 - 0.6154425612670845im	1.74e-09	6.84e-02	7.09e-15
	7	18.588963416145624 - 0.6154425612670775im	1.74e-09	6.84e-02	
5	7	18.58896344138152 - 0.6154425647650038im	9.40e-12	6.84e-02	1.22e-14
	7	18.58896344138154 - 0.615442564765016im	9.40e-12	6.84e-02	
6	6	18.58896525724792 - 0.615443021648839im	1.28e-07	6.84e-02	1.32e-15
	6	18.588965257247917 - 0.6154430216488403im	1.28e-07	6.84e-02	
7	6	18.58896337264796 - 0.6154426444629252im	7.20e-09	6.84e-02	5.00e-15
	6	18.58896337264795 - 0.6154426444629204im	7.20e-09	6.84e-02	
8	6	18.58896344012183 - 0.6154425602437874im	3.14e-10	6.84e-02	4.10e-15
	6	18.58896344012183 - 0.6154425602437833im	3.14e-10	6.84e-02	
9	6	18.58896344139265 - 0.6154425647636592im	9.97e-12	6.84e-02	3.32e-15
	6	18.588963441392664 - 0.6154425647636621im	9.97e-12	6.84e-02	
10	5	18.58896751208772 - 0.6154409952812947im	2.99e-07	6.84e-02	1.72e-14
	5	18.588967512087706 - 0.6154409952812963im	2.99e-07	6.84e-02	
11	5	18.58896364980876 - 0.6154430324053323im	3.50e-08	6.84e-02	3.02e-15
	5	18.588963649808775 - 0.6154430324053345im	3.50e-08	6.84e-02	
12	5	18.58896340016189 - 0.6154425755019333im	2.91e-09	6.84e-02	2.30e-15
	5	18.588963400161894 - 0.6154425755019356im	2.91e-09	6.84e-02	
13	5	18.58896344175409 - 0.6154425626023302im	1.46e-10	6.84e-02	7.94e-15
	5	18.588963441754075 - 0.6154425626023224im	1.46e-10	6.84e-02	
14	5	18.5889634412903 - 0.6154425647328736im	3.66e-12	6.84e-02	1.14e-14
	5	18.58896344129032 - 0.6154425647328835im	3.66e-12	6.84e-02	
15	4	18.5889651021984 - 0.6154429452205046im	1.17e-07	6.84e-02	1.15e-14
	4	18.588965102198415 - 0.6154429452205159im	1.17e-07	6.84e-02	
16	4	18.58896338925333 - 0.6154426111492044im	4.77e-09	6.84e-02	4.64e-15
	4	18.588963389253323 - 0.6154426111492001im	4.77e-09	6.84e-02	
17	4	18.58896344171655 - 0.615442564463893im	3.39e-11	6.84e-02	3.33e-15
	4	18.588963441716555 - 0.6154425644638902im	3.39e-11	6.84e-02	
18	3	18.58896319223808 - 0.6154432829180086im	5.20e-08	6.84e-02	1.36e-14
	3	18.588963192238104 - 0.6154432829180219im	5.20e-08	6.84e-02	
19	3	18.58896424325041 - 0.6154434190101671im	8.02e-08	6.84e-02	1.64e-14
	3	18.588964243250395 - 0.6154434190101592im	8.02e-08	6.84e-02	
20	4	18.58896048827961 - 0.6154427868757306im	2.03e-07	6.84e-02	2.70e-15
	4	18.588960488279607 - 0.615442786875728im	2.03e-07	6.84e-02	

Table S-3: Comparison between the Newton method using ApproxFun (down) and the Newton method using the exact expression of  $D(k)$  (up) in a special variable case  $n_1$  given by  $n_1(r) = \sqrt{2-r^2}$  for  $n_2 = 1$ ,  $\xi = 0.5$  and  $m = 10$ . We took here  $\varepsilon = 1e-6$  and  $l_{\max} = 1000$ .

$k_0$	$l$	$k$	$ D(k) $	$ \partial_k D(k) $	Difference in $k$
21	8	24.31472259294407 - 1.132533380322222im	3.20e-09	4.37e-02	9.86e-14
	8	24.31472259294416 - 1.1325333803221875im	3.20e-09	4.37e-02	
22	5	24.31472055171216 - 1.1325342728376im	9.49e-08	4.37e-02	2.00e-13
	5	24.314720551712146 - 1.1325342728377994im	9.49e-08	4.37e-02	
23	4	24.31472272287542 - 1.132533490562084im	1.05e-08	4.37e-02	5.38e-13
	4	24.314722722875874 - 1.132533490562372im	1.05e-08	4.37e-02	
24	4	24.31472252029847 - 1.132533369059882im	4.79e-10	4.37e-02	6.79e-13
	4	24.314722520299103 - 1.1325333690601302im	4.79e-10	4.37e-02	
25	4	24.31472523590229 - 1.132536800954997im	1.91e-07	4.37e-02	2.42e-13
	4	24.314725235902074 - 1.1325368009548904im	1.91e-07	4.37e-02	
26	7	29.61145921358794 - 1.273583542487957im	6.06e-10	3.46e-02	6.74e-12
	7	29.611459213581508 - 1.2735835424859219im	6.06e-10	3.46e-02	
27	6	34.64993220415352 - 1.329004960610387im	1.63e-07	2.84e-02	5.93e-14
	6	34.64993220415358 - 1.329004960610404im	1.63e-07	2.84e-02	
28	5	29.61145932650436 - 1.273583578719955im	4.22e-09	3.46e-02	9.12e-12
	5	29.611459326495837 - 1.273583578716714im	4.22e-09	3.46e-02	
29	4	29.61145947666278 - 1.27358437975178im	3.09e-08	3.46e-02	1.58e-11
	4	29.611459476646992 - 1.2735843797505257im	3.09e-08	4.37e-02	
30	5	29.6114592173724 - 1.273583525331912im	1.22e-11	3.46e-02	7.69e-12
	5	29.61145921736673 - 1.2735835253267198im	1.18e-11	3.46e-02	
31	7	29.6114592172687 - 1.273583524873477im	1.79e-11	3.46e-02	1.42e-11
	7	29.611459217282782 - 1.2735835248752136im	1.79e-11	3.46e-02	
32	11	38.6889572663705 - 2.600811140151995im	8.55e-11	6.46e-02	2.13e-14
	11	38.68895726637048 - 2.600811140151994im	8.55e-11	6.46e-02	
33	6	34.64993092029182 - 1.32900094885017im	4.53e-08	2.84e-02	2.98e-14
	6	34.64993092029181 - 1.3290009488501437im	4.53e-08	2.84e-02	
34	4	34.64993363068658 - 1.329003274419759im	1.46e-07	2.84e-02	9.44e-15
	4	34.649933630686576 - 1.3290032744197529im	1.46e-07	2.84e-02	
35	5	34.64992990849705 - 1.328999714221655im	1.13e-10	2.84e-02	2.37e-14
	5	34.64992990849707 - 1.3289997142216445im	1.13e-10	2.84e-02	
36	9	34.64992991390228 - 1.328999715144571im	5.92e-11	2.84e-02	3.14e-14
	9	34.6499299139023 - 1.328999715144594im	5.92e-11	2.84e-02	
37	10	39.54722441341892 - 1.357395632339697im	2.07e-08	2.43e-02	7.35e-14
	10	39.54722441341888 - 1.3573956323397613im	2.07e-08	2.43e-02	
38	8	39.54722356873814 - 1.357395665451988im	8.53e-10	2.43e-02	6.00e-15
	8	39.54722356873814 - 1.357395665451982im	8.53e-10	2.43e-02	
39	4	39.5472207449567 - 1.35740325326138im	1.96e-07	2.43e-02	2.98e-14
	4	39.5472207449567 - 1.3574032532614098im	1.96e-07	2.43e-02	
40	5	39.54722423899524 - 1.357395977985056im	1.77e-08	2.43e-02	8.26e-15
	5	39.547224238995234 - 1.3573959779850517im	1.77e-08	2.43e-02	

Table S-4: (Cont'd) Comparison between the Newton method using ApproxFun (down) and the Newton method using the exact expression of  $D(k)$  (up) in a special variable case  $n_1$  given by  $n_1(r) = \sqrt{2 - r^2}$  for  $n_2 = 1$ ,  $\xi = 0.5$  and  $m = 10$ . We took here  $\varepsilon = 1e-6$  and  $l_{\max} = 1000$ .

# S3 Piecewise constant cases

## S3.1 Low-contrast media

$$n_1(r) = 1.5$$

$m$	$k_0$	$l$	$k$	$k_{\text{asympt}}$	$ \det(k) $	$ \partial_k \det(k) $	$\frac{ \det(k) }{\ T(k)\ _F}$	$ k - k_{\text{asympt}} $
1	1.33	10	2.9412214517988846 - 1.0213193155493827im	1.404547952561922	1.07e-14	1.40e+00	3.15e-15	1.85e+00
2	2.67	6	4.567191225356701 - 0.9043901168618548im	3.8338779784797286	3.35e-11	1.32e+00	1.05e-11	1.16e+00
3	4	5	6.153857666206802 - 0.7885737875639456im	5.777332794430966	2.85e-10	1.32e+00	9.29e-11	8.74e-01
4	5.33	5	7.720812756597912 - 0.6808760720924771im	7.549595817571761	3.49e-14	1.35e+00	1.13e-14	7.02e-01
5	6.67	4	9.275045821677303 - 0.5831461096495909im	9.233276944106649	1.64e-08	1.41e+00	5.07e-09	5.85e-01
6	8	4	10.819644524989346 - 0.49566872221472635im	10.862185118573025	6.08e-09	1.49e+00	1.72e-09	4.97e-01
7	9.33	4	12.356132077506965 - 0.41815032448175377im	12.45353017076617	2.37e-08	1.59e+00	5.93e-09	4.29e-01
8	10.67	5	13.885303104340203 - 0.3500580048463525im	14.01731282633191	2.45e-14	1.71e+00	5.31e-15	3.74e-01
9	12	5	15.40758260902961 - 0.2907525346671839im	15.559887746632942	2.35e-13	1.86e+00	4.35e-14	3.28e-01
10	13.33	5	16.923201860866378 - 0.23954558981446541im	17.085561463191144	7.94e-12	2.02e+00	1.24e-12	2.89e-01
11	14.67	5	18.43229438636131 - 0.19572719040605327im	18.597397906363835	1.74e-10	2.21e+00	2.30e-11	2.56e-01
12	16	5	19.93495268796489 - 0.15858126252109225im	20.097661326712466	2.51e-09	2.43e+00	2.78e-10	2.27e-01
13	17.33	5	21.431263593910362 - 0.12739692510813508im	21.588076774547527	2.51e-08	2.68e+00	2.33e-09	2.02e-01
14	18.67	6	22.92133045224094 - 0.10147864059520828im	23.069991730554193	8.62e-15	2.98e+00	6.72e-16	1.80e-01
15	20	6	24.405286333912258 - 0.08015607332740156im	24.544480894183742	9.68e-14	3.32e+00	6.31e-15	1.61e-01
16	21.33	6	25.883300247280477 - 0.06279379760306064im	26.012416645668527	1.81e-12	3.72e+00	9.87e-14	1.44e-01
17	22.67	6	27.355578058896366 - 0.0488000469977541im	27.474517911479982	2.42e-11	4.18e+00	1.10e-12	1.29e-01
18	24	6	28.82235923395287 - 0.037633920115272244im	28.931384960603197	2.36e-10	4.71e+00	9.00e-12	1.15e-01
19	25.33	6	30.283910666495377 - 0.028810397590219156im	30.383524756473076	1.77e-09	5.34e+00	5.62e-11	1.04e-01
20	26.67	6	31.740518796620687 - 0.021902843972756506im	31.831369801672267	1.06e-08	6.07e+00	2.80e-10	9.35e-02
21	28	6	33.19248112357947 - 0.016542983461149904im	33.275292395296674	5.23e-08	6.93e+00	1.16e-09	8.44e-02
22	29.33	6	34.64009803387209 - 0.012418628486121377im	34.715615590296096	2.20e-07	7.94e+00	4.05e-09	7.65e-02
23	30.67	7	36.08366569411309 - 0.009269655772411808im	36.15262173363031	2.30e-14	9.12e+00	3.52e-16	6.96e-02
24	32	7	37.52347003317291 - 0.006882735407147462im	37.586559207022354	3.04e-13	1.05e+01	6.39e-15	6.35e-02
25	33.33	7	38.95978268084367 - 0.005085524861790347im	39.01764780851463	1.79e-12	1.21e+01	1.90e-14	5.81e-02
26	34.67	7	40.39285800647834 - 0.003740648216911396im	40.4460830936776	1.15e-11	1.41e+01	1.01e-13	5.34e-02
27	36	7	41.82293159901168 - 0.002739945476988483im	41.87203991088016	6.20e-11	1.63e+01	4.56e-13	4.92e-02
28	37.33	7	43.25021976549947 - 0.0019992013442696344im	43.295675305305124	2.96e-10	1.90e+01	1.81e-12	4.55e-02
29	38.67	7	44.67491981925316 - 0.0014534978710381067im	44.71713092351226	1.26e-09	2.22e+01	6.37e-12	4.22e-02
30	40	7	46.097210919331935 - 0.0010532410259593333im	46.13653501913951	4.80e-09	2.59e+01	2.02e-11	3.93e-02
31	41.33	7	47.51725525869917 - 0.0007608484539104058im	47.55400413732363	1.68e-08	3.03e+01	5.86e-11	3.68e-02
32	42.67	7	48.93519944041087 - 0.0005480462712514229im	48.96964453826328	5.39e-08	3.56e+01	1.56e-10	3.44e-02
33	44	7	50.351175922319385 - 0.0003937019998486636im	50.383553407409686	1.61e-07	4.18e+01	3.88e-10	3.24e-02
34	45.33	7	51.765304446819925 - 0.0002821135302205254im	51.79581988991895	4.52e-07	4.91e+01	9.02e-10	3.05e-02
35	46.67	7	53.17769340145632 - 0.000201675645007481im	53.20652597942726	1.20e-06	5.78e+01	1.98e-09	2.88e-02
36	48	7	54.58844107861054 - 0.00014385241181050188im	54.61574728533793	3.00e-06	6.82e+01	4.11e-09	2.73e-02
37	49.33	7	55.99763681875335 - 0.00010239298206207897im	56.023553698218514	7.19e-06	8.05e+01	8.14e-09	2.59e-02
38	50.67	8	57.40536220609935 - 7.273843426901466e-5im	57.43000996928929	1.92e-12	9.51e+01	1.80e-15	2.46e-02
39	52	8	58.81169142982313 - 5.157539342094568e-5im	58.83517621711491	5.08e-12	1.12e+02	3.94e-15	2.35e-02
40	53.33	8	60.2166927760122 - 3.650467591420821e-5im	60.23910837231776	1.95e-11	1.33e+02	1.25e-14	2.24e-02
41	54.67	8	61.62042892394215 - 2.579408584689976e-5im	61.64185856928814	6.72e-11	1.58e+02	3.56e-14	2.14e-02
42	56	8	63.0229576449074 - 1.8196704014106916e-5im	63.04347549237541	2.26e-10	1.87e+02	9.91e-14	2.05e-02
43	57.33	8	64.42433233311223 - 1.2817365212355606e-5im	64.44400468283037	7.19e-10	2.22e+02	2.61e-13	1.97e-02
44	58.67	8	65.82460246791646 - 9.015052379810998e-6im	65.84348881177745	2.17e-09	2.64e+02	6.50e-13	1.89e-02
45	60	8	67.22381401657992 - 6.331827028646652e-6im	67.24196792367869	6.26e-09	3.14e+02	1.55e-12	1.82e-02
46	61.33	8	68.62200978567625 - 4.441267884262988e-6im	68.63947965407776	1.72e-08	3.74e+02	3.52e-12	1.75e-02
47	62.67	8	70.01922972835321 - 3.1111868818178037e-6im	70.03605942485238	4.56e-08	4.45e+02	7.68e-12	1.68e-02
48	64	8	71.41551121366949 - 2.1767516562853845e-6im	71.43174061973707	1.16e-07	5.30e+02	1.61e-11	1.62e-02
49	65.33	8	72.81088926336673 - 1.5211649734481785e-6im	72.82655474248713	2.84e-07	6.32e+02	3.26e-11	1.57e-02
50	66.67	8	74.20539676065863 - 1.0618130598726635e-6im	74.2205315597273	6.75e-07	7.55e+02	6.39e-11	1.51e-02
51	68	8	75.59906463493806 - 7.403593777267181e-7im	75.61369923024954	1.55e-06	9.01e+02	1.21e-10	1.46e-02
52	69.33	8	76.99192202571422 - 5.156763493708755e-7im	77.00608442229196	3.46e-06	1.08e+03	2.23e-10	1.42e-02
53	70.67	8	78.38399642858849 - 3.588131191863404e-7im	78.39771242012931	7.52e-06	1.29e+03	3.99e-10	1.37e-02
54	72	8	79.77531382564938 - 2.4941999169469316e-7im	79.78860722113613	1.59e-05	1.54e+03	6.95e-10	1.33e-02
55	73.33	8	81.16589880230521 - 1.7321305547435112e-7im	81.17879162433847	3.29e-05	1.84e+03	1.18e-09	1.29e-02
56	74.67	8	82.55577465226776 - 1.2017942719862094e-7im	82.56828731134388	6.64e-05	2.20e+03	1.97e-09	1.25e-02
57	76	8	83.94496347214364 - 8.330917110366931e-8im	83.95711492043253	1.31e-04	2.64e+03	3.20e-09	1.22e-02
58	77.33	8	85.333486246874 - 5.770068968393716e-8im	85.34529411449975	2.54e-04	3.16e+03	5.11e-09	1.18e-02
59	78.67	8	86.72136292708211 - 3.993064464643193e-8im	86.73284364345857	4.83e-04	3.79e+03	7.99e-09	1.15e-02
60	80	9	88.10861269709926 - 2.7610951207716043e-8im	88.11978140164216	1.23e-10	4.55e+03	1.68e-15	1.12e-02

Table S-5: Results obtained by the Newton method for  $n_1 = 1.5$ ,  $n_2 = 1$ ,  $\xi = 0.5$  starting from  $k_0 = \frac{m}{\xi n_0}$ . We took here  $\varepsilon = 1e-8$  and  $l_{\text{max}} = 2000$ .

### S3.2 High-contrast media

$$n_1(r) = 5$$

$m$	$k_0$	$l$	$k$	$k_{\text{asympt}}$	$ \det(k) $	$ \partial_k \det(k) $	$\frac{ \det(k) }{\ T(k)\ _F}$	$ k - k_{\text{asympt}} $
1	0.4	5	0.9289987680826443 - 0.04523834315971972im	0.8842557552463222	1.44e-15	9.62e+00	4.39e-16	6.36e-02
2	0.8	4	1.4998099150133781 - 0.010215157356845911im	1.4892827214976112	1.19e-11	1.99e+01	1.25e-12	1.47e-02
3	1.2	5	2.0304915035306306 - 0.0016737245701525074im	2.0224106828300403	1.90e-11	4.78e+01	6.16e-13	8.25e-03
4	1.6	5	2.5332600608053313 - 0.0002250224324238292im	2.5260265729729126	2.37e-07	1.27e+02	2.32e-09	7.24e-03
5	2	6	3.0190057464666977 - 2.6964505481422285e-5im	3.0127828023877194	1.39e-11	3.60e+02	4.06e-14	6.22e-03
6	2.4	6	3.4936803250165007 - 3.004752173541452e-6im	3.4883629888379457	1.34e-08	1.06e+03	1.17e-11	5.32e-03
7	2.8	6	3.960459416225663 - 3.183017415564268e-7im	3.9558733069976633	2.31e-06	3.21e+03	5.96e-10	4.59e-03
8	3.2	7	4.421228115261558 - 3.2466894902410785e-8im	4.4172227083710744	4.57e-12	9.90e+03	3.47e-16	4.01e-03
9	3.6	7	4.8772204014868334 - 3.215018134396133e-9im	4.873680280984354	1.06e-09	3.11e+04	2.36e-14	3.54e-03
10	4	7	5.329300472271188 - 3.1083242783367133e-10im	5.3261387153376285	1.36e-07	9.88e+04	8.81e-13	3.16e-03
11	4.4	7	5.778102650797891 - 2.9461255850545655e-11im	5.775253241560408	8.67e-06	3.17e+05	1.64e-11	2.85e-03
12	4.8	7	6.224109026375009 - 2.74609859775701e-12im	6.221521063701407	3.34e-04	1.03e+06	1.83e-10	2.59e-03
13	5.2	7	6.66769609164898 - 2.52045570457135e-13im	6.665329694374709	8.71e-03	3.36e+06	1.38e-09	2.37e-03
14	5.6	7	7.109164413438445 - 2.3274506929752e-14im	7.106987860964534	1.68e-01	1.11e+07	7.68e-09	2.18e-03
15	6	8	7.548758419736942 - 1.8945155713887954e-15im	7.546746083387481	3.26e-07	3.66e+07	4.30e-15	2.01e-03
16	6.4	8	7.9866798674345905 - 3.8812025647829594e-16im	7.984810843791047	1.54e-05	1.22e+08	5.82e-14	1.87e-03
17	6.8	8	8.423097625006472 + 2.1348936193935203e-16im	8.421354625124714	5.13e-04	4.07e+08	5.57e-13	1.74e-03
18	7.2	8	8.858154611496365 + 2.1389462948567035e-16im	8.856523198362067	1.32e-02	1.37e+09	4.10e-12	1.63e-03
19	7.6	8	9.291973019898002 + 1.544785566106463e-16im	9.290441025297994	2.70e-01	4.61e+09	2.40e-11	1.53e-03
20	8	8	9.724638257653362 + 2.3736960931177923e-16im	9.723215338890416	4.56e+00	1.56e+10	1.16e-10	1.44e-03
21	8.4	8	10.156301976717426 - 1.1900052185417522e-16im	10.154939275489847	6.53e+01	5.30e+10	4.72e-10	1.36e-03
22	8.8	8	10.586984437022778 - 4.561232924811838e-16im	10.585694314365664	8.13e+02	1.80e+11	1.67e-09	1.29e-03
23	9.2	8	11.016776373179304 - 1.6122235478306528e-17im	11.015552202535067	8.95e+03	6.15e+11	5.22e-09	1.22e-03
24	9.6	9	11.445740526787104 - 1.4137056688608484e-16im	11.44457649133396	8.32e-03	2.11e+12	1.38e-15	1.16e-03
25	10	9	11.87393274714286 + 2.706494241818125e-16im	11.872823776087106	1.63e-01	7.23e+12	7.66e-15	1.11e-03
26	10.4	9	12.3014030996562 + 4.67401212600892e-16im	12.300344705913306	3.65e+00	2.48e+13	4.84e-14	1.06e-03
27	10.8	9	12.728196607607492 - 7.157505437405707e-16im	12.72718481354921	6.19e+01	8.56e+13	2.33e-13	1.01e-03
28	11.2	9	13.154353938405894 + 5.93980437663009e-17im	13.153385202789783	9.52e+02	2.95e+14	1.01e-12	9.69e-04
29	11.6	9	13.57991196479966 - 6.522172009112395e-17im	13.57898312221752	1.30e+04	1.02e+15	3.89e-12	9.29e-04
30	12	9	14.004904236941927 + 3.756874765840019e-16im	14.004012447322797	1.59e+05	3.54e+15	1.35e-11	8.92e-04
31	12.4	9	14.429361381966812 + 2.9441554944916877e-16im	14.428504088223606	1.78e+06	1.23e+16	4.25e-11	8.57e-04
32	12.8	9	14.853311444171052 - 2.0966686788064463e-17im	14.852486336506397	1.84e+07	4.27e+16	1.23e-10	8.25e-04
33	13.2	9	15.27678017617792 + 1.419957217980044e-17im	15.275985161904302	1.75e+08	1.48e+17	3.31e-10	7.95e-04
34	13.6	9	15.699791289360771 - 5.1286366559267425e-17im	15.699024467373523	1.56e+09	1.57e+17	8.29e-10	7.67e-04
35	14	9	16.122366670164638 - 1.4816623354636735e-16im	16.12162630945759	1.31e+10	1.81e+18	1.95e-09	7.40e-04
36	14.4	9	16.544526567671234 - 1.952231859209583e-16im	16.543811089523164	1.04e+11	6.31e+18	4.33e-09	7.15e-04
37	14.8	9	16.966289756724333 + 4.855898963602317e-16im	16.96559772042216	7.79e+11	2.21e+19	9.14e-09	6.92e-04
38	15.2	10	17.38673752461428 + 6.149710739788696e-16im	17.387003772318206	1.01e+06	7.73e+19	3.32e-15	6.70e-04
39	15.6	10	17.808694714368958 + 6.586981462266349e-16im	17.80804560076339	1.22e+07	2.71e+20	1.13e-14	6.49e-04
40	16	10	18.229367835970436 + 1.0305930546274741e-15im	18.22873845958632	1.44e+08	9.50e+20	3.71e-14	6.29e-04
41	16.4	10	18.64970728310631 + 4.626528310361964e-16im	18.64909660072809	1.65e+09	3.34e+21	1.19e-13	6.11e-04
42	16.8	10	19.06972631669211 - 2.1480752494321374e-16im	19.069133362817244	1.77e+10	1.17e+22	3.58e-13	5.93e-04
43	17.2	10	19.4894373705534 + 5.452325986420823e-16im	19.488861249992212	1.80e+11	4.13e+22	1.02e-12	5.76e-04
44	17.6	10	19.90885212091889 - 4.699501904353818e-16im	19.90829200224708	1.72e+12	1.45e+23	2.72e-12	5.60e-04
45	18	10	20.327981548633637 + 1.3682878643361967e-16im	20.32743665838434	1.56e+13	5.13e+23	6.88e-12	5.45e-04
46	18.4	10	20.746835994998264 + 6.278049097308506e-16im	20.746305612498908	1.34e+14	1.81e+24	1.65e-11	5.30e-04
47	18.8	10	21.165425212009033 - 1.1986754289783127e-16im	21.164908664784164	1.10e+15	6.39e+24	3.80e-11	5.17e-04
48	19.2	10	21.583758407663527 - 1.0182255257250858e-15im	21.583255067339692	8.69e+15	2.26e+25	8.34e-11	5.03e-04
49	19.6	10	22.001844286903584 + 3.640542269852532e-16im	22.00135356556624	6.57e+16	7.98e+25	1.76e-10	4.91e-04
50	20	10	22.419691088687355 - 6.18490848432868e-16im	22.41921243565446	4.79e+17	2.82e+26	3.57e-10	4.79e-04
51	20.4	10	22.83730661961448 - 2.2150447016920813e-16im	22.836839518606798	3.37e+18	1.00e+27	7.00e-10	4.67e-04
52	20.8	10	23.254698284469086 - 4.914840523818897e-17im	23.25424225117478	2.29e+19	3.54e+27	1.33e-09	4.56e-04
53	21.2	10	23.671873113994433 + 5.596041454992709e-16im	23.67142769404527	1.51e+20	1.26e+28	2.44e-09	4.45e-04
54	21.6	10	24.08883779016825 - 6.429348935550911e-17im	24.088402557567772	9.70e+20	4.46e+28	4.35e-09	4.35e-04
55	22	10	24.50559866920907 + 4.3767788983932454e-16im	24.505173225278554	6.05e+21	1.58e+29	7.55e-09	4.25e-04
56	22.4	11	24.922161868047585 + 4.610593529399424e-16im	24.921745775447178	4.26e+15	5.62e+29	1.48e-15	4.16e-04
57	22.8	11	25.338533065227093 + 3.7988448079297595e-16im	25.33812600084375	4.87e+16	2.00e+30	4.70e-15	4.07e-04
58	23.2	11	25.754717804739506 + 4.637562128573648e-16im	25.754319426902597	5.29e+17	7.10e+30	1.42e-14	3.98e-04
59	23.6	11	26.170721343078498 - 4.652091377522209e-16im	26.170331328437797	4.48e+18	2.52e+31	3.34e-14	3.90e-04
60	24	11	26.586548702785926 + 5.921555087660197e-16im	26.586166745048544	3.93e+19	8.99e+31	8.14e-14	3.82e-04

Table S-6: Results obtained by the Newton method for  $n_1 = 5$ ,  $n_2 = 1$ ,  $\xi = 0.5$  starting from  $k_0 = \frac{m}{\xi n_0}$ . We took here  $\varepsilon = 1e-8$  and  $l_{\text{max}} = 2000$ .

# S4 Variable cases

## S4.1 $n_1$ variable and $n_2 = 1$

$$n_1(r) = 2 - r$$

$m$	$k_0$	$l$	$k$	$k_{\text{asympt}}$	$ \det(k) $	$ \partial_k \det(k) $	$\frac{ \det(k) }{\ T(k)\ _F}$	$ k - k_{\text{asympt}} $
1	1.33	13	6.319821637534675 - 0.8852775094525012im	1.4051097872513703	3.67e-08	1.40e+00	7.33e-09	4.99e+00
2	2.67	7	4.311909988078464 - 0.6755610763676703im	3.708252723915477	4.23e-14	1.69e+00	1.41e-14	9.06e-01
3	4	6	5.847774226712011 - 0.5742451453806543im	5.553028501041968	3.01e-15	1.72e+00	1.00e-15	6.45e-01
4	5.33	5	7.369474014406212 - 0.4824173452925744im	7.243859029864192	5.15e-11	1.81e+00	1.63e-11	4.99e-01
5	6.67	5	8.881738598735172 - 0.4012506982673458im	8.857569745641534	3.92e-14	1.94e+00	1.12e-14	4.02e-01
6	8	4	10.386432418688315 - 0.3305887598822313im	10.424704364080949	2.80e-08	2.10e+00	7.01e-09	3.33e-01
7	9.33	4	11.884338704967615 - 0.26981120308410683im	11.96046139230838	6.11e-09	2.31e+00	1.30e-09	2.80e-01
8	10.67	4	13.37578266508728 - 0.21811726428386907im	13.473512159036872	9.31e-09	2.55e+00	1.67e-09	2.39e-01
9	12	4	14.860893950499706 - 0.17463510421081396im	14.969283929659495	3.80e-08	2.84e+00	5.66e-09	2.06e-01
10	13.33	5	16.339732830319488 - 0.13847163034852053im	16.451408547954802	5.89e-15	3.18e+00	7.26e-16	1.78e-01
11	14.67	5	17.81235607739828 - 0.10874070551653621im	17.92244243971538	3.92e-14	3.58e+00	3.99e-15	1.55e-01
12	16	5	19.27885240444428 - 0.08458332178990707im	19.38425760969737	5.23e-13	4.05e+00	4.40e-14	1.35e-01
13	17.33	5	20.739359449488816 - 0.0651844152847684im	20.83826906158287	5.70e-12	4.61e+00	3.95e-13	1.18e-01
14	18.67	5	22.19406875016445 - 0.049787138856965944im	22.285574533020405	4.95e-11	5.28e+00	2.82e-12	1.04e-01
15	20	5	23.64322235514991 - 0.037704130271580184im	23.727044292985035	3.47e-10	6.06e+00	1.63e-11	9.19e-02
16	21.33	5	25.087103955017668 - 0.028325032827833788im	25.163381045578042	2.01e-09	7.00e+00	7.77e-11	8.14e-02
17	22.67	5	26.526027002981284 - 0.02111984735632102im	26.5951611758174	9.75e-09	8.11e+00	3.10e-10	7.23e-02
18	24	5	27.960321925394275 - 0.01563822376370771im	28.022863929013774	4.06e-08	9.43e+00	1.06e-09	6.45e-02
19	25.33	5	29.390324046939536 - 0.011505293221968506im	29.446892544290492	1.48e-07	1.10e+01	3.19e-09	5.77e-02
20	26.67	5	30.816363305868975 - 0.008414958132371654im	30.86758987847692	4.80e-07	1.29e+01	8.50e-09	5.19e-02
21	28	6	32.23875637360949 - 0.006121712007226923im	32.285250167946494	5.81e-14	1.51e+01	8.47e-16	4.69e-02
22	29.33	6	33.65780095674447 - 0.0044315961584975964im	33.70012802673084	2.38e-13	1.78e+01	2.86e-15	4.26e-02
23	30.67	6	35.07377266505265 - 0.0031937641604689844im	35.112445430103556	1.19e-12	2.10e+01	1.17e-14	3.88e-02
24	32	6	36.48692343281727 - 0.0022922972500740925im	36.52239720526705	5.59e-12	2.48e+01	4.52e-14	3.55e-02
25	33.33	6	37.89748144428805 - 0.001639145256703826im	37.93015539909595	2.31e-11	2.94e+01	1.54e-13	3.27e-02
26	34.67	6	39.30565201178321 - 0.001168097760956254im	39.33587278972773	8.85e-11	3.48e+01	4.83e-13	3.02e-02
27	36	6	40.711619067040566 - 0.000829808869153259im	40.739685737330724	3.09e-10	4.14e+01	1.39e-12	2.81e-02
28	37.33	6	42.11554698444382 - 0.0005877903340540705im	42.141716519049346	9.96e-10	4.93e+01	3.67e-12	2.62e-02
29	38.67	6	43.51758253056944 - 0.0004152489726177944im	43.5420752571355	3.00e-09	5.87e+01	9.06e-12	2.45e-02
30	40	6	44.91785680017337 - 0.00029263215496138945im	44.940861523175606	8.48e-09	7.00e+01	2.10e-11	2.30e-02
31	41.33	6	46.31648705093649 - 0.00020574963913845464im	46.338165682152905	2.27e-08	8.36e+01	4.62e-11	2.17e-02
32	42.67	6	47.71357838808876 - 0.00014433538289591733im	47.73407002583552	5.79e-08	1.00e+02	9.67e-11	2.05e-02
33	44	6	49.10922527721022 - 0.0001010759175823941im	49.12864973427281	1.41e-07	1.20e+02	1.93e-10	1.94e-02
34	45.33	6	50.50351288143034 - 7.064013199559534e-5im	50.5219736960527	3.30e-07	1.43e+02	3.71e-10	1.85e-02
35	46.67	6	51.896518230256646 - 4.928105446065974e-5im	51.91410521174152	7.45e-07	1.72e+02	6.87e-10	1.76e-02
36	48	6	53.28831123336809 - 3.432059000254276e-5im	53.305102600109706	1.63e-06	2.06e+02	1.23e-09	1.68e-02
37	49.33	6	54.678955555504935 - 2.3859325232465636e-5im	54.69501972298854	3.43e-06	2.48e+02	2.13e-09	1.61e-02
38	50.67	6	56.06850936926672 - 1.65535538070986e-5im	56.083906441651365	7.05e-06	2.98e+02	3.58e-09	1.54e-02
39	52	6	57.4570260020398 - 1.1454881383505394e-5im	57.47180901527443	1.41e-05	3.58e+02	5.87e-09	1.48e-02
40	53.33	6	58.844554491998004 - 7.89539371171078e-6im	58.858770450169544	2.75e-05	4.31e+02	9.39e-09	1.42e-02
41	54.67	7	60.2311400888562 - 5.504763771922583e-6im	60.24483080698625	1.36e-12	5.19e+02	3.81e-16	1.37e-02
42	56	7	61.61682461690494 - 3.8025787084092296e-6im	61.63002747187329	9.70e-12	6.25e+02	2.22e-15	1.32e-02
43	57.33	7	63.00164687597391 - 2.6237196223681195e-6im	63.0143953966109	1.30e-11	7.54e+02	2.44e-15	1.27e-02
44	58.67	7	64.38564293488696 - 1.8083336183506224e-6im	64.39796731192381	3.38e-11	9.09e+02	5.19e-15	1.23e-02
45	60	7	65.76884640297767 - 1.245036996841289e-6im	65.78077391752967	9.45e-11	1.10e+03	1.19e-14	1.19e-02
46	61.33	7	67.1512886655986 - 8.563429367810468e-7im	67.16284405193512	2.50e-10	1.32e+03	2.57e-14	1.16e-02
47	62.67	7	68.53299909062868 - 5.884272825165588e-7im	68.5442048445434	6.01e-10	1.60e+03	5.05e-14	1.12e-02
48	64	7	69.91400521023789 - 4.039560133030205e-7im	69.9248818522636	1.42e-09	1.93e+03	9.75e-14	1.09e-02
49	65.33	7	71.29433288147527 - 2.7706833097430426e-7im	71.3048991824997	3.27e-09	2.34e+03	1.84e-13	1.06e-02
50	66.67	7	72.67400642867003 - 1.898739574324792e-7im	72.68427960413494	7.44e-09	2.83e+03	3.42e-13	1.03e-02
51	68	7	74.0530487701553 - 1.300119158986604e-7im	74.06304464790618	1.64e-08	3.42e+03	6.18e-13	1.00e-02
52	69.33	7	75.43148153142653 - 8.895187402806668e-8im	75.44121469737641	3.54e-08	4.14e+03	1.09e-12	9.73e-03
53	70.67	7	76.80932514651717 - 6.08140945395583e-8im	76.81880907155451	7.47e-08	5.01e+03	1.88e-12	9.48e-03
54	72	7	78.18659894910083 - 4.1550928163256736e-8im	78.19584610007617	1.55e-07	6.07e+03	3.19e-12	9.25e-03
55	73.33	7	79.5633212546024 - 2.837987828767068e-8im	79.57234319174495	3.16e-07	7.36e+03	5.31e-12	9.02e-03
56	74.67	7	80.93950943441125 - 1.9391509296903456e-8im	80.94831689713264	6.31e-07	8.92e+03	8.67e-12	8.81e-03
57	76	7	82.31517998313323 - 1.327854609878886e-8im	82.32378296585331	1.24e-06	1.08e+04	1.39e-11	8.60e-03
58	77.33	7	83.69034857968562 - 9.148766232561071e-9im	83.69875639905239	2.40e-06	1.31e+04	2.21e-11	8.41e-03
59	78.67	7	85.06503014292879 - 6.395640208352229e-9im	85.07325149758765	4.59e-06	1.59e+04	3.44e-11	8.22e-03
60	80	7	86.43923888243577 - 4.608391378408978e-9im	86.44728190632462	8.62e-06	1.93e+04	5.28e-11	8.04e-03

Table S-7: Results obtained by the Newton method for  $n_1(r) = 2 - r$ ,  $n_2 = 1$ ,  $\xi = 0.5$  starting from  $k_0 = \frac{m}{\xi n_0}$ . We took here  $\varepsilon = 1e-8$  and  $l_{\text{max}} = 2000$ .

$$n_1(r) = 1.5 + r$$

$m$	$k_0$	$l$	$k$	$k_{\text{asympt}}$	$ \det(k) $	$ \partial_k \det(k) $	$\frac{ \det(k) }{\ T(k)\ _F}$	$ k - k_{\text{asympt}} $
1	1	6	2.3573676407577873 - 0.5820419051788126im	1.8200470263362465	1.57e-15	1.71e+00	6.10e-16	7.92e-01
2	2	4	3.676563387273686 - 0.43451946674734865im	3.542548925725047	2.25e-08	1.81e+00	8.74e-09	4.55e-01
3	3	4	4.9645216831943495 - 0.3132395128737777im	4.979499565390129	2.58e-10	2.03e+00	8.57e-11	3.14e-01
4	4	5	6.2318202354950385 - 0.21855409808217305im	6.308316746647625	1.42e-14	2.35e+00	3.59e-15	2.32e-01
5	5	5	7.480957938826707 - 0.1474128807045029im	7.578289435972096	1.40e-10	2.78e+00	2.53e-11	1.77e-01
6	6	5	8.712536676603357 - 0.09598428277781516im	8.810501058485475	5.20e-08	3.36e+00	6.64e-09	1.37e-01
7	7	6	9.926896921138045 - 0.06030041686723931im	10.016070612813092	1.25e-12	4.12e+00	1.11e-13	1.08e-01
8	8	6	11.124682864606768 - 0.03657763695264314im	11.201649081379276	4.38e-10	5.15e+00	2.70e-11	8.52e-02
9	9	6	12.306988672724527 - 0.021466411871924853im	12.371565391471394	3.41e-08	6.54e+00	1.45e-09	6.81e-02
10	10	7	13.475279254512278 - 0.012224951146831323im	13.528813195439396	6.91e-14	8.45e+00	2.03e-15	5.49e-02
11	11	7	14.63120648103238 - 0.00677943788410014im	14.67555940908813	1.03e-11	1.11e+01	2.09e-13	4.49e-02
12	12	7	15.776419738148194 - 0.003674002402732517im	15.813429359972528	5.77e-10	1.47e+01	8.01e-12	3.72e-02
13	13	7	16.91243065132815 - 0.001952137147955008im	16.94367743551207	1.55e-08	1.97e+01	1.47e-10	3.13e-02
14	14	7	18.040546516976722 - 0.0010198704617168162im	18.067294642970015	2.42e-07	2.67e+01	1.57e-09	2.68e-02
15	15	8	19.16185796057901 - 0.0005251556197799022im	19.185079333131803	1.88e-13	3.66e+01	8.32e-16	2.32e-02
16	16	8	20.27725778042725 - 0.00026704487704611507im	20.29768536713728	5.14e-12	5.04e+01	1.55e-14	2.04e-02
17	17	8	21.3874742426067617 - 0.00013431599979152925im	21.40565590968485	1.33e-10	6.98e+01	2.73e-13	1.82e-02
18	18	8	22.49309454921572 - 6.690861416570675e-5im	22.509447748359143	2.28e-09	9.74e+01	3.17e-12	1.64e-02
19	19	8	23.59461159693222 - 3.304543402363117e-5im	23.609449184542648	2.81e-08	1.36e+02	2.65e-11	1.48e-02
20	20	8	24.692428900104026 - 1.6196705740375406e-5im	24.705993450867247	2.65e-07	1.92e+02	1.69e-10	1.36e-02
21	21	8	25.786887539073486 - 7.887557155910364e-6im	25.79936894593014	1.99e-06	2.72e+02	8.57e-10	1.25e-02
22	22	8	26.87827788874823 - 3.823950202481914e-6im	26.889827159800383	1.24e-05	3.86e+02	3.61e-09	1.15e-02
23	23	9	27.966849944790354 - 1.8329333580810445e-6im	27.977588894610072	6.26e-12	5.49e+02	1.22e-15	1.07e-02
24	24	9	29.052820810206107 - 8.766364380636033e-7im	29.06284920654482	9.33e-11	7.84e+02	1.23e-14	1.00e-02
25	25	9	30.136380880710707 - 4.172070040049025e-7im	30.1457813753308	1.14e-09	1.12e+03	1.01e-13	9.40e-03
26	26	9	31.2176982713856 - 1.9764484924768173e-7im	31.226540124522074	1.11e-08	1.61e+03	6.57e-13	8.84e-03
27	27	9	32.29692243097661 - 9.320610295038761e-8im	32.305264257862746	9.00e-08	2.32e+03	3.58e-12	8.34e-03
28	28	9	33.374186991337105 - 4.371441071891802e-8im	33.38207883567084	6.25e-07	3.36e+03	1.67e-11	7.89e-03
29	29	9	34.44961206260746 - 2.0459804717643096e-8im	34.457096985326004	3.78e-06	4.86e+03	6.75e-11	7.48e-03
30	30	9	35.523306104315296 - 1.0641877146982796e-8im	35.53042141806988	2.02e-05	7.04e+03	2.42e-10	7.12e-03
31	31	9	36.595367466796716 - 1.1265680222109211e-8im	36.60214570811019	9.73e-05	1.02e+04	7.75e-10	6.78e-03
32	32	9	37.66588567142305 - 2.8513979650907355e-8im	37.672355377857365	4.24e-04	1.49e+04	2.26e-09	6.47e-03
33	33	9	38.73494247915084 - 7.92147613395413e-8im	38.741128823903914	1.70e-03	2.17e+04	6.03e-09	6.19e-03
34	34	10	39.80261284730119 - 4.39217646395791e-10im	39.808538111302695	9.00e-10	3.17e+04	2.13e-15	5.93e-03
35	35	10	40.868965643398674 - 2.0202369694082143e-10im	40.874649658250384	8.43e-09	4.63e+04	1.33e-14	5.68e-03
36	36	10	41.93406434311159 - 9.345971072353194e-11im	41.93952482903842	6.13e-08	6.78e+04	6.44e-14	5.46e-03
37	37	10	42.997967599819276 - 4.609836046602509e-11im	43.00322044980071	3.96e-07	9.95e+04	2.77e-13	5.25e-03
38	38	10	44.060729740027114 - 2.940002741054361e-11im	44.06578925895063	2.29e-06	1.46e+05	1.07e-12	5.06e-03
39	39	10	45.122401195888116 - 1.9493422840842457e-11im	45.12728030209938	1.21e-05	2.15e+05	3.74e-12	4.88e-03
40	40	10	46.1830288344493 + 4.866384905060397e-11im	46.18773927956334	5.88e-05	3.16e+05	1.20e-11	4.71e-03
41	41	10	47.24265653480356 + 3.791227230191699e-10im	47.24720885320857	2.63e-04	4.67e+05	3.58e-11	4.55e-03
42	42	10	48.30132499107982 + 1.4686769375326877e-9im	48.30572891827697	1.10e-03	6.89e+05	9.91e-11	4.40e-03
43	43	10	49.35907246188665 + 4.217386704837359e-9im	49.363336844938146	4.29e-03	1.02e+06	2.57e-10	4.26e-03
44	44	10	50.415934756216246 + 9.669805674472577e-9im	50.420067693571504	1.58e-02	1.50e+06	6.25e-10	4.13e-03
45	45	10	51.47194548863522 + 1.7730719998937296e-8im	51.47595440717377	5.49e-02	2.23e+06	1.44e-09	4.01e-03
46	46	10	52.52713626356818 + 2.390699063123695e-8im	52.531027983781414	1.82e-01	3.30e+06	3.16e-09	3.89e-03
47	47	10	53.58153683905053 + 1.3151384438663937e-8im	53.58531763137755	5.73e-01	4.90e+06	6.59e-09	3.78e-03
48	48	11	54.635175036559104 - 1.6943669372972442e-14im	54.63885090740074	2.85e-07	7.27e+06	2.17e-15	3.68e-03
49	49	11	55.688077623105926 + 6.92655536290001e-14im	55.69165384467785	1.94e-06	1.08e+07	9.76e-15	3.58e-03
50	50	11	56.740269497531784 + 5.370357023749876e-13im	56.74375106535498	1.05e-05	1.61e+07	3.49e-14	3.48e-03
51	51	11	57.791774330993064 + 2.1470789016016066e-12im	57.79516588418901	5.14e-05	2.39e+07	1.13e-13	3.39e-03
52	52	11	58.84261454853737 + 5.848969316166994e-12im	58.8459204023848	2.36e-04	3.56e+07	3.42e-13	3.31e-03
53	53	11	59.89281141811578 + 1.0362770107215933e-11im	59.89603559300906	1.02e-03	5.30e+07	9.77e-13	3.22e-03
54	54	11	60.94238513161088 + 4.1812227296686558e-12im	60.94553137888412	4.18e-03	7.91e+07	2.64e-12	3.15e-03
55	55	11	61.99135487873204 - 5.221027830990682e-11im	61.99442670375053	1.62e-02	1.18e+08	6.75e-12	3.07e-03
56	56	11	63.03973891451266 - 2.5335983166155016e-10im	63.042739597393776	6.01e-02	1.76e+08	1.65e-11	3.00e-03
57	57	11	64.08755462104384 - 7.6911035912675e-10im	64.09048723534612	2.12e-01	2.64e+08	3.83e-11	2.93e-03
58	58	11	65.13481856400033 - 1.8103995980296717e-9im	65.13768599370314	7.19e-01	3.94e+08	8.55e-11	2.87e-03
59	59	11	66.1815465444749 - 3.449010178245752e-9im	66.18435149953305	2.34e+00	5.90e+08	1.83e-10	2.80e-03
60	60	11	67.2277536466534 - 5.1623420435234645e-9im	67.2304986773022	7.33e+00	8.84e+08	3.78e-10	2.75e-03

Table S-8: Results obtained by the Newton method for  $n_1(r) = 1.5 + r$ ,  $n_2 = 1$ ,  $\xi = 0.5$  starting from  $k_0 = \frac{m}{\xi n_0}$ . We took here  $\varepsilon = 1e-8$  and  $l_{\text{max}} = 2000$ .

$$n_1(r) = 1 + r$$

$m$	$k_0$	$l$	$k$	$k_{\text{asympt}}$	$ \det(k) $	$ \partial_k \det(k) $	$\frac{ \det(k) }{\ T(k)\ _F}$	$ k - k_{\text{asympt}} $
1	1.33	9	13.602746351567303 - 1.2941451159878599im	0.97222155979372	1.50e-11	1.09e+00	1.73e-12	1.27e+01
2	2.67	6	4.800842869405789 - 1.183070967313181im	3.739093521053414	3.75e-11	1.05e+00	1.08e-11	1.59e+00
3	4	5	6.435809549914782 - 1.0457273636322453im	5.852012676075551	1.46e-10	1.02e+00	4.53e-11	1.20e+00
4	5.33	5	8.044440569723108 - 0.918011144092654im	7.73893601066758	6.66e-14	1.02e+00	2.15e-14	9.68e-01
5	6.67	5	9.636426835812768 - 0.8011294949004661im	9.510506071020615	1.11e-14	1.04e+00	3.55e-15	8.11e-01
6	8	5	11.216277798909314 - 0.6951459775408366im	11.211474721375804	2.64e-14	1.07e+00	8.12e-15	6.95e-01
7	9.33	5	12.786368558462707 - 0.5996993138799153im	12.864406898379844	1.56e-12	1.12e+00	4.44e-13	6.05e-01
8	10.67	5	14.348045195688 - 0.5142616881099401im	14.48231292039349	7.10e-11	1.17e+00	1.80e-11	5.32e-01
9	12	5	15.902103958028206 - 0.4382396502466293im	16.073405701871685	1.97e-09	1.24e+00	4.39e-10	4.71e-01
10	13.33	5	17.44902725545988 - 0.37101500363312206im	17.64322015807435	3.37e-08	1.32e+00	6.48e-09	4.19e-01
11	14.67	6	18.98911213006 - 0.3119615421532im	19.195675362475026	5.12e-14	1.41e+00	8.46e-15	3.74e-01
12	16	6	20.522546323740904 - 0.2604515540393857im	20.733655528929173	2.10e-12	1.51e+00	2.97e-13	3.35e-01
13	17.33	6	22.04945656131828 - 0.21585932877096295im	22.25935008430728	7.02e-11	1.63e+00	8.43e-12	3.01e-01
14	18.67	6	23.56994101652031 - 0.17756367539278137im	23.77446379652114	1.41e-09	1.76e+00	1.44e-10	2.71e-01
15	20	6	25.08409185062345 - 0.14495128270767368im	25.280352483656912	1.85e-08	1.91e+00	1.60e-09	2.44e-01
16	21.33	7	26.5920108576689 - 0.11742119548418033im	26.778113950309482	1.55e-14	2.09e+00	1.13e-15	2.20e-01
17	22.67	7	28.093820003084957 - 0.0943903852758443im	28.268650851725607	2.67e-13	2.29e+00	1.65e-14	1.99e-01
18	24	7	29.58966745672592 - 0.07530001975990316im	29.75271532810661	6.84e-12	2.51e+00	3.58e-13	1.80e-01
19	25.33	7	31.079730076218894 - 0.05962189516545331im	31.230941437449935	1.17e-10	2.77e+00	5.16e-12	1.63e-01
20	26.67	7	32.56421272289772 - 0.046864387643311654im	32.70386920428691	1.38e-09	3.07e+00	5.15e-11	1.47e-01
21	28	7	34.043345106794526 - 0.03657735239555499im	34.17196277287918	1.20e-08	3.41e+00	3.78e-10	1.34e-01
22	29.33	7	35.51737684558089 - 0.028355531654709637im	35.63562432925074	8.06e-08	3.81e+00	2.14e-09	1.22e-01
23	30.67	7	36.98657145553082 - 0.021840221964071024im	37.0952049307877	4.34e-07	4.27e+00	9.70e-09	1.11e-01
24	32	8	38.45120033698413 - 0.016719286265063603im	38.55101303848046	4.16e-13	4.80e+00	7.83e-15	1.01e-01
25	33.33	8	39.91153584655681 - 0.012725380198164082im	40.00332131716136	5.29e-12	5.42e+00	8.38e-14	9.27e-02
26	34.67	8	41.36784677100592 - 0.009633156582191504im	41.45237211242877	5.28e-11	6.13e+00	7.03e-13	8.51e-02
27	36	8	42.82039335645103 - 0.007255392838604364im	42.89838190415723	4.15e-10	6.96e+00	4.65e-12	7.83e-02
28	37.33	8	44.269423991668 - 0.0054386626979423865im	44.34154495968992	2.67e-09	7.92e+00	2.51e-11	7.23e-02
29	38.67	8	45.71517284980216 - 0.004058817661396753im	45.782036354765616	1.44e-08	9.04e+00	1.14e-10	6.70e-02
30	40	8	47.157858490294146 - 0.0030165632734921216im	47.220014490234455	6.69e-08	1.04e+01	4.43e-10	6.22e-02
31	41.33	8	48.59768326837528 - 0.00223332872743454im	48.65562320317919	2.73e-07	1.19e+01	1.51e-09	5.80e-02
32	42.67	8	50.03483337581177 - 0.0016475546272814875im	50.088993549139026	9.90e-07	1.37e+01	4.60e-09	5.42e-02
33	44	9	51.46947926720615 - 0.0012112618157749586im	51.52024531563029	3.89e-13	1.57e+01	1.51e-15	5.08e-02
34	45.33	9	52.90177678374547 - 0.0008877332098896368im	52.94948831460949	3.14e-12	1.82e+01	1.02e-14	4.77e-02
35	46.67	9	54.33186780756634 - 0.0006486994944277913im	54.3768234918904	2.07e-11	2.10e+01	5.64e-14	4.50e-02
36	48	9	55.75988159374283 - 0.0004727144170449162im	55.80234388406681	1.21e-10	2.43e+01	2.75e-13	4.25e-02
37	49.33	9	57.18593586701386 - 0.000343572960575929im	57.22613544766607	6.21e-10	2.83e+01	1.18e-12	4.02e-02
38	50.67	9	58.610137938101595 - 0.0002490969327138568im	58.64827778067497	2.86e-09	3.28e+01	4.55e-12	3.81e-02
39	52	9	60.0325857605627 - 0.00018017973874448622im	60.068844752945786	1.19e-08	3.82e+01	1.58e-11	3.63e-02
40	53.33	9	61.453368909229795 - 0.00013004249337385338im	61.48790505909003	4.53e-08	4.46e+01	5.01e-11	3.45e-02
41	54.67	9	62.87256947137938 - 9.365957120010886e-5im	62.905522705138985	1.59e-07	5.20e+01	1.46e-10	3.30e-02
42	56	9	64.29026284903895 - 6.731802422403697e-5im	64.32175743836696	5.15e-07	6.08e+01	3.96e-10	3.15e-02
43	57.33	9	65.7065184759801 - 4.828168127268904e-5im	65.73666512814364	1.56e-06	7.12e+01	1.00e-09	3.01e-02
44	58.67	9	67.1214004562677 - 3.453720344330811e-5im	67.15029810443183	4.45e-06	8.34e+01	2.37e-09	2.89e-02
45	60	9	68.5349681326056 - 2.4605905537424205e-5im	68.56270545951888	1.20e-05	9.78e+01	5.33e-09	2.77e-02
46	61.33	10	69.94727646902473 - 1.7648735177175025e-5im	69.97393331772325	4.76e-12	1.15e+02	1.76e-15	2.67e-02
47	62.67	10	71.35837670547025 - 1.2576414170964056e-5im	71.38402507711324	2.52e-11	1.35e+02	7.74e-15	2.56e-02
48	64	10	72.76831653700052 - 8.948319875666202e-6im	72.79302162669013	1.19e-10	1.59e+02	3.04e-14	2.47e-02
49	65.33	10	74.17714053420661 - 6.357610752242654e-6im	74.20096154199649	5.08e-10	1.87e+02	1.08e-13	2.38e-02
50	66.67	10	75.58489042225375 - 4.510645260220755e-6im	75.60788126169965	2.01e-09	2.20e+02	3.55e-13	2.30e-02
51	68	10	76.99160533979665 - 3.195931630331396e-6im	77.01381524735261	7.45e-09	2.60e+02	1.09e-12	2.22e-02
52	69.33	10	78.39732206776739 - 2.261435651376025e-6im	78.41879612824042	2.59e-08	3.07e+02	3.15e-12	2.15e-02
53	70.67	10	79.80207523208226 - 1.598044315861328e-6im	79.82285483297078	8.46e-08	3.63e+02	8.56e-12	2.08e-02
54	72	10	81.20589748377536 - 1.1275753513992965e-6im	81.22602070925426	2.62e-07	4.29e+02	2.20e-11	2.01e-02
55	73.33	10	82.60881965956104 - 7.941980566180889e-7im	82.62832163313803	7.71e-07	5.07e+02	5.36e-11	1.95e-02
56	74.67	10	84.01087092532448 - 5.585030665995034e-7im	84.02978410880078	2.16e-06	6.01e+02	1.25e-10	1.89e-02
57	76	10	85.41207890450451 - 3.9369579149573007e-7im	85.43043335988082	5.79e-06	7.12e+02	2.77e-10	1.84e-02
58	77.33	10	86.8124697927887 - 2.834113226663404e-7im	86.83029341319607	1.49e-05	8.44e+02	5.91e-10	1.78e-02
59	78.67	10	88.21206846009586 - 2.2037563320102512e-7im	88.22938717561152	3.69e-05	1.00e+03	1.21e-09	1.73e-02
60	80	10	89.61089854069313 - 2.045670437835238e-7im	89.62773650472413	8.79e-05	1.19e+03	2.39e-09	1.68e-02

Table S-9: Results obtained by the Newton method for  $n_1(r) = 1 + r$ ,  $n_2 = 1$ ,  $\xi = 0.5$  starting from  $k_0 = \frac{m}{\xi n_0}$ . We took here  $\varepsilon = 1e-8$  and  $l_{\text{max}} = 2000$ .

$$n_1(r) = 3(1 - r)$$

$m$	$k_0$	$l$	$k$	$k_{\text{asympt}}$	$ \det(k) $	$ \partial_k \det(k) $	$\frac{ \det(k) }{\ T(k)\ _F}$	$ k - k_{\text{asympt}} $
1	1.33	9	5.0550018091851285 - 0.6248886757558838im	4.161760458079524	8.68e-11	2.43e+00	1.91e-11	1.09e+00
2	2.67	9	3.793068555579194 - 0.3612720296024689im	5.495093791412857	1.43e-10	2.73e+00	5.06e-11	1.74e+00
3	4	7	5.211463134482563 - 0.2775990463435686im	6.82842712474619	3.45e-11	2.96e+00	1.11e-11	1.64e+00
4	5.33	6	6.624138531594931 - 0.20983062483433862im	8.161760458079524	1.13e-08	3.33e+00	3.09e-09	1.55e+00
5	6.67	6	8.031924435987753 - 0.15618584407704272im	9.495093791412858	1.32e-10	3.82e+00	2.94e-11	1.47e+00
6	8	6	9.43467283612071 - 0.11452520508310852im	10.82842712474619	7.23e-12	4.46e+00	1.28e-12	1.40e+00
7	9.33	6	10.832115071451929 - 0.08276743632092393im	12.161760458079524	1.03e-12	5.27e+00	1.43e-13	1.33e+00
8	10.67	6	12.224109392150245 - 0.05900049580566784im	13.495093791412856	2.74e-13	6.30e+00	2.99e-14	1.27e+00
9	12	6	13.610702991933767 - 0.04152903086484195im	14.828427124746192	1.15e-13	7.59e+00	9.80e-15	1.22e+00
10	13.33	6	14.992120493693493 - 0.02890000576220863im	16.161760458079524	5.41e-14	9.22e+00	3.62e-15	1.17e+00
11	14.67	6	16.368720814112155 - 0.019910647327633115im	17.495093791412856	2.29e-14	1.13e+01	1.20e-15	1.13e+00
12	16	6	17.74094464337479 - 0.013598881140339688im	18.82842712474619	1.01e-14	1.38e+01	4.15e-16	1.09e+00
13	17.33	6	19.10926590189109 - 0.0092194476200337im	20.161760458079524	2.21e-14	1.70e+01	7.13e-16	1.05e+00
14	18.67	6	20.474154021357652 - 0.006211382402557667im	21.495093791412856	1.03e-13	2.11e+01	2.62e-15	1.02e+00
15	20	6	21.836048870841775 - 0.004162806103337918im	22.828427124746188	2.13e-13	2.61e+01	4.26e-15	9.92e-01
16	21.33	5	23.195346967046568 - 0.002777559860439838im	24.16176045807952	6.32e-07	3.24e+01	9.97e-09	9.66e-01
17	22.67	5	24.552396255705496 - 0.0018464326046760664im	25.49509379141286	6.98e-07	4.03e+01	8.69e-09	9.43e-01
18	24	5	25.907496497829097 - 0.0012236249096686767im	26.828427124746188	7.95e-07	5.01e+01	7.83e-09	9.21e-01
19	25.33	5	27.260902896557074 - 0.0008087541002688868im	28.161760458079524	9.33e-07	6.24e+01	7.27e-09	9.01e-01
20	26.67	5	28.612831244149334 - 0.000533344601000589im	29.49509379141286	1.13e-06	7.78e+01	6.95e-09	8.82e-01
21	28	5	29.963463459116507 - 0.00035104269172285324im	30.82842712474619	1.40e-06	9.71e+01	6.84e-09	8.65e-01
22	29.33	5	31.312952886979065 - 0.0002306655575914565im	32.16176045807952	1.78e-06	1.21e+02	6.91e-09	8.49e-01
23	30.67	5	32.66142905441303 - 0.00015134362795646687im	33.495093791412856	2.33e-06	1.51e+02	7.17e-09	8.34e-01
24	32	5	34.00900176615905 - 9.916882923930642e-5im	34.82842712474619	3.12e-06	1.89e+02	7.62e-09	8.19e-01
25	33.33	5	35.35576454652956 - 6.490505276795219e-5im	36.16176045807952	4.27e-06	2.36e+02	8.28e-09	8.06e-01
26	34.67	5	36.70179748338277 - 4.2436693726562156e-5im	37.495093791412856	5.96e-06	2.94e+02	9.19e-09	7.93e-01
27	36	6	38.04716957090624 - 2.7740466390310082e-5im	38.82842712474619	1.72e-12	3.67e+02	2.10e-15	7.81e-01
28	37.33	6	39.39194054619569 - 1.8111278402523637e-5im	40.16176045807953	6.86e-13	4.59e+02	6.69e-16	7.70e-01
29	38.67	6	40.736162489797366 - 1.1816353040657862e-5im	41.495093791412856	2.20e-12	5.73e+02	1.71e-15	7.59e-01
30	40	6	42.079881041701725 - 7.704546109343315e-6im	42.82842712474619	6.50e-12	7.16e+02	4.01e-15	7.49e-01
31	41.33	6	43.42313642010548 - 5.020722490734482e-6im	44.16176045807953	7.83e-13	8.94e+02	3.85e-16	7.39e-01
32	42.67	6	44.765964248473665 - 3.2701218933887567e-6im	45.495093791412856	1.05e-11	1.12e+03	4.10e-15	7.29e-01
33	44	6	46.10839623325855 - 2.128925424223715e-6im	46.8284271247462	1.40e-11	1.40e+03	4.37e-15	7.20e-01
34	45.33	6	47.45046072205144 - 1.3853949067354885e-6im	48.16176045807953	2.26e-11	1.74e+03	5.61e-15	7.11e-01
35	46.67	6	48.79218316579931 - 9.01195840046244e-7im	49.495093791412856	4.75e-11	2.18e+03	9.40e-15	7.03e-01
36	48	6	50.13358650378857 - 5.860184658471562e-7im	50.828427124746185	6.31e-11	2.72e+03	9.96e-15	6.95e-01
37	49.33	6	51.47469148618586 - 3.809452233432185e-7im	52.16176045807953	1.42e-10	3.40e+03	1.79e-14	6.87e-01
38	50.67	6	52.81551694584535 - 2.4756209937630865e-7im	53.495093791412856	2.66e-10	4.25e+03	2.67e-14	6.80e-01
39	52	6	54.15608002867527 - 1.608371619236838e-7im	54.82842712474619	5.81e-10	5.31e+03	4.65e-14	6.72e-01
40	53.33	6	55.49639638996398 - 1.0446688437585891e-7im	56.16176045807952	1.06e-09	6.63e+03	6.79e-14	6.65e-01
41	54.67	6	56.83648036258345 - 6.783747098060616e-8im	57.49509379141285	2.18e-09	8.28e+03	1.11e-13	6.59e-01
42	56	6	58.17634510182636 - 4.404206286732895e-8im	58.82842712474619	4.47e-09	1.03e+04	1.82e-13	6.52e-01
43	57.33	6	59.516002710717785 - 2.858772448619e-8im	60.16176045807953	8.93e-09	1.29e+04	2.91e-13	6.46e-01
44	58.67	6	60.8554643489219 - 1.8552747286546934e-8im	61.495093791412856	1.85e-08	1.61e+04	4.79e-13	6.40e-01
45	60	6	62.194740327791585 - 1.2037716510580575e-8im	62.82842712474619	3.65e-08	2.02e+04	7.56e-13	6.34e-01
46	61.33	6	63.533840193653994 - 7.808136365496758e-9im	64.16176045807953	7.33e-08	2.52e+04	1.21e-12	6.28e-01
47	62.67	6	64.87277280105982 - 5.061904355440123e-9im	65.49509379141284	1.46e-07	3.14e+04	1.93e-12	6.22e-01
48	64	6	66.21154637743213 - 3.278163104214401e-9im	66.82842712474618	2.90e-07	3.93e+04	3.07e-12	6.17e-01
49	65.33	6	67.550168580312 - 2.1191076120991594e-9im	68.16176045807953	5.74e-07	4.90e+04	4.85e-12	6.12e-01
50	66.67	6	68.88864654820604 - 1.3663536644811713e-9im	69.49509379141286	1.13e-06	6.12e+04	7.63e-12	6.06e-01
51	68	6	70.22698694588337 - 8.797308830994168e-10im	70.82842712474618	2.21e-06	7.65e+04	1.19e-11	6.01e-01
52	69.33	6	71.56519600483867 - 5.706680383336926e-10im	72.16176045807951	4.31e-06	9.55e+04	1.86e-11	5.97e-01
53	70.67	6	72.90327955953245 - 3.849281561085858e-10im	73.49509379141287	8.35e-06	1.19e+05	2.88e-11	5.92e-01
54	72	6	74.24124307992899 - 2.91249068141831e-10im	74.8284271247462	1.61e-05	1.49e+05	4.44e-11	5.87e-01
55	73.33	6	75.57909170077959 - 2.735230847935135e-10im	76.16176045807953	3.08e-05	1.86e+05	6.80e-11	5.83e-01
56	74.67	6	76.91683024803483 - 3.2480477018546124e-10im	77.49509379141286	5.87e-05	2.32e+05	1.04e-10	5.78e-01
57	76	6	78.25446326271873 - 4.4191674367209546e-10im	78.8284271247462	1.11e-04	2.90e+05	1.57e-10	5.74e-01
58	77.33	6	79.59199502255204 - 6.196090149136291e-10im	80.16176045807951	2.09e-04	3.62e+05	2.36e-10	5.70e-01
59	78.67	6	80.92942956157428 - 8.434936713466322e-10im	81.49509379141287	3.91e-04	4.51e+05	3.53e-10	5.66e-01
60	80	6	82.26677068798257 - 1.0810012371326823e-9im	82.82842712474618	7.28e-04	5.63e+05	5.26e-10	5.62e-01

Table S-10: Results obtained by the Newton method for  $n_1(r) = 3(1 - r)$ ,  $n_2 = 1$ ,  $\xi = 0.5$  starting from  $k_0 = \frac{m}{\xi n_0}$ . We took here  $\varepsilon = 1e-8$  and  $l_{\text{max}} = 2000$ .

$$n_1(r) = -2.8r + 2.5$$

$m$	$k_0$	$l$	$k$	$k_{\text{asympt}}$	$ \det(k) $	$ \partial_k \det(k) $	$\frac{ \det(k) }{\ T(k)\ _F}$	$ k - k_{\text{asympt}} $
1	1.82	17	7.924919667036129 - 2.7112347145700677im	3.059135351886293	5.18e-08	7.76e+00	4.36e-09	5.57e+00
2	3.64	7	8.37697526088352 - 1.1970651616679695im	4.851135351886293	9.84e-09	2.13e+00	1.11e-09	3.72e+00
3	5.45	7	10.164172357599108 - 1.1715053777822293im	6.643135351886293	3.11e-14	1.85e+00	3.69e-15	3.71e+00
4	7.27	7	11.945784263931984 - 1.1385426036460573im	8.435135351886293	5.35e-14	1.71e+00	6.59e-15	3.69e+00
5	9.09	7	13.724183225760296 - 1.1022390897528125im	10.227135351886291	8.15e-14	1.64e+00	1.03e-14	3.67e+00
6	10.91	7	15.500792465870116 - 1.0645281109812703im	12.019135351886291	2.05e-12	1.61e+00	2.65e-13	3.64e+00
7	12.73	7	17.276486339139304 - 1.0264260048504945im	13.811135351886294	1.31e-10	1.60e+00	1.73e-11	3.61e+00
8	14.55	7	19.051817511163566 - 0.9885010118022203im	15.603135351886294	1.63e-08	1.60e+00	2.20e-09	3.59e+00
9	16.36	8	20.827143637265124 - 0.9510827663087211im	17.395135351886296	1.91e-12	1.60e+00	2.63e-13	3.56e+00
10	18.18	9	22.60269991987898 - 0.9143659662302194im	19.187135351886294	5.00e-14	1.62e+00	7.02e-15	3.54e+00
11	20	10	24.378642374743507 - 0.8784655205985158im	20.979135351886296	1.17e-13	1.63e+00	1.68e-14	3.51e+00
12	21.82	17	30.38943218753896 - 2.2460769149097035im	22.77113535188629	5.13e-13	6.83e-01	5.23e-14	7.94e+00
13	23.64	13	24.711964653174864 - 0.35390624826554373im	24.56313535188629	2.88e-09	2.19e+00	6.09e-10	3.84e-01
14	25.45	10	26.504913721208297 - 0.32890589273895im	26.355135351886297	3.11e-09	2.26e+00	6.37e-10	3.61e-01
15	27.27	9	28.298019385287773 - 0.30559492302475816im	28.147135351886295	3.66e-08	2.34e+00	7.23e-09	3.41e-01
16	29.09	9	30.091268883439273 - 0.2838537452584024im	29.939135351886293	4.39e-11	2.42e+00	8.36e-12	3.22e-01
17	30.91	9	31.88464488214092 - 0.263574304576328im	31.731135351886287	1.36e-13	2.51e+00	2.50e-14	3.05e-01
18	32.73	8	33.678127668323974 - 0.24465832960536904im	33.523135351886296	3.93e-08	2.61e+00	6.91e-09	2.90e-01
19	34.55	8	35.471696351962656 - 0.22701592385323294im	35.3151353518863	3.78e-09	2.72e+00	6.38e-10	2.76e-01
20	36.36	8	37.26532995608981 - 0.2105643988931974im	37.107135351886285	4.49e-10	2.83e+00	7.25e-11	2.63e-01
21	38.18	8	39.059007878190805 - 0.19522735188970902im	38.899135351886294	6.21e-11	2.95e+00	9.61e-12	2.52e-01
22	40	8	40.852710395471384 - 0.18093388034508504im	40.691135351886295	9.52e-12	3.07e+00	1.41e-12	2.43e-01
23	41.82	8	42.646418921109 - 0.16761795535340046im	42.4831353518863	1.54e-12	3.21e+00	2.18e-13	2.34e-01
24	43.64	8	44.44011618187979 - 0.15521789627445226im	44.27513535188629	2.32e-13	3.35e+00	3.14e-14	2.27e-01
25	45.45	8	46.23378632248428 - 0.14367593674467627im	46.067135351886286	6.41e-14	3.50e+00	8.27e-15	2.20e-01
26	47.27	8	48.02741495748448 - 0.1329378626305127im	47.859135351886295	6.31e-14	3.66e+00	7.78e-15	2.14e-01
27	49.09	7	49.820989172745755 - 0.12295271033715599im	49.651135351886296	4.70e-08	3.83e+00	5.53e-09	2.10e-01
28	50.91	7	51.614497571948604 - 0.11367250609978563im	51.44313535188629	1.58e-08	4.00e+00	1.78e-09	2.06e-01
29	52.73	7	53.40793011811359 - 0.10505204623755078im	53.23513535188629	4.82e-09	4.19e+00	5.16e-10	2.02e-01
30	54.55	7	55.2012782028307 - 0.09704873257476901im	55.027135351886294	1.30e-09	4.39e+00	1.32e-10	1.99e-01
31	56.36	7	56.99453452942706 - 0.0896223816056731im	56.819135351886295	3.01e-10	4.60e+00	2.93e-11	1.97e-01
32	58.18	7	58.787693045713475 - 0.08273509879291595im	58.61113535188629	5.88e-11	4.82e+00	5.46e-12	1.95e-01
33	60.00	7	60.58074887182462 - 0.07635115204247592im	60.403135351886284	9.42e-12	5.06e+00	8.34e-13	1.93e-01
34	61.82	7	62.37369821961381 - 0.07043685830493594im	62.195135351886286	1.25e-12	5.31e+00	1.05e-13	1.92e-01
35	63.64	7	64.16653831024476 - 0.06496048156938178im	63.987135351886295	1.48e-13	5.57e+00	1.19e-14	1.91e-01
36	65.45	7	65.95926729145538 - 0.05989213883492715im	65.77913535188628	1.17e-14	5.85e+00	8.99e-16	1.90e-01
37	67.27	6	67.75188415614063 - 0.05520370580526653im	67.5711353518863	4.06e-08	6.14e+00	2.97e-09	1.89e-01
38	69.09	6	69.54438865714904 - 0.05086876577786841im	69.3631353518863	7.82e-09	6.45e+00	5.46e-10	1.88e-01
39	70.91	6	71.33678123858921 - 0.0468624709739395im	71.15513535188627	1.22e-09	6.78e+00	8.11e-11	1.88e-01
40	72.73	6	73.12906294884523 - 0.04316152173560448im	72.94713535188629	1.48e-10	7.12e+00	9.45e-12	1.87e-01
41	74.55	6	74.92123537496299 - 0.039744071128104734im	74.73913535188628	1.37e-11	7.48e+00	8.30e-13	1.86e-01
42	76.36	6	76.71330057236737 - 0.0365896564435685im	76.53113535188629	9.37e-13	7.87e+00	5.43e-14	1.86e-01
43	78.18	6	78.50526100024688 - 0.03367913124926142im	78.3231353518863	6.52e-14	8.27e+00	3.61e-15	1.85e-01
44	80	5	80.2971194614906 - 0.030994607229059584im	80.1151353518863	7.31e-08	8.70e+00	3.86e-09	1.85e-01
45	81.82	5	82.08887904554395 - 0.02851934840480773im	81.9071353518863	9.82e-09	9.15e+00	4.95e-10	1.84e-01
46	83.64	5	83.88054307876568 - 0.02623778682844393im	83.6991353518863	9.61e-10	9.62e+00	4.63e-11	1.83e-01
47	85.45	5	85.67211507550046 - 0.02413538750749404im	85.4911353518863	6.37e-11	1.01e+01	2.93e-12	1.83e-01
48	87.27	5	87.46359869546593 - 0.022198621256883697im	87.28313535188629	2.59e-12	1.06e+01	1.14e-13	1.82e-01
49	89.09	5	89.25499770494528 - 0.020414903202032327im	89.07513535188627	1.94e-13	1.12e+01	8.17e-15	1.81e-01
50	90.91	4	91.04631594295964 - 0.01877254069238944im	90.86713535188629	5.00e-08	1.18e+01	2.01e-09	1.80e-01
51	92.73	4	92.83755728442577 - 0.01726065951862863im	92.65913535188629	2.59e-09	1.24e+01	9.95e-11	1.79e-01
52	94.55	4	94.62872562404067 - 0.0158691922971560005im	94.4511353518863	5.16e-11	1.30e+01	1.90e-12	1.78e-01
53	96.36	4	96.41982484069513 - 0.014588790429884878im	96.2431353518863	4.76e-13	1.37e+01	1.67e-14	1.77e-01
54	98.18	3	98.21085878294456 - 0.013410795421105522im	98.0351353518863	1.14e-08	1.44e+01	3.84e-10	1.76e-01
55	100.00	3	100.00183124581129 - 0.012327190597652627im	99.82713535188628	7.86e-12	1.52e+01	2.52e-13	1.75e-01
56	101.82	3	101.79274596357453 - 0.011330558581350531im	101.6191353518863	6.31e-09	1.60e+01	1.94e-10	1.74e-01
57	103.64	4	103.58360658711511 - 0.010414041062372249im	103.4111353518863	3.92e-13	1.68e+01	1.15e-14	1.73e-01
58	105.45	4	105.37441668055968 - 0.00957129888327655im	105.20313535188627	4.37e-10	1.77e+01	1.23e-11	1.72e-01
59	107.27	4	107.16517970551287 - 0.008796474723500942im	106.99513535188628	7.39e-08	1.96e+01	1.99e-09	1.70e-01
60	109.09	5	108.95589902956841 - 0.008084171985163967im	108.78713535188628	2.92e-12	1.96e+01	7.53e-14	1.69e-01

Table S-11: Results obtained by the Newton method for  $n_1(r) = -2.8r + 2.5$ ,  $n_2 = 1$ ,  $\xi = 0.5$  starting from  $k_0 = \frac{m}{\xi n_0}$ . We took here  $\varepsilon = 1e-8$  and  $l_{\text{max}} = 2000$ .

$$n_1(r) = -2.8r + 2.5$$

$m$	$k_0$	$l$	$k$	$k_{\text{asympt}}$	$ \det(k) $	$ \partial_k \det(k) $	$\frac{ \det(k) }{\ T(k)\ _F}$	$ k - k_{\text{asympt}} $
1	1.79	19	7.924919673377272 - 2.711234712507853im	3.059135351886293	1.15e-12	7.76e+00	9.73e-14	5.57e+00
2	3.58	8	8.376975264130033 - 1.1970651649564188im	4.851135351886293	4.52e-12	2.13e+00	5.08e-13	3.72e+00
3	5.38	6	10.164172393807487 - 1.1715053821567618im	6.643135351886293	6.75e-08	1.85e+00	8.01e-09	3.71e+00
4	7.17	6	11.94578427594684 - 1.1385426064549284im	8.435135351886293	2.11e-08	1.71e+00	2.60e-09	3.69e+00
5	8.96	7	13.724183225760338 - 1.1022390897528427im	10.227135351886291	5.62e-15	1.64e+00	7.10e-16	3.67e+00
6	10.75	7	15.500792465869143 - 1.0645281109805322im	12.019135351886291	9.42e-14	1.61e+00	1.22e-14	3.64e+00
7	12.54	7	17.276486339104792 - 1.0264260047759763im	13.811135351886294	1.93e-12	1.60e+00	2.55e-13	3.61e+00
8	14.34	7	19.051817519765606 - 0.9885010062749388im	15.603135351886294	5.62e-11	1.60e+00	7.58e-12	3.59e+00
9	16.13	7	20.827143635948605 - 0.951082765741548im	17.395135351886296	2.30e-09	1.60e+00	3.17e-10	3.56e+00
10	17.92	8	22.602699919878983 - 0.9143659662302159im	19.187135351886294	1.73e-14	1.62e+00	2.43e-15	3.54e+00
11	19.71	8	24.378642374744476 - 0.878465520596773im	20.979135351886296	3.38e-12	1.63e+00	4.83e-13	3.51e+00
12	21.50	8	26.1550743394299 - 0.8434476980538193im	22.77113535188629	2.90e-09	1.65e+00	4.23e-10	3.49e+00
13	23.30	9	27.932063307100197 - 0.8093484385248295im	24.56313535188629	6.77e-13	1.67e+00	1.01e-13	3.46e+00
14	25.09	10	29.70965188059457 - 0.7761845360689912im	26.355135351886297	1.33e-12	1.69e+00	2.01e-13	3.44e+00
15	26.88	17	38.42563994255149 - 1.2007889285996445im	28.147135351886295	6.21e-11	9.63e-01	5.92e-12	1.03e+01
16	28.67	16	38.35400182165353 - 2.17185385340075im	29.939135351886293	9.68e-10	7.10e-01	1.02e-10	8.69e+00
17	30.46	10	35.046205454111096 - 0.6823154450946716im	31.731135351886287	9.93e-13	1.78e+00	1.57e-13	3.38e+00
18	32.26	12	40.2471711994572 - 0.9488770557754486im	33.523135351886296	2.68e-13	1.00e+00	3.52e-14	6.79e+00
19	34.05	12	44.264192424464945 - 2.133710259325852im	35.3151353518863	2.56e-12	5.75e-01	2.72e-13	9.20e+00
20	35.84	13	46.22470677080104 - 2.1231348503504854im	37.107135351886285	5.08e-09	5.28e-01	5.44e-10	9.36e+00
21	37.63	11	45.569311378109795 - 0.8705637649228068im	38.899135351886294	2.57e-10	1.16e+00	3.40e-11	6.73e+00
22	39.42	8	47.343958147106754 - 0.8452524356204417im	40.691135351886295	6.46e-13	1.20e+00	8.58e-14	6.71e+00
23	41.22	7	49.11894304059512 - 0.8203401210184359im	42.4831353518863	2.49e-13	1.25e+00	3.32e-14	6.69e+00
24	43.01	7	50.89428278704891 - 0.7958271190797321im	44.27513535188629	4.07e-12	1.30e+00	5.46e-13	6.67e+00
25	44.80	8	52.66999089881322 - 0.7717133642402609im	46.067135351886286	6.78e-14	1.35e+00	9.13e-15	6.65e+00
26	46.59	10	54.44607813660672 - 0.7479986257853766im	47.859135351886295	1.89e-10	1.39e+00	2.56e-11	6.63e+00
27	48.38	11	59.84539855701591 - 2.067947442775565im	49.651135351886296	7.11e-11	4.01e-01	7.83e-12	1.04e+01
28	50.18	12	61.77911175631261 - 2.0619738377747474im	51.44313535188629	1.26e-11	4.18e-01	1.39e-12	1.05e+01
29	51.97	11	63.71030649676497 - 2.0563448024082094im	53.23513535188629	1.63e-12	4.41e-01	1.81e-13	1.07e+01
30	53.76	10	65.63911580713739 - 2.0510295885880967im	55.027135351886294	1.93e-08	4.68e-01	2.15e-09	1.08e+01
31	55.55	12	67.56566180261024 - 2.046001227879538im	56.819135351886295	1.18e-14	4.97e-01	1.32e-15	1.09e+01
32	57.34	13	69.49005703801322 - 2.041235669209688im	58.61113535188629	1.80e-08	5.25e-01	2.02e-09	1.11e+01
33	59.14	16	71.4124054424669 - 2.036711590754209im	60.403135351886284	5.37e-15	5.51e-01	6.04e-16	1.12e+01
34	60.93	12	73.33280302966797 - 2.0324100538965197im	62.195135351886286	1.18e-09	5.72e-01	1.33e-10	1.13e+01
35	62.72	10	75.25133894442197 - 2.028314047452006im	63.987135351886295	1.07e-08	5.86e-01	1.22e-09	1.14e+01
36	64.51	9	77.16809583675624 - 2.0244082190058155im	65.77913535188628	6.11e-08	5.92e-01	6.97e-09	1.16e+01
37	66.30	12	79.08315105340095 - 2.020679035286402im	67.5711353518863	4.33e-10	5.90e-01	4.96e-11	1.17e+01
38	68.10	8	75.79006974904964 - 0.4946169873841978im	69.3631353518863	3.44e-08	1.96e+00	4.90e-09	6.45e+00
39	69.89	13	80.99552405281761 - 0.7048215855697035im	71.15513535188627	1.33e-08	9.27e-01	1.82e-09	9.87e+00
40	71.68	13	82.77126419913428 - 0.6866546920113008im	72.94713535188629	9.37e-10	9.75e-01	1.29e-10	9.85e+00
41	73.47	10	81.13478699994599 - 0.44039064295231917im	74.73913535188628	1.49e-08	2.11e+00	2.10e-09	6.41e+00
42	75.26	10	88.63525715467108 - 2.0042838629433155im	76.53113535188629	1.81e-09	5.07e-01	2.12e-10	1.23e+01
43	77.06	12	90.54145848955929 - 2.0013893674065426im	78.3231353518863	2.40e-10	4.86e-01	2.81e-11	1.24e+01
44	78.85	10	96.90526797195834 - 0.934574763791481im	80.1151353518863	1.09e-07	1.27e+00	8.92e-09	1.68e+01
45	80.64	11	94.35005233794624 - 1.9959236786640566im	81.9071353518863	3.71e-08	4.48e-01	4.39e-09	1.26e+01
46	82.43	11	96.25253431436398 - 1.9933400030764068im	83.6991353518863	8.01e-10	4.33e-01	9.52e-11	1.27e+01
47	84.22	9	95.20916041037414 - 0.5652744960706997im	85.4911353518863	2.97e-12	1.32e+00	4.11e-13	9.73e+00
48	86.02	9	96.98713837643704 - 0.5487905726372811im	87.28313535188629	5.15e-11	1.37e+00	7.14e-12	9.72e+00
49	87.81	12	101.95320841254598 - 1.9861200346047678im	89.07513535188627	8.95e-11	4.09e-01	1.08e-11	1.30e+01
50	89.60	14	104.01454891156557 - 0.7040192148694097im	90.86713535188629	1.27e-13	5.14e-01	1.70e-14	1.32e+01
51	91.39	12	105.7483785913666 - 1.9817027629996653im	92.65913535188629	8.93e-12	4.13e-01	1.09e-12	1.32e+01
52	93.18	10	118.10228692796544 - 2.0996424340138904im	94.4511353518863	1.94e-11	3.61e-01	1.39e-12	2.37e+01
53	94.98	10	116.40656455949774 - 0.9262750834116645im	96.2431353518863	4.46e-09	1.21e+00	3.46e-10	2.02e+01
54	96.77	16	111.43386300120069 - 1.9755920886559317im	98.0351353518863	8.28e-12	4.47e-01	1.02e-12	1.35e+01
55	98.56	10	113.32720121999776 - 1.9736792075378702im	99.82713535188628	3.20e-09	4.64e-01	3.97e-10	1.36e+01
56	100.35	10	115.21967204040102 - 1.9718233857620906im	101.6191353518863	3.06e-11	4.84e-01	3.81e-12	1.37e+01
57	102.14	10	117.11130020288623 - 1.9700219583098941im	103.4111353518863	9.33e-12	5.05e-01	1.17e-12	1.38e+01
58	103.94	11	119.00210931466334 - 1.9682724149409456im	105.20313535188627	2.75e-10	5.26e-01	3.46e-11	1.39e+01
59	105.73	15	120.89212194455617 - 1.9665724081133815im	106.99513535188628	1.11e-09	5.48e-01	1.40e-10	1.40e+01
60	107.52	11	121.77094976606186 - 0.5570322903639797im	108.78713535188628	2.25e-08	7.28e-01	3.14e-09	1.30e+01

Table S-12: Results obtained by the Newton method for  $n_1(r) = -2.8r + 2.5$ ,  $n_2 = 1$ ,  $\xi = 0.5$  starting from  $k_0 = \frac{m}{\xi_0 n(\xi_0)}$  (leading term in the asymptotics). We took here  $\varepsilon = 1e-8$  and  $l_{\text{max}} = 2000$ .

$$n_1(r) = -2.8r + 2.5$$

$m$	$k_0$	$l$	$k$	$k_{\text{asympt}}$	$ \det(k) $	$ \partial_k \det(k) $	$\frac{ \det(k) }{\ T(k)\ _F}$	$ k - k_{\text{asympt}} $
1	3.06	8	3.126030006549902 - 0.8490620306257869im	3.059135351886293	9.45e-09	2.32e+00	2.24e-09	8.52e-01
2	4.85	8	4.960265572425262 - 0.7930888853914064im	4.851135351886293	2.58e-15	2.21e+00	6.01e-06	8.01e-01
3	6.64	7	6.770901080871078 - 0.7367987701752973im	6.643135351886293	1.14e-14	2.05e+00	2.72e-15	7.48e-01
4	8.44	6	8.572070703674939 - 0.6839781193220764im	8.435135351886293	1.98e-11	1.97e+00	4.79e-12	6.98e-01
5	10.23	6	10.36876216651674 - 0.6350860184782311im	10.227135351886291	1.55e-14	1.92e+00	3.78e-15	6.51e-01
6	12.02	5	12.16318428414382 - 0.5899319796825272im	12.019135351886291	1.49e-08	1.91e+00	3.63e-09	6.07e-01
7	13.81	5	13.956444792753562 - 0.5481968118098185im	13.811135351886294	1.27e-09	1.91e+00	3.07e-10	5.67e-01
8	15.60	5	15.749141359003909 - 0.5095603531707246im	15.603135351886294	1.40e-10	1.94e+00	3.33e-11	5.30e-01
9	17.40	5	17.541609891834206 - 0.4737332319979154im	17.395135351886296	1.86e-11	1.97e+00	4.37e-12	4.96e-01
10	19.19	5	19.33404195716356 - 0.4404616747071416im	19.187135351886294	2.96e-12	2.01e+00	6.80e-13	4.64e-01
11	20.98	5	21.126545358575086 - 0.4095246562003437im	20.979135351886296	5.26e-13	2.06e+00	1.18e-13	4.35e-01
12	22.77	5	22.91917748890154 - 0.3807292820246637im	22.77113535188629	9.91e-14	2.12e+00	2.16e-14	4.08e-01
13	24.56	5	24.71196465218663 - 0.35390624739203197im	24.56313535188629	2.73e-14	2.19e+00	5.78e-15	3.84e-01
14	26.36	5	26.504913720701992 - 0.32890589145736715im	26.355135351886297	1.95e-14	2.26e+00	3.99e-15	3.61e-01
15	28.15	5	28.298019400924126 - 0.30559492191913357im	28.147135351886295	8.64e-15	2.34e+00	1.71e-15	3.41e-01
16	29.94	4	30.09126889687436 - 0.28385374115283685im	29.939135351886293	3.40e-08	2.42e+00	6.47e-09	3.22e-01
17	31.73	4	31.884644887082175 - 0.2635742983927942im	31.731135351886287	1.99e-08	2.51e+00	3.64e-09	3.05e-01
18	33.52	4	33.67812765344491 - 0.2446583257529659im	33.523135351886296	1.23e-08	2.61e+00	2.16e-09	2.90e-01
19	35.32	4	35.47169635124586 - 0.22701592061898712im	35.3151353518863	8.03e-09	2.72e+00	1.35e-09	2.76e-01
20	37.11	4	37.26532995412398 - 0.21056439864554935im	37.107135351886285	5.56e-09	2.83e+00	8.98e-10	2.63e-01
21	38.90	4	39.05900787699128 - 0.1952273525762515im	38.899135351886294	4.08e-09	2.95e+00	6.32e-10	2.52e-01
22	40.69	4	40.852710395190186 - 0.18093388134672558im	40.691135351886295	3.19e-09	3.07e+00	4.73e-10	2.43e-01
23	42.48	4	42.64641892150247 - 0.1676179560810548im	42.4831353518863	2.65e-09	3.21e+00	3.75e-10	2.34e-01
24	44.28	4	44.44011618254973 - 0.1552178964789759im	44.27513535188629	2.34e-09	3.35e+00	3.17e-10	2.27e-01
25	46.07	4	46.233786323042004 - 0.14367593645362683im	46.067135351886286	2.20e-09	3.50e+00	2.84e-10	2.20e-01
26	47.86	4	48.02741495767278 - 0.13293786206248964im	47.859135351886295	2.19e-09	3.66e+00	2.70e-10	2.14e-01
27	49.65	4	49.82098918464871 - 0.1229527080522311im	49.651135351886296	2.30e-09	3.83e+00	2.70e-10	2.10e-01
28	51.44	4	51.61449757089832 - 0.11367250192530574im	51.44313535188629	2.54e-09	4.00e+00	2.85e-10	2.06e-01
29	53.24	4	53.407930116296434 - 0.10505204649514722im	53.23513535188629	2.94e-09	4.19e+00	3.15e-10	2.02e-01
30	55.03	4	55.201278202362595 - 0.09704873355045542im	55.027135351886294	3.55e-09	4.39e+00	3.63e-10	1.99e-01
31	56.82	4	56.994534529574615 - 0.08962238258991599im	56.819135351886295	4.45e-09	4.60e+00	4.33e-10	1.97e-01
32	58.61	4	58.787693046501445 - 0.0827350996855552im	58.61113535188629	5.76e-09	4.82e+00	5.35e-10	1.95e-01
33	60.40	4	60.58074887328337 - 0.07635115243807007im	60.403135351886284	7.66e-09	5.06e+00	6.78e-10	1.93e-01
34	62.20	4	62.373698221490464 - 0.07043685773895014im	62.195135351886286	1.04e-08	5.31e+00	8.79e-10	1.92e-01
35	63.99	4	64.16653831201282 - 0.06496047968182814im	63.987135351886295	1.44e-08	5.57e+00	1.16e-09	1.91e-01
36	65.78	4	65.95926729234613 - 0.05989213549073176im	65.77913535188628	2.02e-08	5.85e+00	1.55e-09	1.90e-01
37	67.57	4	67.75188415440033 - 0.05520370777326841im	67.5711353518863	2.87e-08	6.14e+00	2.11e-09	1.89e-01
38	69.36	4	69.54438865376642 - 0.05086876177463293im	69.3631353518863	4.12e-08	6.45e+00	2.88e-09	1.88e-01
39	71.16	4	71.33678123121109 - 0.04686246661499633im	71.15513535188627	5.92e-08	6.78e+00	3.95e-09	1.88e-01
40	72.95	4	73.12906293702491 - 0.043161519746097755im	72.94713535188629	8.55e-08	7.12e+00	5.44e-09	1.87e-01
41	74.74	4	74.92123535872258 - 0.03974407407034693im	74.73913535188628	1.24e-07	7.48e+00	7.50e-09	1.86e-01
42	76.53	5	76.71330057236749 - 0.03658965644355615im	76.53113535188629	8.48e-15	7.87e+00	4.91e-16	1.86e-01
43	78.32	5	78.50526100024689 - 0.033679131249257734im	78.3231353518863	9.76e-14	8.27e+00	5.40e-15	1.85e-01
44	80.12	5	80.29711946124657 - 0.030994598827928963im	80.1151353518863	7.39e-14	8.70e+00	3.91e-15	1.85e-01
45	81.91	5	82.08887904545642 - 0.028519347335157565im	81.9071353518863	5.34e-14	9.15e+00	2.70e-15	1.84e-01
46	83.70	5	83.8805430787561 - 0.02623778672902819im	83.6991353518863	2.67e-13	9.62e+00	1.29e-14	1.83e-01
47	85.49	5	85.67211507550007 - 0.02413538750122882im	85.4911353518863	2.02e-13	1.01e+01	9.30e-15	1.83e-01
48	87.28	5	87.46359869546592 - 0.022198621256683832im	87.28313535188629	6.04e-13	1.06e+01	2.66e-14	1.82e-01
49	89.08	5	89.2549977049453 - 0.02041490320210765im	89.07513535188627	9.38e-13	1.12e+01	3.94e-14	1.81e-01
50	90.87	5	91.04631594181848 - 0.01877253660841756im	90.86713535188629	1.65e-12	1.18e+01	6.61e-14	1.80e-01
51	92.66	5	92.83755728442789 - 0.017260659309688977im	92.65913535188629	3.14e-12	1.24e+01	1.21e-13	1.79e-01
52	94.45	5	94.628725624043 - 0.015869192293885618im	94.4511353518863	5.75e-12	1.30e+01	2.11e-13	1.78e-01
53	96.24	5	96.41982484069588 - 0.014588790430014055im	96.2431353518863	1.04e-11	1.37e+01	3.63e-13	1.77e-01
54	98.04	5	98.21085878215642 - 0.013410795363359575im	98.0351353518863	1.81e-11	1.44e+01	6.08e-13	1.76e-01
55	99.83	5	100.00183124581334 - 0.012327190596469492im	99.82713535188628	3.16e-11	1.52e+01	1.02e-12	1.75e-01
56	101.62	5	101.79274596322634 - 0.011330558759372413im	101.6191353518863	5.50e-11	1.60e+01	1.69e-12	1.74e-01
57	103.41	5	103.5836065871191 - 0.010414041058545102im	103.4111353518863	9.27e-11	1.68e+01	2.73e-12	1.73e-01
58	105.20	5	105.37441668058895 - 0.009571298881057701im	105.20313535188627	1.56e-10	1.77e+01	4.39e-12	1.72e-01
59	107.00	5	107.16517970831693 - 0.00879647751848351im	106.99513535188628	2.58e-10	1.86e+01	6.95e-12	1.70e-01
60	108.79	5	108.95589902957423 - 0.008084171964339585im	108.78713535188628	4.21e-10	1.96e+01	1.09e-11	1.69e-01

Table S-13: Results obtained by the Newton method for  $n_1(r) = -2.8r + 2.5$ ,  $n_2 = 1$ ,  $\xi = 0.5$  starting from  $k_{\text{asympt}}$ . We took here  $\varepsilon = 1e-8$  and  $l_{\text{max}} = 2000$ .

$$n_1(r) = 1.5 + 6r(\xi - r)$$

$m$	$k_0$	$l$	$k$	$k_{\text{asympt}}$	$ \det(k) $	$ \partial_k \det(k) $	$\frac{ \det(k) }{\ T(k)\ _F}$	$ k - k_{\text{asympt}} $
1	1.33	15	6.2127404455770465 - 0.8387720532805358im	5.333333333333333	4.74e-08	1.54e+00	9.63e-09	1.22e+00
2	2.67	7	4.047468166574287 - 0.5246463375796181im	6.666666666666666	2.97e-09	2.06e+00	1.03e-09	2.67e+00
3	4	6	5.499773898985259 - 0.41551950976663776im	8.0	4.90e-11	2.20e+00	1.63e-11	2.53e+00
4	5.33	6	6.942042250192962 - 0.3249938617322503im	9.333333333333332	1.06e-14	2.42e+00	3.15e-15	2.41e+00
5	6.67	5	8.377083767868388 - 0.25104186154205443im	10.666666666666668	1.58e-09	2.71e+00	3.99e-10	2.30e+00
6	8	5	9.805651396895824 - 0.1914390997765093im	12.0	6.90e-11	3.10e+00	1.42e-11	2.20e+00
7	9.33	5	11.227871705396403 - 0.1440755955003027im	13.333333333333334	5.52e-12	3.57e+00	9.16e-13	2.11e+00
8	10.67	5	12.643719983784923 - 0.10700280743933707im	14.666666666666666	7.89e-13	4.17e+00	1.05e-13	2.03e+00
9	12	5	14.053205886767062 - 0.07844113090471486im	16.0	2.17e-13	4.90e+00	2.29e-14	1.95e+00
10	13.33	5	15.45644573095469 - 0.056788606811771926im	17.333333333333336	1.23e-13	5.81e+00	1.03e-14	1.88e+00
11	14.67	5	16.853679377000322 - 0.0406329592884618im	18.666666666666664	1.47e-13	6.94e+00	9.73e-15	1.81e+00
12	16	5	18.24525650899839 - 0.02876099706336247im	20.0	3.62e-13	8.34e+00	1.90e-14	1.75e+00
13	17.33	5	19.631607045470435 - 0.02015999112976365im	21.333333333333332	1.16e-12	1.01e+01	4.83e-14	1.70e+00
14	18.67	5	21.013206317835145 - 0.014008883480562343im	22.666666666666668	4.42e-12	1.22e+01	1.47e-13	1.65e+00
15	20	5	22.390542498864544 - 0.009660446116447376im	24.0	1.76e-11	1.49e+01	4.64e-13	1.61e+00
16	21.33	5	23.764090605059305 - 0.006617514295846039im	25.333333333333332	6.88e-11	1.82e+01	1.44e-12	1.57e+00
17	22.67	5	25.13429459907233 - 0.00450691709848621im	26.666666666666668	2.54e-10	2.23e+01	4.22e-12	1.53e+00
18	24	5	26.501557133646475 - 0.003054141348471122im	28.0	8.67e-10	2.74e+01	1.15e-11	1.50e+00
19	25.33	5	27.86623542604793 - 0.0020607083619374293im	29.333333333333332	2.74e-09	3.38e+01	2.89e-11	1.47e+00
20	26.67	5	29.22864145347032 - 0.0013852005658552956im	30.666666666666664	8.04e-09	4.17e+01	6.76e-11	1.44e+00
21	28	5	30.589044823112157 - 0.0009280913142047934im	32.0	2.20e-08	5.14e+01	1.47e-10	1.41e+00
22	29.33	5	31.947677034215655 - 0.0006200563019577831im	33.33333333333333	5.66e-08	6.36e+01	3.02e-10	1.39e+00
23	30.67	5	33.30473624114756 - 0.00041322502402054323im	34.666666666666664	1.37e-07	7.87e+01	5.85e-10	1.36e+00
24	32	5	34.66039196055549 - 0.0002747811977017059im	36.0	3.17e-07	9.74e+01	1.08e-09	1.34e+00
25	33.33	5	36.01478941462949 - 0.0001823661869239611im	37.333333333333334	7.00e-07	1.21e+02	1.90e-09	1.32e+00
26	34.67	5	37.368053370860004 - 0.00012082550734374668im	38.666666666666664	1.48e-06	1.50e+02	3.21e-09	1.30e+00
27	36	5	38.72029144303944 - 7.993313059442592e-5im	40.0	3.04e-06	1.86e+02	5.25e-09	1.28e+00
28	37.33	5	40.07159687700538 - 5.281505140981158e-5im	41.333333333333336	6.01e-06	2.30e+02	8.29e-09	1.26e+00
29	38.67	6	41.42205088983924 - 3.4829017528121486e-5im	42.666666666666664	1.35e-13	2.86e+02	1.49e-16	1.24e+00
30	40	6	42.771724529412595 - 2.295162615587744e-5im	44.0	8.56e-13	3.55e+02	7.54e-16	1.23e+00
31	41.33	6	44.12068034843971 - 1.510894241801592e-5im	45.333333333333336	1.82e-12	4.42e+02	1.28e-15	1.21e+00
32	42.67	6	45.468973653525445 - 9.936702073015925e-6im	46.666666666666664	5.40e-12	5.49e+02	3.03e-15	1.20e+00
33	44	6	46.81665359370749 - 6.52939098066515e-6im	48.0	1.68e-11	6.82e+02	7.55e-15	1.18e+00
34	45.33	6	48.1637640485406 - 4.287024163546314e-6im	49.33333333333333	4.20e-11	8.48e+02	1.51e-14	1.17e+00
35	46.67	6	49.51034436402416 - 2.81267363719003e-6im	50.666666666666666	9.65e-11	1.05e+03	2.77e-14	1.16e+00
36	48	6	50.85642996501854 - 1.8441120268841887e-6im	52.0	2.24e-10	1.31e+03	5.14e-14	1.14e+00
37	49.33	6	52.20205286731895 - 1.2083192829491815e-6im	53.333333333333336	4.88e-10	1.63e+03	8.98e-14	1.13e+00
38	50.67	6	53.54724210802752 - 7.912656613817324e-7im	54.666666666666664	1.04e-09	2.03e+03	1.53e-13	1.12e+00
39	52	6	54.89202410918219 - 5.178775612524181e-7im	56.0	2.19e-09	2.53e+03	2.57e-13	1.11e+00
40	53.33	6	56.23642298663918 - 3.387759201125526e-7im	57.333333333333336	4.48e-09	3.14e+03	4.22e-13	1.10e+00
41	54.67	6	57.58046081384112 - 2.2151043838481372e-7im	58.666666666666664	8.97e-09	3.91e+03	6.75e-13	1.09e+00
42	56	6	58.92415784822177 - 1.4477298629786244e-7im	60.0	1.76e-08	4.87e+03	1.06e-12	1.08e+00
43	57.33	6	60.26753272650486 - 9.458222093653786e-8im	61.33333333333333	3.38e-08	6.06e+03	1.63e-12	1.07e+00
44	58.67	6	61.61060263396972 - 6.177062394669382e-8im	62.666666666666666	6.40e-08	7.55e+03	2.47e-12	1.06e+00
45	60	6	62.953383451813416 - 4.033097421728913e-8im	64.0	1.19e-07	9.39e+03	3.68e-12	1.05e+00
46	61.33	6	64.29588988598876 - 2.632935394068613e-8im	65.333333333333334	2.18e-07	1.17e+04	5.39e-12	1.04e+00
47	62.67	6	65.63813558029733 - 1.719113959210712e-8im	66.666666666666666	3.93e-07	1.46e+04	7.79e-12	1.03e+00
48	64	6	66.98013321603476 - 1.1232376085990485e-8im	68.0	7.00e-07	1.81e+04	1.11e-11	1.02e+00
49	65.33	6	68.32189460009721 - 7.352420852697811e-9im	69.33333333333333	1.23e-06	2.26e+04	1.56e-11	1.01e+00
50	66.67	6	69.66343074314386 - 4.8325246537300444e-9im	70.666666666666667	2.14e-06	2.81e+04	2.17e-11	1.00e+00
51	68	6	71.00475192915357 - 3.2038794712988905e-9im	72.0	3.66e-06	3.50e+04	2.98e-11	9.95e-01
52	69.33	6	72.34586777750499 - 2.161278103989485e-9im	73.33333333333333	6.22e-06	4.36e+04	4.06e-11	9.87e-01
53	70.67	6	73.68678729853677 - 1.506640754693074e-9im	74.666666666666667	1.04e-05	5.43e+04	5.46e-11	9.80e-01
54	72	6	75.0275189434026 - 1.1121009678437038e-9im	76.0	1.74e-05	6.76e+04	7.27e-11	9.72e-01
55	73.33	6	76.36807064891696 - 8.959223437358086e-10im	77.33333333333333	2.86e-05	8.42e+04	9.60e-11	9.65e-01
56	74.67	6	77.70844987798952 - 8.067738510232788e-10im	78.666666666666667	4.67e-05	1.05e+05	1.26e-10	9.58e-01
57	76	6	79.0486636561628 - 8.13538256177321e-10im	80.0	7.57e-05	1.31e+05	1.63e-10	9.51e-01
58	77.33	6	80.38871860469843 - 8.986408058929852e-10im	81.33333333333333	1.22e-04	1.63e+05	2.10e-10	9.45e-01
59	78.67	6	81.72862097059803 - 1.0537837800712185e-9im	82.666666666666667	1.94e-04	2.03e+05	2.68e-10	9.38e-01
60	80	6	83.06837665389524 - 1.2771752050448571e-9im	84.0	3.06e-04	2.53e+05	3.39e-10	9.32e-01

Table S-14: Results obtained by the Newton method for  $n_1(r) = 1.5 + 6r(\xi - r)$ ,  $n_2 = 1$ ,  $\xi = 0.5$  starting from  $k_0 = \frac{m}{\xi n_0}$ . We took here  $\varepsilon = 1e-8$  and  $l_{\text{max}} = 2000$ .

$$n_1(r) = 1.5 - 6r(\xi - r)$$

$m$	$k_0$	$l$	$k$	$k_{\text{asympt}}$	$ \det(k) $	$ \partial_k \det(k) $	$\frac{ \det(k) }{\ T(k)\ _F}$	$ k - k_{\text{asympt}} $
1	1.33	8	5.81160775798412 - 1.9882387793184597im	0.8013387620671644	1.80e-08	1.77e+00	2.61e-09	5.39e+00
2	2.67	7	5.062619436026797 - 1.553700758832008im	3.797740929268689	7.67e-15	8.14e-01	1.93e-15	2.00e+00
3	4	5	6.77380298797884 - 1.4179046129451796im	6.073077254855459	6.90e-09	7.44e-01	1.92e-09	1.58e+00
4	5.33	5	8.45020498175942 - 1.2821303643219im	8.090067850271312	5.62e-11	7.03e-01	1.69e-11	1.33e+00
5	6.67	5	10.104099467260863 - 1.1519395713087264im	9.971935246328307	1.46e-10	6.78e-01	4.63e-11	1.16e+00
6	8	5	11.741692047461065 - 1.0294931116728006im	11.769619297419684	3.13e-09	6.64e-01	1.01e-09	1.03e+00
7	9.33	6	13.366517237596524 - 0.9155941154546037im	13.509248610554106	8.05e-15	6.58e-01	2.55e-15	9.27e-01
8	10.67	6	14.98074645506607 - 0.810439080050228im	15.20609811692434	6.88e-13	6.60e-01	2.07e-13	8.41e-01
9	12	6	16.58578221880767 - 0.7139320883539408im	16.869920941709644	6.57e-11	6.67e-01	1.83e-11	7.68e-01
10	13.33	6	18.1825610824244 - 0.6258282561079307im	18.507353103333447	3.08e-09	6.81e-01	7.73e-10	7.05e-01
11	14.67	7	19.771722085562967 - 0.5458031296479617im	20.12313157252302	1.13e-14	7.01e-01	2.50e-15	6.49e-01
12	16	7	21.3537072499469 - 0.4734875928702209im	21.720766810922786	1.33e-12	7.27e-01	2.60e-13	5.99e-01
13	17.33	7	22.928825323253086 - 0.40848573349055417im	23.3029397237446	1.42e-10	7.59e-01	2.41e-11	5.54e-01
14	18.67	7	24.497294437943346 - 0.35038424833760756im	24.871748760768263	7.28e-09	7.99e-01	1.07e-09	5.13e-01
15	20	8	26.05927208698891 - 0.29875763810264205im	26.428870570507165	2.94e-14	8.47e-01	3.74e-15	4.75e-01
16	21.33	8	27.61487724646199 - 0.253171422589353im	27.97566830021137	8.28e-12	9.04e-01	9.07e-13	4.41e-01
17	22.67	8	29.16420706728268 - 0.21318483452405346im	29.51326687181421	8.90e-10	9.71e-01	8.40e-11	4.09e-01
18	24	8	30.70734992040343 - 0.17835356493220092im	31.042606693777397	4.55e-08	1.05e+00	3.70e-09	3.80e-01
19	25.33	9	32.24439557697803 - 0.1482327525726876im	32.56448286658304	8.78e-13	1.14e+00	6.14e-14	3.53e-01
20	26.67	9	33.77544283302587 - 0.12238116745805495im	34.07957437378488	2.10e-10	1.25e+00	1.26e-11	3.28e-01
21	28	9	35.300605169565344 - 0.10036507878491609im	35.5884662007339	2.03e-08	1.38e+00	1.05e-09	3.05e-01
22	29.33	10	36.82001424187622 - 0.08176319045794235im	37.09166635731883	3.37e-13	1.52e+00	1.49e-14	2.84e-01
23	30.67	10	38.3338215807056 - 0.06617118402167377im	38.5896191624115	1.59e-10	1.69e+00	6.06e-12	2.64e-01
24	32	10	39.842198519805656 - 0.05320635137017992im	40.08271574158209	2.83e-08	1.89e+00	9.23e-10	2.46e-01
25	33.33	11	41.34533475187802 - 0.0425115161634788im	41.57130241712368	1.65e-12	2.12e+00	4.61e-14	2.30e-01
26	34.67	11	42.84343551459938 - 0.033758093499018274im	43.05568748289943	3.66e-09	2.39e+00	8.75e-11	2.15e-01
27	36	12	44.3367181970127 - 0.026648319845037696im	44.536146726553724	2.44e-12	2.70e+00	4.99e-14	2.01e-01
28	37.33	13	45.82540828132224 - 0.020916276131486566im	46.01292796957732	9.08e-14	3.06e+00	1.59e-15	1.89e-01
29	38.67	14	47.30973532965186 - 0.016327848040097348im	47.486254829544706	2.76e-07	3.49e+00	4.12e-09	1.77e-01
30	40	21	48.78992874440157 - 0.012680027990721484im	48.95632986061902	5.79e-09	3.98e+00	7.37e-11	1.67e-01
31	41.33	15	49.54815198304445 - 1.5004008989314472im	50.42333719283394	3.53e-08	6.14e+00	2.95e-10	1.74e+00
32	42.67	14	50.959375181804376 - 1.4969061429014117im	51.88744476409404	2.09e-12	7.19e+00	1.45e-14	1.76e+00
33	44	13	52.36909732448825 - 1.493588499801763im	53.34880621878611	7.21e-10	8.43e+00	4.15e-12	1.79e+00
34	45.33	12	53.77738878330252 - 1.4904341928154838im	54.807562531610856	1.83e-06	9.90e+00	8.72e-09	1.81e+00
35	46.67	12	55.18431521355908 - 1.4874303037999197im	56.26384340348819	6.48e-08	1.17e+01	2.56e-10	1.84e+00
36	48	12	56.58993700463793 - 1.4845660767067208im	57.71776846726354	3.78e-09	1.38e+01	1.24e-11	1.86e+00
37	49.33	12	57.99431077247717 - 1.4818312920260552im	59.16944833380403	3.37e-10	1.63e+01	9.16e-13	1.89e+00
38	50.67	12	59.39748921623315 - 1.4792168366347098im	60.618985503444605	4.31e-11	1.93e+01	9.71e-14	1.92e+00
39	52	12	60.799521568645616 - 1.476714460242559im	62.06647516327467	7.50e-12	2.28e+01	1.40e-14	1.95e+00
40	53.33	12	62.2004539005513 - 1.4743166706991813im	63.51200588718237	2.14e-12	2.71e+01	3.31e-15	1.97e+00
41	54.67	11	63.60032945421428 - 1.4720167837069529im	64.95566025269903	4.82e-06	3.22e+01	6.16e-09	2.00e+00
42	56	11	64.99918862117494 - 1.4698080940076035im	66.39751538635942	3.25e-06	3.83e+01	3.43e-09	2.03e+00
43	57.33	11	66.39706950594349 - 1.4676855328797151im	67.83764344739843	2.41e-06	4.57e+01	2.11e-09	2.06e+00
44	58.67	11	67.7940082152335 - 1.4656435740514988im	69.27611205805583	1.95e-06	5.44e+01	1.41e-09	2.08e+00
45	60	11	69.1900383469208 - 1.4636773727192671im	70.71298468748388	1.71e-06	6.49e+01	1.02e-09	2.11e+00
46	61.33	11	70.58519181550102 - 1.4617826543790025im	72.1483209951994	1.60e-06	7.76e+01	7.90e-10	2.14e+00
47	62.67	11	71.97949886007858 - 1.459955337275967im	73.5821771391457	1.58e-06	9.27e+01	6.47e-10	2.17e+00
48	64	11	73.3729879896958 - 1.4581916103586914im	75.0146060527	1.65e-06	1.11e+02	5.57e-10	2.20e+00
49	65.33	11	74.76568617903543 - 1.4564880159846245im	76.44565769434918	1.80e-06	1.33e+02	5.02e-10	2.22e+00
50	66.67	11	76.15761905301581 - 1.4548413735871701im	77.87537927324334	2.04e-06	1.59e+02	4.69e-10	2.25e+00
51	68	11	77.54881095543021 - 1.4532486977855292im	79.30381545340158	2.39e-06	1.90e+02	4.54e-10	2.28e+00
52	69.33	11	78.93928499141157 - 1.4517071909006252im	80.73100853897594	2.89e-06	2.28e+02	4.53e-10	2.31e+00
53	70.67	11	80.32906311003086 - 1.450214262202928im	82.15699864266743	3.58e-06	2.74e+02	4.62e-10	2.33e+00
54	72	11	81.7181662083232 - 1.4487675200657144im	83.5818238391983	4.53e-06	3.29e+02	4.83e-10	2.36e+00
55	73.33	11	83.1066142156225 - 1.4473647371520915im	85.00552030488963	5.85e-06	3.95e+02	5.15e-10	2.39e+00
56	74.67	11	84.49442614677518 - 1.446003817789399im	86.42812244639255	7.70e-06	4.74e+02	5.58e-10	2.41e+00
57	76	11	85.8816201413242 - 1.4446827858259799im	87.84966301705946	1.03e-05	5.70e+02	6.14e-10	2.44e+00
58	77.33	11	87.26821350851205 - 1.4433997882838847im	89.27017322478824	1.39e-05	6.86e+02	6.84e-10	2.47e+00
59	78.67	11	88.6542227836228 - 1.4421530991666498im	90.68968283065038	1.90e-05	8.25e+02	7.70e-10	2.49e+00
60	80	11	90.03966378763893 - 1.4409411125369873im	92.10822023970314	2.62e-05	9.93e+02	8.76e-10	2.52e+00

Table S-15: Results obtained by the Newton method for  $n_1(r) = 1.5 - 6r(\xi - r)$ ,  $n_2 = 1$ ,  $\xi = 0.5$  starting from  $k_0 = \frac{m}{\xi n_0}$ . We took here  $\varepsilon = 1e-8$  and  $l_{\text{max}} = 2000$ .

$$n_1(r) = 1.5 - 6r(\xi - r)$$

$m$	$k_0$	$l$	$k$	$k_{\text{asympt}}$	$ \det(k) $	$ \partial_k \det(k) $	$\frac{ \det(k) }{\ T(k)\ _F}$	$ k - k_{\text{asympt}} $
1	0.80	7	5.811607768328178 - 1.988238794791164im	0.8013387620671644	1.71e-08	1.77e+00	2.48e-09	5.39e+00
2	3.80	5	5.0626194360283705 - 1.553700758846383im	3.797740929268689	1.18e-11	8.14e-01	2.96e-12	2.00e+00
3	6.07	5	6.773802979521228 - 1.4179046167704703im	6.073077254855459	2.43e-14	7.44e-01	6.74e-15	1.58e+00
4	8.09	5	8.450204981711662 - 1.2821303643861277im	8.090067850271312	1.52e-14	7.03e-01	4.58e-15	1.33e+00
5	9.97	5	10.104099467097347 - 1.1519395711676987im	9.971935246328307	3.14e-15	6.78e-01	9.95e-16	1.16e+00
6	11.77	5	11.741692042775735 - 1.0294931112001742im	11.769619297419684	8.57e-15	6.64e-01	2.76e-15	1.03e+00
7	13.51	5	13.366517237596518 - 0.9155941154545839im	13.509248610554106	6.86e-15	6.58e-01	2.17e-15	9.27e-01
8	15.21	5	14.980746455066289 - 0.8104390800492021im	15.20609811692434	2.74e-15	6.60e-01	8.27e-16	8.41e-01
9	16.87	5	16.585782218836684 - 0.7139320884480772im	16.869920941709644	8.44e-15	6.67e-01	2.35e-15	7.68e-01
10	18.51	5	18.18256108427598 - 0.6258282519781904im	18.507353103333447	1.22e-14	6.81e-01	3.07e-15	7.05e-01
11	20.12	4	19.77172208787727 - 0.5458030937107814im	20.12313157252302	2.52e-08	7.01e-01	5.61e-09	6.49e-01
12	21.72	4	21.353707257761574 - 0.4734875744889059im	21.720766810922786	1.45e-08	7.27e-01	2.83e-09	5.99e-01
13	23.30	4	22.928825329847758 - 0.40848572611806816im	23.3029397237446	7.60e-09	7.59e-01	1.29e-09	5.54e-01
14	24.87	4	24.49729443439167 - 0.3503842512946039im	24.871748760768263	3.63e-09	7.99e-01	5.34e-10	5.13e-01
15	26.43	4	26.05927208883804 - 0.29875763783286263im	26.428870570507165	1.58e-09	8.47e-01	2.01e-10	4.75e-01
16	27.98	4	27.614877247143667 - 0.2531714227150877im	27.97566830021137	6.34e-10	9.04e-01	6.95e-11	4.41e-01
17	29.51	4	29.164207067067967 - 0.21318483383093023im	29.51326687181421	2.34e-10	9.71e-01	2.21e-11	4.09e-01
18	31.04	4	30.70734992989217 - 0.1783535227438839im	31.042606693777397	8.04e-11	1.05e+00	6.54e-12	3.80e-01
19	32.56	4	32.244395576987344 - 0.1482327525924103im	32.56448286658304	2.58e-11	1.14e+00	1.80e-12	3.53e-01
20	34.08	4	33.77544283318981 - 0.1223811674226783im	34.07957437378488	7.79e-12	1.25e+00	4.68e-13	3.28e-01
21	35.59	4	35.30060516754089 - 0.10036509337515626im	35.5884662007339	2.24e-12	1.38e+00	1.16e-13	3.05e-01
22	37.09	4	36.8200142418763 - 0.08176319045827857im	37.09166635731883	6.26e-13	1.52e+00	2.77e-14	2.84e-01
23	38.59	4	38.33382158061727 - 0.06617118398908536im	38.5896191624115	1.61e-13	1.69e+00	6.10e-15	2.64e-01
24	40.08	4	39.8421985316791 - 0.05320636050749595im	40.08271574158209	3.58e-14	1.89e+00	1.17e-15	2.46e-01
25	41.57	3	41.345334665316656 - 0.042511480419606604im	41.57130241712368	1.98e-07	2.12e+00	5.55e-09	2.30e-01
26	43.06	3	42.84343547624253 - 0.033758072017691106im	43.05568748289943	1.07e-07	2.39e+00	2.57e-09	2.15e-01
27	44.54	3	44.336718178809235 - 0.026648308314174463im	44.536146726553724	5.82e-08	2.70e+00	1.19e-09	2.01e-01
28	46.01	3	45.82540827298592 - 0.020916270014147306im	46.01292796957732	3.17e-08	3.06e+00	5.54e-10	1.89e-01
29	47.49	3	47.309735263377135 - 0.016327893594047314im	47.486254829544706	1.74e-08	3.49e+00	2.60e-10	1.77e-01
30	48.96	3	48.789928741679844 - 0.01268002524940858im	48.95632986061902	9.64e-09	3.98e+00	1.23e-10	1.67e-01
31	50.42	3	50.26621487601802 - 0.009798695233349789im	50.42333719283394	5.41e-09	4.56e+00	5.87e-11	1.57e-01
32	51.89	3	51.73881345695214 - 0.007536816440139551im	51.88744476409404	3.08e-09	5.24e+00	2.84e-11	1.49e-01
33	53.35	3	53.20793557295723 - 0.005771517424899524im	53.34880621878611	1.77e-09	6.04e+00	1.40e-11	1.41e-01
34	54.81	3	54.67378192259304 - 0.004401303929614971im	54.807562531610856	1.04e-09	6.97e+00	6.96e-12	1.34e-01
35	56.26	3	56.13654172123126 - 0.003343212156988141im	56.26384340348819	6.19e-10	8.06e+00	3.52e-12	1.27e-01
36	57.72	3	57.59639212818031 - 0.0025300791803372167im	57.71776846726354	3.74e-10	9.34e+00	1.81e-12	1.21e-01
37	59.17	3	59.05349810375713 - 0.0019080173266816868im	59.16944833380403	2.30e-10	1.08e+01	9.44e-13	1.16e-01
38	60.62	3	60.508012602134876 - 0.0014341445050873511im	60.618985503444605	1.44e-10	1.26e+01	4.99e-13	1.11e-01
39	62.07	3	61.9600770109525 - 0.0010745937071258431im	62.06647516327467	9.10e-11	1.47e+01	2.68e-13	1.06e-01
40	63.51	3	63.40982175922705 - 0.0008028031124788853im	63.51200588718237	5.84e-11	1.71e+01	1.46e-13	1.02e-01
41	64.96	3	64.85736702821121 - 0.0005980731049173792im	64.95566025269903	3.81e-11	2.00e+01	8.04e-14	9.83e-02
42	66.40	3	66.3028235134053 - 0.00044436711489528587im	66.39751538635942	2.53e-11	2.34e+01	4.51e-14	9.47e-02
43	67.84	3	67.74629319861782 - 0.00032932835783914405im	67.83764344739843	1.68e-11	2.74e+01	2.54e-14	9.14e-02
44	69.28	3	69.18787011403191 - 0.0002434830257600566im	69.27611205805583	1.12e-11	3.22e+01	1.43e-14	8.82e-02
45	70.71	3	70.62764105937768 - 0.00017960124403453595im	70.71298468748388	7.94e-12	3.77e+01	8.54e-15	8.53e-02
46	72.15	3	72.06568628053444 - 0.0001321892566268073im	72.1483209951994	5.63e-12	4.43e+01	5.10e-15	8.26e-02
47	73.58	3	73.50208009336106 - 9.708919533637164e-5im	73.5821771391457	4.04e-12	5.21e+01	3.09e-15	8.01e-02
48	75.01	3	74.93689145253359 - 7.116595797260401e-5im	75.0146060527	2.99e-12	6.13e+01	1.93e-15	7.77e-02
49	76.45	3	76.37018446593372 - 5.20638590741509e-5im	76.44565769434918	1.74e-12	7.23e+01	9.43e-16	7.55e-02
50	77.88	3	77.8020188569453 - 3.801864144976839e-5im	77.87537927324334	1.19e-12	8.52e+01	5.43e-16	7.34e-02
51	79.30	2	79.23245041995015 - 2.7495964319784174e-5im	79.30381545340158	2.22e-05	1.00e+02	8.54e-09	7.14e-02
52	80.73	2	80.66153122478687 - 1.9993289476428555e-5im	80.73100853897594	2.12e-05	1.19e+02	6.86e-09	6.95e-02
53	82.16	2	82.0893101862088 - 1.4512637084699177e-5im	82.15699864266743	2.04e-05	1.40e+02	5.54e-09	6.77e-02
54	83.58	2	83.51583320173428 - 1.0516734912868861e-5im	83.58182383911983	1.97e-05	1.66e+02	4.49e-09	6.60e-02
55	85.01	2	84.94114344834584 - 7.608766658725639e-6im	85.00552030488963	1.91e-05	1.96e+02	3.67e-09	6.44e-02
56	86.43	2	86.36528161431569 - 5.496349350011826e-6im	86.42812244639255	1.87e-05	2.32e+02	3.01e-09	6.28e-02
57	87.85	2	87.78828610590729 - 3.964537457598681e-6im	87.84966301705946	1.84e-05	2.75e+02	2.48e-09	6.14e-02
58	89.27	2	89.21019323198405 - 2.8556566744662813e-6im	89.27017322478824	1.82e-05	3.26e+02	2.06e-09	6.00e-02
59	90.69	2	90.63103736921536 - 2.054285280731795e-6im	90.68968283065038	1.81e-05	3.86e+02	1.72e-09	5.86e-02
60	92.11	2	92.05085111025026 - 1.4761009236742952e-6im	92.10822023970314	1.82e-05	4.58e+02	1.45e-09	5.74e-02

Table S-16: Results obtained by the Newton method for  $n_1(r) = 1.5 - 6r(\xi - r)$ ,  $n_2 = 1$ ,  $\xi = 0.5$  starting from  $k_0 = k_{\text{asympt}}$ . We took here  $\varepsilon = 1e-8$  and  $l_{\text{max}} = 2000$ .

$$n_1(r) = 3 - r(r + 1)$$

$m$	$k_0$	$l$	$k$	$k_{\text{asympt}}$	$ \det(k) $	$ \partial_k \det(k) $	$\frac{ \det(k) }{\ T(k)\ _F}$	$ k - k_{\text{asympt}} $
1	0.89	6	1.8143997879339349 - 0.2594411374549328im	1.3379979374850162	2.17e-10	3.21e+00	8.99e-11	5.42e-01
2	1.78	5	2.91191502137055 - 0.15714010829805797im	2.7985740610105108	8.42e-12	3.95e+00	2.74e-12	1.94e-01
3	2.67	4	3.989187559993246 - 0.08804724456565523im	3.9793015281921194	2.68e-08	5.21e+00	5.66e-09	8.86e-02
4	3.56	4	5.046457936436096 - 0.04590716693828803im	5.069595700420508	8.50e-09	7.19e+00	1.09e-09	5.14e-02
5	4.44	5	6.083657425358343 - 0.022395492175469326im	6.1155946033931174	7.50e-15	1.03e+01	5.74e-16	3.90e-02
6	5.33	5	7.10244321017077 - 0.01031427758860502im	7.13522154082962	2.96e-12	1.52e+01	1.34e-13	3.44e-02
7	6.22	5	8.105641723913287 - 0.00453303804189889im	8.137248806935698	2.46e-10	2.30e+01	6.63e-12	3.19e-02
8	7.11	5	9.09629705149306 - 0.0019207003212467918im	9.126620408847002	7.23e-09	3.55e+01	1.16e-10	3.04e-02
9	8	5	10.077057838148097 - 0.00079121446645147im	10.106402246988473	1.10e-07	5.56e+01	1.04e-09	2.94e-02
10	8.89	5	11.049988123956235 - 0.0003188841155858794im	11.078631522046942	1.07e-06	8.81e+01	6.01e-09	2.86e-02
11	9.78	6	12.016619144582757 - 0.00012632048736484165im	12.044734415373396	1.47e-13	1.41e+02	4.91e-16	2.81e-02
12	10.67	6	12.978074525384939 - 4.934533275288302e-5im	13.005750892775744	4.68e-12	2.27e+02	9.24e-15	2.77e-02
13	11.56	6	13.9351878942644 - 1.905469935186866e-5im	13.962464479646409	6.75e-11	3.67e+02	7.89e-14	2.73e-02
14	12.44	6	14.888591265516324 - 7.28665038850242e-6im	14.915481492622492	6.96e-10	5.96e+02	4.82e-13	2.69e-02
15	13.33	6	15.838775710941064 - 2.7632885541148306e-6im	15.865281680140358	5.79e-09	9.73e+02	2.37e-12	2.65e-02
16	14.22	6	16.786131833906488 - 1.0403123908601436e-6im	16.812251848292313	4.00e-08	1.59e+03	9.67e-12	2.61e-02
17	15.11	6	17.73097678764507 - 3.8911862768557336e-7im	17.75670892143953	2.37e-07	2.62e+03	3.38e-11	2.57e-02
18	16	6	18.673572622923604 - 1.4471245155330312e-7im	18.69891620082147	1.24e-06	4.32e+03	1.04e-10	2.53e-02
19	16.89	6	19.6141390586735 - 5.3829831083068225e-8im	19.6390951055044	5.80e-06	7.13e+03	2.89e-10	2.50e-02
20	17.78	6	20.55286261094203 - 2.1219848334306016e-8im	20.577433830477847	2.48e-05	1.18e+04	7.29e-10	2.46e-02
21	18.67	6	21.489903287240704 - 1.1952220461806549e-8im	21.51409385039327	9.84e-05	1.69e+04	1.70e-09	2.42e-02
22	19.56	6	22.42539960937155 - 1.384724325018149e-8im	22.449214885786407	3.65e-04	3.25e+04	3.72e-09	2.38e-02
23	20.44	6	23.359472457935173 - 2.2427038890462892e-8im	23.382918751246727	1.27e-03	5.41e+04	7.64e-09	2.34e-02
24	21.33	7	24.29222803294353 - 3.5005105016500306e-10im	24.31531237678209	1.65e-10	9.02e+04	5.82e-16	2.31e-02
25	22.22	7	25.223760302419645 - 1.2672125077392315e-10im	25.246490208424966	1.83e-09	1.50e+05	3.80e-15	2.27e-02
26	23.11	7	26.154152803722756 - 4.573533198619007e-11im	26.176536136338278	5.43e-09	2.51e+05	6.64e-15	2.24e-02
27	24	7	27.083480223596514 - 1.6438364793557694e-11im	27.10552505874944	2.37e-08	4.20e+05	1.71e-14	2.20e-02
28	24.89	7	28.011809641814473 - 5.887648323220467e-12im	28.03352416198367	1.10e-07	7.04e+05	4.63e-14	2.17e-02
29	25.78	7	28.93920156527407 - 2.2478170852486575e-12im	28.96059397684492	4.90e-07	1.18e+06	1.22e-13	2.14e-02
30	26.67	7	29.865710788232374 - 1.5100932735458871e-12im	29.886789257100936	2.07e-06	1.98e+06	3.01e-13	2.11e-02
31	27.56	7	30.791387113232513 - 2.651437521933138e-12im	30.812159715203567	8.28e-06	3.33e+06	7.08e-13	2.08e-02
32	28.44	7	31.716275959392508 - 5.68000994613624e-12im	31.73675064248916	3.16e-05	5.59e+06	1.59e-12	2.05e-02
33	29.33	7	32.640418878869305 - 1.0275232231132076e-11im	32.660603435186864	1.15e-04	9.40e+06	3.40e-12	2.02e-02
34	30.22	7	33.56385399789767 - 1.3962926709561803e-11im	33.58375604307552	4.05e-04	1.58e+07	7.00e-12	1.99e-02
35	31.11	7	34.486616395441395 - 9.395896898081724e-12im	34.50624335419536	1.37e-03	2.67e+07	1.39e-11	1.96e-02
36	32	7	35.408738429906364 + 1.9042859437151042e-11im	35.42809752636727	4.47e-03	4.50e+07	2.66e-11	1.94e-02
37	32.89	7	36.33025002235431 + 9.818377845301142e-11im	36.34934827420518	1.41e-02	7.58e+07	4.93e-11	1.91e-02
38	33.78	7	37.25117890308059 + 2.663557366796432e-10im	37.270023118685245	4.34e-02	1.28e+08	8.87e-11	1.88e-02
39	34.67	7	38.171550827175125 + 5.676865187699158e-10im	38.19014760505062	1.30e-01	2.16e+08	1.55e-10	1.86e-02
40	35.56	7	39.0913897636969 + 1.0364628401956892e-9im	39.10974549380959	3.79e-01	3.65e+08	2.65e-10	1.84e-02
41	36.44	7	40.01071806229986 + 1.667870238439818e-9im	40.02883892876365	1.08e+00	6.17e+08	4.42e-10	1.81e-02
42	37.33	7	40.92955660051002 + 2.372980121097757e-9im	40.94744858534206	3.00e+00	1.04e+09	7.21e-10	1.79e-02
43	38.22	7	41.84792491433578 + 2.9189380966653997e-9im	41.865593801981795	8.20e+00	1.77e+09	1.15e-09	1.77e-02
44	39.11	7	42.76584131446933 + 2.8598161343109784e-9im	42.78329269685433	2.20e+01	2.99e+09	1.81e-09	1.75e-02
45	40	7	43.68332298998767 + 1.4690211978652767e-9im	43.7005622718813	5.78e+01	5.07e+09	2.78e-09	1.72e-02
46	40.89	7	44.60038610117116 - 2.31011046506217e-9im	44.61741850568467	1.50e+02	8.59e+09	4.21e-09	1.70e-02
47	41.78	7	45.51704586281256 - 9.874225587381451e-9im	45.53387643687215	3.81e+02	1.46e+10	6.27e-09	1.68e-02
48	42.67	7	46.43331661918322 - 2.2906020901797492e-8im	46.44995023885362	9.57e+02	2.47e+10	9.20e-09	1.66e-02
49	43.56	8	47.349211948133735 + 9.715013286542166e-17im	47.36565328721461	8.89e-05	4.19e+10	4.99e-16	1.64e-02
50	44.44	8	48.2647445766819 - 4.01961094482128e-15im	48.28099822052871	6.39e-04	7.11e+10	2.10e-15	1.63e-02
51	45.33	8	49.17992664490387 - 8.282008571205506e-15im	49.19599699537067	1.20e-03	1.21e+11	2.31e-15	1.61e-02
52	46.22	8	50.094769623773566 - 1.9953576261353675e-14im	50.110660936189944	4.27e-03	2.05e+11	4.78e-15	1.59e-02
53	47.11	8	51.00928439188993 - 2.619976850035069e-14im	51.02500078061719	1.37e-02	3.48e+11	8.96e-15	1.57e-02
54	48	8	51.92348127687054 - 2.7418000375379606e-14im	51.93902672070318	4.98e-02	5.92e+11	1.91e-14	1.55e-02
55	48.89	8	52.837370093125024 + 2.2915125370414225e-15im	52.852748440526156	1.39e-01	1.01e+12	3.11e-14	1.54e-02
56	49.78	8	53.75096017638625 + 8.966460381378414e-14im	53.76617515054948	4.09e-01	1.71e+12	5.33e-14	1.52e-02
57	50.67	8	54.66426041533159 + 2.9317513491851894e-13im	54.679315619065136	1.26e+00	2.91e+12	9.60e-14	1.51e-02
58	51.56	8	55.57727928058732 + 6.669856507697361e-13im	55.59217820101886	3.65e+00	4.95e+12	1.62e-13	1.49e-02
59	52.44	8	56.490024851375004 + 1.2576257632256149e-12im	56.504770864477095	1.06e+01	8.43e+12	2.76e-13	1.47e-02
60	53.33	8	57.40250484002879 + 2.057300130187329e-12im	57.41710121496701	3.04e+01	1.44e+13	4.61e-13	1.46e-02

Table S-17: Results obtained by the Newton method for  $n_1(r) = 3 - r(r + 1)$ ,  $n_2 = 1$ ,  $\xi = 0.5$  starting from  $k_0 = \frac{m}{\xi n_0}$ . We took here  $\varepsilon = 1e-8$  and  $l_{\text{max}} = 2000$ .

$$n_1(r) = \sqrt{2 - r^2}$$

$m$	$k_0$	$l$	$k$	$k_{\text{asympt}}$	$ \det(k) $	$ \partial_k \det(k) $	$\frac{ \det(k) }{\ T(k)\ _F}$	$ k - k_{\text{asympt}} $
1	1.51	6	7.8876676918624335 - 1.4052428170656204im	0.2779979601087338	2.81e-10	1.26e+00	3.85e-11	7.74e+00
2	3.02	14	5.043983011022969 - 1.255099671399734im	3.3992834444609796	5.01e-15	1.21e+00	1.26e-15	2.07e+00
3	4.54	7	6.78117621695404 - 1.1657519246857233im	5.725929985613505	6.55e-14	1.15e+00	1.72e-14	1.57e+00
4	6.05	6	8.495101178211378 - 1.07544263327515im	7.79147286644759	4.59e-13	1.13e+00	1.26e-13	1.29e+00
5	7.56	5	10.195114750093254 - 0.9876143271520355im	9.728823554860602	2.67e-09	1.12e+00	7.47e-10	1.09e+00
6	9.07	5	11.885660825533378 - 0.9037283263467333im	11.590106722069358	9.57e-12	1.13e+00	2.69e-12	9.51e-01
7	10.58	5	13.569145340854345 - 0.8244171609148544im	13.400921462365059	5.13e-14	1.16e+00	1.42e-14	8.41e-01
8	12.09	5	15.246985869189647 - 0.7499224015735996im	15.175695528301567	8.34e-15	1.19e+00	2.24e-15	7.53e-01
9	13.61	4	16.92006707378542 - 0.6802860309642261im	16.92335793384409	2.06e-08	1.23e+00	5.28e-09	6.80e-01
10	15.12	4	18.588963438926466 - 0.6154425735324377im	18.649822497140867	1.17e-08	1.27e+00	2.81e-09	6.18e-01
11	16.63	4	20.25405846400167 - 0.5552662491807356im	20.35921278656442	1.43e-08	1.33e+00	3.20e-09	5.65e-01
12	18.14	4	21.91561283345459 - 0.4995968822063811im	22.054522399365098	2.87e-08	1.38e+00	5.93e-09	5.19e-01
13	19.65	5	23.573806065132025 - 0.4482539446905049im	23.737996269812598	1.86e-15	1.45e+00	3.53e-16	4.77e-01
14	21.17	5	25.228762703203294 - 0.40104513354552523im	25.411363359680134	8.39e-15	1.52e+00	1.44e-15	4.41e-01
15	22.68	5	26.88057007926093 - 0.3577711376938493im	27.07598521694322	2.50e-14	1.60e+00	3.90e-15	4.08e-01
16	24.19	5	28.529290339792915 - 0.31822875082956303im	28.732954464055243	1.84e-13	1.69e+00	2.60e-14	3.78e-01
17	25.70	5	30.174969098145972 - 0.2822128436144401im	30.383162209814778	1.32e-12	1.79e+00	1.69e-13	3.51e-01
18	27.21	5	31.817641755053966 - 0.2495177669299015im	32.02734547195008	7.84e-12	1.89e+00	9.00e-13	3.26e-01
19	28.73	5	33.45733822007791 - 0.21993845764532083im	33.666121339938215	4.17e-11	2.01e+00	4.31e-12	3.03e-01
20	30.24	5	35.09408648067281 - 0.19327141118804717im	35.30001210299622	1.98e-10	2.13e+00	1.84e-11	2.82e-01
21	31.75	5	36.72791530333781 - 0.169315611687572im	36.92946407521561	8.40e-10	2.27e+00	7.02e-11	2.63e-01
22	33.26	5	38.358856251937304 - 0.1478734630760819im	38.55486193098055	3.22e-09	2.42e+00	2.42e-10	2.46e-01
23	34.77	5	39.98694514743349 - 0.12875173309777965im	40.176539782137446	1.12e-08	2.58e+00	7.54e-10	2.29e-01
24	36.28	5	41.612223056585655 - 0.11176250128443142im	41.79478985078074	3.54e-08	2.76e+00	2.15e-09	2.14e-01
25	37.80	5	43.23473687585615 - 0.09672408871799562im	43.409869340807994	1.03e-07	2.96e+00	5.63e-09	2.00e-01
26	39.31	6	44.85453947841087 - 0.08346192594523981im	45.02200594152324	2.44e-14	3.18e+00	1.19e-15	1.87e-01
27	40.82	6	46.47168987682354 - 0.07180945664714387im	46.63140227932789	6.90e-14	3.41e+00	3.03e-15	1.75e-01
28	42.33	6	48.086252638315386 - 0.0616087205398996im	48.238239551259575	1.06e-13	3.68e+00	4.19e-15	1.64e-01
29	43.84	6	49.69829750735879 - 0.05271101103002523im	49.842680515504235	6.86e-13	3.96e+00	2.43e-14	1.54e-01
30	45.36	6	51.30789870021302 - 0.04497729220240343im	51.44487197162949	2.87e-12	4.28e+00	9.11e-14	1.44e-01
31	46.87	6	52.91513412276551 - 0.03827847623086779im	53.04494683226257	1.11e-11	4.62e+00	3.16e-13	1.35e-01
32	48.38	6	54.520084525857655 - 0.032495541285245004im	54.64302586494729	3.89e-11	5.01e+00	9.92e-13	1.27e-01
33	49.89	6	56.12283263854753 - 0.027519494964598643im	56.239219165691665	1.26e-10	5.43e+00	2.88e-12	1.20e-01
34	51.40	6	57.72346231452474 - 0.023251194798049584im	57.8336274126814	3.78e-10	5.89e+00	7.75e-12	1.13e-01
35	52.92	6	59.3220577207673 - 0.01960104244809687im	59.42634293866988	1.06e-09	6.40e+00	1.95e-11	1.06e-01
36	54.43	6	60.91870259095307 - 0.016488571728510423im	61.01745065287239	2.80e-09	6.96e+00	4.61e-11	1.00e-01
37	55.94	6	62.51347955955712 - 0.013841952399153236im	62.60702883721701	6.99e-09	7.58e+00	1.03e-10	9.46e-02
38	57.45	6	64.10646958637228 - 0.011597432061328336im	64.19514983712165	1.66e-08	8.27e+00	2.19e-10	8.94e-02
39	58.96	6	65.6977514756854 - 0.009698737591804106im	65.78188066326851	3.76e-08	9.02e+00	4.44e-10	8.47e-02
40	60.47	6	67.28740148972052 - 0.008096455718707863im	67.36728351790704	8.15e-08	9.86e+00	8.63e-10	8.03e-02
41	61.99	6	68.87549305231263 - 0.0067474098697211235im	68.95141625686348	1.70e-07	1.08e+01	1.61e-09	7.62e-02
42	63.50	6	70.46209653610099 - 0.0056140476019024im	70.53433279653885	3.42e-07	1.18e+01	2.91e-09	7.25e-02
43	65.01	6	72.04727912476118 - 0.0046638500017582695im	72.11608347364279	6.66e-07	1.29e+01	5.06e-09	6.90e-02
44	66.52	6	73.63110474081267 - 0.0038687716186946563im	73.69671536415952	1.26e-06	1.42e+01	8.56e-09	6.57e-02
45	68.03	7	75.21363390603155 - 0.0032048001897794632im	75.27627256701744	8.20e-14	1.55e+01	5.00e-16	6.27e-02
46	69.55	7	76.79492419646647 - 0.0026512066731211466im	76.85479645709125	5.93e-13	1.71e+01	3.23e-15	5.99e-02
47	71.06	7	78.3750297440144 - 0.002190445857498904im	78.43232591146872	7.22e-13	1.87e+01	3.52e-15	5.73e-02
48	72.57	7	79.95400167111424 - 0.0018075605195045199im	80.0088975123329	1.71e-12	2.06e+01	7.47e-15	5.49e-02
49	74.08	7	81.53188813078424 - 0.0014898692154344784im	81.58454572933054	4.60e-12	2.27e+01	1.79e-14	5.27e-02
50	75.59	7	83.10873443898353 - 0.0012266498074444237im	83.1593030838892	1.14e-11	2.50e+01	3.96e-14	5.06e-02
51	77.10	7	84.68458321676113 - 0.0010088602689774257im	84.73320029760687	2.70e-11	2.75e+01	8.41e-14	4.86e-02
52	78.62	7	86.25947453773435 - 0.0008288939553513338im	86.30626642655	6.21e-11	3.03e+01	1.73e-13	4.68e-02
53	80.13	7	87.83344607729113 - 0.0006803663287910885im	87.87852898305114	1.39e-10	3.34e+01	3.46e-13	4.51e-02
54	81.64	7	89.40653326067101 - 0.0005579300735463695im	89.45001404639164	3.01e-10	3.68e+01	6.70e-13	4.35e-02
55	83.15	7	90.97876940774276 - 0.00045711558993282234im	91.02074636357649	6.33e-10	4.07e+01	1.26e-12	4.20e-02
56	84.66	7	92.55018587286162 - 0.00037419398532698655im	92.5907494412576	1.30e-09	4.49e+01	2.31e-12	4.06e-02
57	86.18	7	94.12081217866209 - 0.0003060598597716603im	94.16004562973256	2.60e-09	4.96e+01	4.13e-12	3.92e-02
58	87.69	7	95.6906761430302 - 0.00025013139405633905im	95.72865619983267	5.09e-09	5.48e+01	7.22e-12	3.80e-02
59	89.20	7	97.25980399881186 - 0.0002042654732892163im	97.29660141341809	9.75e-09	6.06e+01	1.24e-11	3.68e-02
60	90.71	7	98.82822050605951 - 0.0001666858070041872im	98.86390058811422	1.83e-08	6.70e+01	2.07e-11	3.57e-02

Table S-18: Results obtained by the Newton method for  $n_1(r) = \sqrt{2 - r^2}$ ,  $n_2 = 1$ ,  $\xi = 0.5$  starting from  $k_0 = \frac{m}{\xi n_0}$ . We took here  $\varepsilon = 1e-8$  and  $l_{\text{max}} = 2000$ .

## S4.2 $n_1$ and $n_2$ variable

$$n_1(r) = \sqrt{2 - r^2} \quad n_2(r) = r + 0.5$$

$m$	$k_0$	$l$	$k$	$ \det(k) $	$ \partial_k \det(k) $	$\frac{ \det(k) }{\ T(k)\ _F}$
1	1.51	17	0.40053408329828327 - 1.2449374864234752im	8.48e-09	1.30e+00	5.31e-09
2	3.02	15	11.44346347372721 - 2.286602295636471im	3.34e-13	6.05e+00	1.80e-14
3	4.54	15	-7.6810822010348785 - 1.774902301665455im	1.10e-10	3.66e+00	1.48e-11
4	6.05	6	8.89369366419431 - 1.0592866230998579im	3.32e-11	1.39e+00	7.37e-12
5	7.56	5	10.40252005138865 - 0.9746801306001142im	6.80e-09	1.36e+00	1.69e-09
6	9.07	5	11.971622435387683 - 1.0228695592136103im	1.53e-12	1.16e+00	3.84e-13
7	10.58	4	13.757647634726336 - 1.0978647143490887im	3.83e-11	8.58e-01	8.39e-12
8	12.09	4	15.48100038031874 - 0.911212326380654im	2.92e-09	1.14e+00	6.36e-10
9	13.61	4	17.07327704713775 - 0.8058922932781359im	1.79e-08	1.24e+00	3.98e-09
10	15.12	4	18.67383953495821 - 0.7774007935679721im	2.48e-08	1.22e+00	5.43e-09
11	16.63	4	20.335853556473555 - 0.7720721899006605im	4.07e-09	1.14e+00	8.29e-10
12	18.14	4	22.02269488484835 - 0.7064482797854552im	7.06e-10	1.21e+00	1.33e-10
13	19.65	4	23.657401810238266 - 0.6247091538432159im	1.63e-08	1.35e+00	2.89e-09
14	21.17	5	25.27256539257801 - 0.5757135851089986im	1.15e-14	1.42e+00	1.92e-15
15	22.68	5	26.90303045005347 - 0.5494429062124283im	9.97e-14	1.44e+00	1.55e-14
16	24.19	5	28.552704067003997 - 0.5149480245783592im	2.35e-13	1.50e+00	3.32e-14
17	25.70	5	30.193232777159285 - 0.46377513595984887im	7.55e-13	1.62e+00	9.74e-14
18	27.21	5	31.816485149659695 - 0.4184330845561557im	1.03e-11	1.75e+00	1.21e-12
19	28.73	5	33.43738986807831 - 0.3874233900625147im	1.25e-10	1.85e+00	1.34e-11
20	30.24	5	35.06586021939024 - 0.36173659656435037im	7.00e-10	1.95e+00	6.83e-11
21	31.75	5	36.696699983610564 - 0.33075521933880614im	2.03e-09	2.08e+00	1.79e-10
22	33.26	5	38.32010519332835 - 0.29728228279642593im	6.37e-09	2.26e+00	5.04e-10
23	34.77	5	39.93705255000444 - 0.2693461139451231im	2.42e-08	2.43e+00	1.73e-09
24	36.28	5	41.55388130414437 - 0.24767727328796607im	8.43e-08	2.61e+00	5.42e-09
25	37.80	6	43.17277724501983 - 0.22733441134357557im	2.15e-14	2.79e+00	1.24e-15
26	39.31	6	44.79013136454209 - 0.20532802012716414im	7.44e-14	3.02e+00	3.85e-15
27	40.82	6	46.40290773513727 - 0.1840638348842305im	9.36e-14	3.28e+00	4.34e-15
28	42.33	6	48.012550596554 - 0.16632781039738778im	4.31e-13	3.55e+00	1.79e-14
29	43.84	6	49.621663248113734 - 0.15154108249306403im	1.88e-12	3.83e+00	7.00e-14
30	45.36	6	51.230495839369716 - 0.1373827953945077im	6.68e-12	4.15e+00	2.22e-13
31	46.87	6	52.837253320128994 - 0.12307349064724347im	2.13e-11	4.51e+00	6.34e-13
32	48.38	6	54.441021992630574 - 0.10988600426384472im	6.74e-11	4.91e+00	1.79e-12
33	49.89	6	56.04271985844161 - 0.09878152795125739im	2.08e-10	5.34e+00	4.95e-12
34	51.40	6	57.643429576819486 - 0.08921651184519115im	5.88e-10	5.81e+00	1.25e-11
35	52.92	6	59.243065344333026 - 0.08013242792385902im	1.51e-09	6.33e+00	2.87e-11
36	54.43	6	60.84081516301014 - 0.07132329339079532im	3.65e-09	6.91e+00	6.20e-11
37	55.94	6	62.43641583560084 - 0.06338568432176445im	8.64e-09	7.54e+00	1.31e-10
38	57.45	6	64.03037250007489 - 0.05665186938013002im	1.99e-08	8.24e+00	2.71e-10
39	58.96	6	65.62316470813552 - 0.05078254933103091im	4.37e-08	9.00e+00	5.31e-10
40	60.47	6	67.21471808852614 - 0.045284459305748im	9.08e-08	9.85e+00	9.87e-10
41	61.99	6	68.80468354576907 - 0.04008961786533196im	1.82e-07	1.08e+01	1.77e-09
42	63.50	6	70.39299682405083 - 0.035463445717243997im	3.59e-07	1.18e+01	3.11e-09
43	65.01	6	71.97992856594321 - 0.031522717181525495im	6.90e-07	1.30e+01	5.34e-09
44	66.52	6	73.56571352398113 - 0.028080820732719964im	1.29e-06	1.42e+01	8.90e-09
45	68.03	7	75.1503269158149 - 0.024899678467071862im	1.25e-13	1.56e+01	7.73e-16
46	69.55	7	76.73362883365553 - 0.021944642114035778im	3.62e-13	1.71e+01	2.00e-15
47	71.06	7	78.31561526116275 - 0.019329952066174907im	8.50e-13	1.88e+01	4.20e-15
48	72.57	7	79.89643394241597 - 0.017098457670134567im	1.42e-12	2.07e+01	6.27e-15
49	74.08	7	81.47621294586875 - 0.015153813188387636im	4.46e-12	2.28e+01	1.76e-14
50	75.59	7	83.05495895997215 - 0.01337765676775253im	1.04e-11	2.51e+01	3.65e-14
51	77.10	7	84.63262407018541 - 0.01174672204290037im	2.53e-11	2.76e+01	7.95e-14
52	78.62	7	86.20922164524417 - 0.010308524497539044im	5.77e-11	3.05e+01	1.62e-13
53	80.13	7	87.784835735916 - 0.009080043429391947im	1.28e-10	3.36e+01	3.21e-13
54	81.64	7	89.35954283396433 - 0.008013694946652047im	2.77e-10	3.71e+01	6.21e-13
55	83.15	7	90.93336265395388 - 0.007049757225697063im	5.82e-10	4.09e+01	1.17e-12
56	84.66	7	92.50628654088392 - 0.00617188887327263im	1.19e-09	4.52e+01	2.13e-12
57	86.18	7	94.07833162055061 - 0.005398911345104989im	2.39e-09	4.99e+01	3.82e-12
58	87.69	7	95.64954837216531 - 0.004738229023314983im	4.69e-09	5.51e+01	6.68e-12
59	89.20	7	97.21998558968617 - 0.004167257302893625im	8.99e-09	6.09e+01	1.14e-11
60	90.71	7	98.78966562952907 - 0.00365583307117504im	1.69e-08	6.74e+01	1.92e-11

Table S-19: Results obtained by the Newton method for  $n_1(r) = \sqrt{2 - r^2}$ ,  $n_2 = r + 0.5$ ,  $\xi = 0.5$  starting from  $k_0 = \frac{m}{\xi n_0}$ . We took here  $\varepsilon = 1e-8$  and  $l_{\max} = 2000$ .

$$n_1(r) = \sqrt{2 - r^2} \quad n_2(r) = 1 + (r - 0.5)^3$$

$m$	$k_0$	$l$	$k$	$ \det(k) $	$ \partial_k \det(k) $	$\frac{ \det(k) }{\ T(k)\ _F}$
1	1.51	19	8.33731377407904 - 1.5145282232893382im	8.63e-15	1.55e+00	1.00e-15
2	3.02	10	10.018989709571363 - 1.2044185189436711im	9.92e-15	1.56e+00	1.46e-15
3	4.54	8	6.560084964097422 - 0.9823851559418392im	1.05e-12	1.47e+00	3.47e-13
4	6.05	7	8.20434829959099 - 1.1276540761930103im	2.47e-12	1.14e+00	7.43e-13
5	7.56	6	10.30091455556008 - 1.2279993570070407im	7.50e-10	7.14e-01	1.73e-10
6	9.07	5	12.006156469238457 - 0.9155868162462955im	6.06e-10	1.14e+00	1.57e-10
7	10.58	5	13.62772269891376 - 0.7681906372433964im	1.53e-12	1.26e+00	4.19e-13
8	12.09	5	15.247512631208721 - 0.688563536426607im	2.42e-14	1.31e+00	6.67e-15
9	13.61	5	16.885411230477 - 0.6477564871571444im	9.18e-15	1.30e+00	2.45e-15
10	15.12	4	18.55302394816074 - 0.6224977056615771im	2.53e-08	1.26e+00	6.28e-09
11	16.63	4	20.245775572024332 - 0.5824002509835021im	5.92e-09	1.26e+00	1.33e-09
12	18.14	4	21.9311969191144 - 0.5160856026458189im	5.17e-09	1.34e+00	1.06e-09
13	19.65	4	23.592169197883663 - 0.44664418136589723im	2.76e-08	1.45e+00	5.16e-09
14	21.17	5	25.238012015731343 - 0.3899041780709828im	1.71e-14	1.55e+00	2.92e-15
15	22.68	5	26.879640875590262 - 0.3471364866080714im	4.42e-14	1.63e+00	6.90e-15
16	24.19	5	28.52311123036569 - 0.3139759499755985im	4.25e-13	1.71e+00	6.02e-14
17	25.70	5	30.169832791101626 - 0.28462532817560937im	2.54e-12	1.78e+00	3.24e-13
18	27.21	5	31.817125318698583 - 0.2546758884919236im	1.04e-11	1.87e+00	1.20e-12
19	28.73	5	33.46070442737622 - 0.22355729019230391im	3.90e-11	1.99e+00	4.03e-12
20	30.24	5	35.0983430030089 - 0.19374573773877826im	1.61e-10	2.13e+00	1.50e-11
21	31.75	5	36.7306740379862 - 0.1676160686760042im	7.08e-10	2.27e+00	5.91e-11
22	33.26	5	38.35946032512848 - 0.14585820709507277im	2.99e-09	2.43e+00	2.24e-10
23	34.77	5	39.986116933353415 - 0.127798059209067im	1.13e-08	2.59e+00	7.64e-10
24	36.28	5	41.611184708455156 - 0.11221255649030183im	3.75e-08	2.76e+00	2.27e-09
25	37.80	5	43.23438845192361 - 0.09803275791619845im	1.09e-07	2.96e+00	5.93e-09
26	39.31	6	44.85505365703765 - 0.08478104783587495im	1.99e-14	3.17e+00	9.75e-16
27	40.82	6	46.47265563136915 - 0.0725769075135829im	5.02e-14	3.41e+00	2.21e-15
28	42.33	6	48.087123010508904 - 0.0617664691684616im	1.30e-13	3.67e+00	5.11e-15
29	43.84	6	49.69874650828217 - 0.05254589207433802im	6.51e-13	3.96e+00	2.30e-14
30	45.36	6	51.30791316577706 - 0.04483779983313513im	2.88e-12	4.28e+00	9.14e-14
31	46.87	6	52.91490942207569 - 0.03837351700391295im	1.12e-11	4.63e+00	3.20e-13
32	48.38	6	54.519857156230174 - 0.0328362311485477im	3.97e-11	5.00e+00	1.01e-12
33	49.89	6	56.12274868861489 - 0.027977556378603212im	1.28e-10	5.42e+00	2.93e-12
34	51.40	6	57.72353296135894 - 0.023670351894243307im	3.81e-10	5.89e+00	7.81e-12
35	52.92	6	59.32220019696449 - 0.019888440654412975im	1.06e-09	6.40e+00	1.95e-11
36	54.43	6	60.918817874381325 - 0.016641439396329064im	2.79e-09	6.96e+00	4.59e-11
37	55.94	6	62.5135103859406 - 0.013916944869427086im	6.96e-09	7.58e+00	1.03e-10
38	57.45	6	64.1064150286182 - 0.01166138508107885im	1.66e-08	8.27e+00	2.19e-10
39	58.96	6	65.69764844057693 - 0.00979321529497068im	3.76e-08	9.02e+00	4.45e-10
40	60.47	6	67.28729503931662 - 0.008227122548779532im	8.17e-08	9.86e+00	8.66e-10
41	61.99	6	68.87541292365893 - 0.006893814071318529im	1.70e-07	1.08e+01	1.62e-09
42	63.50	6	70.46204845681518 - 0.005748698366079068im	3.43e-07	1.18e+01	2.91e-09
43	65.01	6	72.04725061634329 - 0.004768617948237548im	6.66e-07	1.29e+01	5.07e-09
44	66.52	6	73.63107800740693 - 0.003941100014083659im	1.26e-06	1.42e+01	8.56e-09
45	68.03	7	75.21359673250653 - 0.0032539122061979366im	2.59e-13	1.55e+01	1.57e-15
46	69.55	7	76.79487401653422 - 0.0026899387416524966im	2.96e-13	1.71e+01	1.61e-15
47	71.06	7	78.37497157427148 - 0.002228414520876388im	9.21e-13	1.87e+01	4.49e-15
48	72.57	7	79.95394329718219 - 0.001848283385904822im	1.83e-12	2.06e+01	7.97e-15
49	74.08	7	81.53183570454516 - 0.0015316093319056934im	4.66e-12	2.27e+01	1.82e-14
50	75.59	7	83.10869026236614 - 0.0012653248246673316im	1.14e-11	2.50e+01	3.99e-14
51	77.10	7	84.6845460121082 - 0.0010410500237395487im	2.69e-11	2.75e+01	8.40e-14
52	78.62	7	86.25944130255492 - 0.0008534960943431732im	6.23e-11	3.03e+01	1.74e-13
53	80.13	7	87.8334140984521 - 0.0006985351172374429im	1.39e-10	3.34e+01	3.46e-13
54	81.64	7	89.40650124315063 - 0.0005719409388184836im	3.00e-10	3.68e+01	6.69e-13
55	83.15	7	90.97873751552915 - 0.0004691114755783593im	6.33e-10	4.07e+01	1.26e-12
56	84.66	7	92.55015509265516 - 0.0003854376381595435im	1.30e-09	4.49e+01	2.31e-12
57	86.18	7	94.12078354893717 - 0.0003168253174348326im	2.60e-09	4.96e+01	4.13e-12
58	87.69	7	95.69065022708841 - 0.00026004852980710176im	5.09e-09	5.48e+01	7.22e-12
59	89.20	7	97.2597807457597 - 0.00021281766180367284im	9.75e-09	6.06e+01	1.24e-11
60	90.71	7	98.82819943694307 - 0.00017359159060853342im	1.83e-08	6.70e+01	2.07e-11

Table S-20: Results obtained by the Newton method for  $n_1(r) = \sqrt{2 - r^2}$ ,  $n_2 = 1 + (r - 0.5)^3$ ,  $\xi = 0.5$  starting from  $k_0 = \frac{m}{\xi n_0}$ . We took here  $\varepsilon = 1e-8$  and  $l_{\max} = 2000$ .

# S-Appendix A Additional figures

$l$	$k_l$	$ \det_1(k_l) $	$ \partial_k \det_1(k_l) $
1	15.2027551239541 - 0.0014194570359291362im	4.67e+00	3.35e+00
2	16.595070718259585 - 0.09584456745332563im	7.67e-01	2.26e+00
3	16.910865265369715 - 0.21866765298920093im	4.90e-02	2.03e+00
4	16.92329111475096 - 0.2394557194458im	2.56e-04	2.02e+00
5	16.923201859904534 - 0.239545593149898im	7.01e-09	2.02e+00

(a)  $\det_1$  starting from  $k_0 = 11$ .

$l$	$k_l$	$ \det_2(k_l) $	$ \partial_k \det_2(k_l) $
1	13.396229610406712 + 4.6308732874575025im	3.28e-02	3.63e-03
2	21.37329855682114 + 8.869886753253347im	1.81e-02	7.99e-04
3	42.399466900838604 + 17.295737648975493im	9.11e-03	1.99e-04
4	84.49957023255998 + 34.942960837304014im	4.56e-03	4.99e-05
5	168.80515382942275 + 70.15689112416922im	2.28e-03	1.25e-05
6	337.50591933464125 + 140.53062554154792im	1.14e-03	3.12e-06
7	674.9581092588107 + 281.25208333979583im	5.70e-04	7.79e-07
8	1349.8889995007594 + 562.6826361056818im	2.85e-04	NaN

(b)  $\det_2$  starting from  $k_0 = 11$ .

$l$	$k_l$	$ \det_1(k_l) $	$ \partial_k \det_1(k_l) $
1	16.933172576735238 - 0.24982842615297063im	2.89e-02	2.01e+00
2	16.92321608496663 - 0.23950336537694566im	8.99e-05	2.02e+00
3	16.92320186112372 - 0.23954559016258034im	8.67e-10	2.02e+00

(c)  $\det_1$  starting from  $k_0 = 17$ .

$l$	$k_l$	$ \det_2(k_l) $	$ \partial_k \det_2(k_l) $
1	16.903562544030315 - 0.2594084783861693im	5.85e-04	2.11e-02
2	16.922896121039905 - 0.2394985971301382im	6.44e-06	2.08e-02
3	16.92320187831679 - 0.239545557149322im	7.97e-10	2.08e-02

(d)  $\det_2$  starting from  $k_0 = 17$ .

Table S-21: Newton iterations using  $\det_1$  or  $\det_2$  for  $\xi = 0.5$ ,  $n_1 = 1.5$ ,  $n_2 = 1$  and  $m = 10$ , starting from  $k_0 = 11$  or  $k_0 = 17$ .

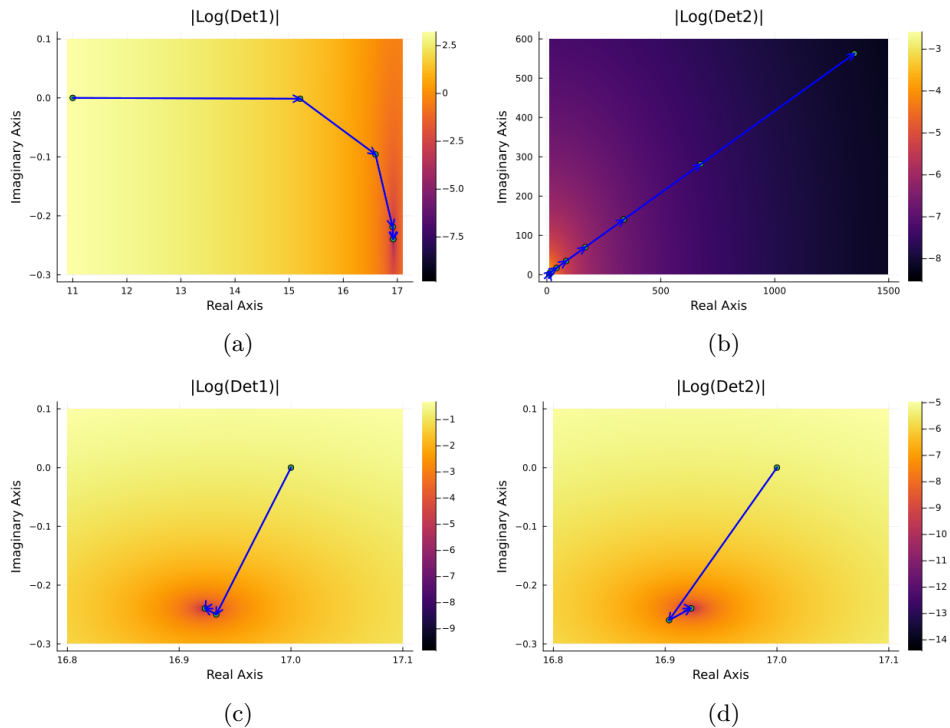


Figure S-2: Newton iterations in the complex plane using  $\det_1$  or  $\det_2$  for  $\xi = 0.5$ ,  $n_1 = 1.5$ ,  $n_2 = 1$  and  $m = 10$ , starting from  $k_0 = 11$  (top) or  $k_0 = 17$  (bottom).

## S-Appendix B Basic properties of nonlinear eigenvalue problems [57]

We gather here some definitions and basic properties of nonlinear eigenvalue problems.

We consider the problem of finding  $\lambda$  such that the linear system

$$T(\lambda)x = 0 \tag{S-1}$$

has a nontrivial solution  $x$ , where  $T(\cdot): D \rightarrow \mathbb{C}^{n \times n}$  is a family of matrices depending on a complex parameter  $\lambda \in D$ .

### Definitions:

$\hat{\lambda} \in D$  is called an eigenvalue of  $T(\cdot)$  if  $T(\hat{\lambda})x = 0$  has a nontrivial solution  $\hat{x} \neq 0$ .  $\hat{x}$  is called a corresponding eigenvector or right eigenvector, and  $(\hat{\lambda}, \hat{x})$  is called eigenpair of  $T(\cdot)$ .

Any nontrivial solution  $\hat{y} \neq 0$  of the adjoint equation  $T(\hat{\lambda})^*y = 0$  is called left eigenvector of  $T(\cdot)$  and the vector-scalar-vector triplet  $(\hat{y}, \hat{\lambda}, \hat{x})$  is called an eigentriplet of  $T(\cdot)$ .

An eigenvalue  $\hat{\lambda}$  of  $T(\cdot)$  has algebraic multiplicity  $k$  if  $\frac{d^\ell}{d\lambda^\ell} \det(T(\lambda))|_{\lambda=\hat{\lambda}} = 0$  for  $\ell = 0, \dots, k-1$  and  $\frac{d^k}{d\lambda^k} \det(T(\lambda))|_{\lambda=\hat{\lambda}} \neq 0$ .

An eigenvalue  $\hat{\lambda}$  is simple if its algebraic multiplicity is one.

The geometric multiplicity of an eigenvalue  $\hat{\lambda}$  is the dimension of the kernel  $\ker(T(\hat{\lambda}))$  of  $T(\hat{\lambda})$ .

An eigenvalue is called semi-simple if its algebraic and geometric multiplicity coincide.

### Properties:

If  $\hat{\lambda}$  is an algebraically simple eigenvalue of  $T(\cdot)$ , then  $\hat{\lambda}$  is geometrically simple. [53]

Let  $(\hat{y}, \hat{\lambda}, \hat{x})$  be an eigentriplet of  $T(\cdot)$ . Then  $\hat{\lambda}$  is algebraically simple if and only if  $\hat{\lambda}$  is geometrically simple and  $\hat{y}^*T'(\hat{\lambda})\hat{x} \neq 0$ . [42, 53]

## S-Appendix C Asymptotic expansions of quasi-resonances in dimension 2 [10]

We gather here some of the results in [10] regarding the construction of quasimodes  $(\underline{k}(m), \underline{u}(m))$  as  $m \rightarrow \infty$ , i.e. approximate solutions of (7) with  $\hat{g}_m = 0$ , in three different configurations. Moreover, it is shown in [10] that the constructed quasi-resonances  $\underline{k}_j(m)$  are real and positive and close to true resonances  $k_j(m)$  modulo a super-algebraic error  $O(m^{-\infty})$ .

*Assumption 1.1.* The radial function  $n: r \mapsto n(r)$  satisfies the following properties:

1.  $n(r) = 1$  if  $r > \xi$  ;
2. The function  $n$  belongs to  $C^\infty([0, \xi])$  and  $n(r) > 1$  for all  $r \leq \xi$ .

*Notation 1.2.*

$$n_0 = \lim_{r \nearrow \xi} n(r), \quad n_I = \lim_{r \nearrow \xi} n'(r), \quad n_{II} = \lim_{r \nearrow \xi} n''(r). \tag{S-2}$$

Effective adimensional curvature:

$$\check{\kappa} := \xi \left( \frac{1}{\xi} + \frac{n_I}{n_0} \right). \tag{S-3}$$

Adimensional Hessian:

$$\check{\mu} := \xi^2 \left( \frac{2}{\xi^2} - \frac{n_{II}}{n_0} \right). \tag{S-4}$$

*Theorem 1.A.* Assume the radial function  $n$  satisfies Assumption 1.1 and

$$\check{\kappa} > 0. \tag{S-5}$$

Then, for any integer  $j \geq 0$ , there exists a quasi-pair  $(\underline{k}_j(m), \underline{u}_j(m))$  such that the quasi-resonance  $\underline{k}_j(m)$  has an expansion in integer powers of  $m^{-1/3}$  starting as

$$\begin{aligned} \underline{k}_j(m) = \frac{m}{\xi n_0} & \left[ 1 + \frac{a_j}{2} \left( \frac{2\check{\kappa}}{m} \right)^{\frac{2}{3}} - \frac{n_0}{2\sqrt{n_0^2 - 1}} \left( \frac{2\check{\kappa}}{m} \right) + \frac{a_j^2}{15} \left( \frac{17}{8} - \frac{3}{\check{\kappa}} + \frac{\check{\mu}}{\check{\kappa}^2} \right) \left( \frac{2\check{\kappa}}{m} \right)^{\frac{4}{3}} \right. \\ & \left. - \frac{a_j n_0}{12\sqrt{n_0^2 - 1}} \left( \frac{n_0^2}{n_0^2 - 1} + 2 - \frac{6}{\check{\kappa}} + \frac{2\check{\mu}}{\check{\kappa}^2} \right) \left( \frac{2\check{\kappa}}{m} \right)^{\frac{5}{3}} + O(m^{-2}) \right] \end{aligned} \tag{S-6}$$

with the numbers  $a_j$  being the successive roots of the flipped Airy function  $z \in \mathbb{C} \mapsto \text{Ai}(-z)$  where  $\text{Ai}$  denotes the Airy function [1, 19].

*Theorem 1.B.* Assume the radial function  $n$  satisfies Assumption 1.1 and

$$\tilde{\kappa} = 0 \quad \text{with} \quad \tilde{\mu} > 0. \quad (\text{S-7})$$

Then, for any integer  $j \geq 0$ , there exists a quasi-pair  $(\underline{k}_j(m), \underline{u}_j(m))$  such that the quasi-resonance  $\underline{k}_j(m)$  has an expansion in integer powers of  $m^{-1/2}$  starting as

$$\underline{k}_j(m) = \frac{m}{\xi n_0} \left[ 1 + \frac{4j+3}{2} \left( \frac{\sqrt{\tilde{\mu}}}{m} \right) + O(m^{-3/2}) \right], \quad (\text{S-8})$$

the coefficient of degree 1 being zero.

*Theorem 1.C.* Assume the radial function  $n$  satisfies Assumption 1.1 and that

$$\tilde{\kappa} < 0. \quad (\text{S-9})$$

Let  $\xi_0 \in (0, \xi)$  such that  $1 + \frac{\xi_0 n'(\xi_0)}{n(\xi_0)} = 0$  and assume further that

$$\tilde{\mu}_0 := \xi_0^2 \left( \frac{2}{\xi_0^2} - \frac{n''(\xi_0)}{n(\xi_0)} \right) > 0. \quad (\text{S-10})$$

Then, for any integer  $j \geq 0$ , there exists a quasi-pair  $(\underline{k}_j(m), \underline{u}_j(m))$  such that the quasi-resonance  $\underline{k}_j(m)$  has an expansion in integer powers of  $m^{-1/2}$  starting as

$$\underline{k}_j(m) = \frac{m}{\xi_0 n(\xi_0)} \left[ 1 + \frac{2j+1}{2} \left( \frac{\sqrt{\tilde{\mu}_0}}{m} \right) + O(m^{-2}) \right], \quad (\text{S-11})$$

the coefficients of degree 1 and 3 being zero.

## S-Appendix D Special variable $n$ with explicit solution (Luneburg lens)

The fundamental solutions of the second-order differential equation

$$-y''(x) - \frac{y'(x)}{x} + \left( \frac{m^2}{x^2} - k^2(2-x^2) \right) y(x) = 0 \quad (\text{S-12})$$

(where  $n(x) = \sqrt{2-x^2}$ ) are given by

- $f_1(x) = \frac{1}{x} M_{\frac{k}{2}, \frac{m}{2}}(kx^2)$  (vanishes at  $x = 0$ )
- $f_2(x) = \frac{1}{x} W_{\frac{k}{2}, \frac{m}{2}}(kx^2)$  (singular at  $x = 0$ )

where  $M_{k,m}(z)$  and  $W_{k,m}(z)$  are the Whittaker functions [1, 59, 43], solutions of the Whittaker differential equation

$$w'' + \left( \frac{1/4 - m^2}{z^2} + \frac{k}{z} - \frac{1}{4} \right) w = 0. \quad (\text{S-13})$$

Indeed, if one looks for a solution of (S-12) in the form  $y(x) = \frac{1}{x} w(kx^2)$  then using

$$y'(x) = 2kw'(kx^2) - \frac{1}{x^2} w(kx^2) \quad (\text{S-14})$$

$$y''(x) = 4k^2 x w''(kx^2) - \frac{2k}{x} w'(kx^2) + \frac{2}{x^3} w(kx^2), \quad (\text{S-15})$$

the differential equation (S-12) becomes

$$-4k^2 x w''(kx^2) - \left( \frac{1-m^2}{x^3} + \frac{k^2(2-x^2)}{x} \right) w(kx^2) = 0 \quad (\text{S-16})$$

$$w''(kx^2) + \left( \frac{1-m^2}{4k^2 x^4} + \frac{1}{2x^2} - \frac{1}{4} \right) w(kx^2) = 0, \quad (\text{S-17})$$

hence the announced result.

We have used the Whittaker representation in our implementation for its convenience and reduced form.

This special case is linked to the Luneburg lens which is a spherically symmetric gradient-index lens, whose typical refractive index has the same form considered here [13, 34, 35, 36].